

SUBSURFACE STRATIGRAPHY OF THE WASATCH AND MESAVERDE FORMATIONS,
PICEANCE BASIN, N.W. COLORADO

by

Richard Ryan

ORAU Geologist

April, 1987

TABLE OF CONTENTS

	<u>PAGE</u>
I. <u>SUMMARY</u>	
II. <u>INTRODUCTION</u>	
Purpose	
Study Area and Scope	
Background Geology	
III. <u>METHODOLOGY</u>	
IV. <u>COMPILATION AND DOCUMENTATION OF DATA</u>	
Production Data	
Geophysical Well Log Data	
Completion Report Data	
Synthetic aperture Radar Imagery	
V. <u>DISCUSSION OF RESULTS</u>	
Correlation of Stratigraphic Horizons	
Structure Features and Basin Evolution	
Reservoir Distribution	
VI. <u>CONCLUSIONS</u>	
VII. <u>SUGGESTIONS FOR FUTURE WORK</u>	
VIII. <u>BIBLIOGRAPHY</u>	
IX. <u>APPENDIX A</u> - Cross Sections A-A' Through V-V'	

- X. APPENDIX B - Well Logs Showing Intersection With Sl-S11
- XI. APPENDIX C - A Portion of the Geologic Map of Colorado
- XII. APPENDIX D - SAR Image

LIST OF FIGURES AND TABLES

PAGE

FIGURE 1: General geography and stratigraphy of the Piceance Basin	
FIGURE 2: Geography during earliest Mesaverde deposition	
FIGURE 3: Geography during middle Mesaverde deposition	
FIGURE 4: Geography before the end of Mesaverde deposition	
FIGURE 5: Geography during earliest Tertiary deposition	
FIGURE 6: Relationship between existing stratigraphic nomenclature and the correlated horizons S1 through S11	
FIGURE 7: Well and Cross section location map showing the top of the Wasatch Formation outcrop for reference	
FIGURE 8: Structure on the S4 horizon	
FIGURE 9: Structure on the S8 horizon	
FIGURE 10: Structure on top of the Rollins sandstone (?), base of the Williams Fork formation, Mesaverde Group	
FIGURE 11: Thickness of the S1/S6 interval (approximately the Wasatch formation)	
FIGURE 12: Thickness of the S6/S11 interval (approximately the Williams Fork formation)	
FIGURE 13: Thickness of the S8/S9 interval	
FIGURE 14: Thickness of the S3/S4 interval	
FIGURE 15: Detail of White River Dome area	
FIGURE 16: Detail of the Piceance Creek area	
FIGURE 17: Anatomy of a flower structure	

FIGURE 18: Detail of Rulison field area

FIGURE 19: Sand isolith map of the "Fluvial Interval", Mesaverde Group rocks, Rulison field

I. SUMMARY

Correlation of gamma radiation well logs resulted in definition of eleven stratigraphic horizons through the Wasatch and Williams Fork formations. The digital form of gamma radiation well logs was responsible for the success of the correlation exercise - only "condensed vertical scale displays" of the data revealed correlatable horizons. Stratigraphic correlation provides the basis for structural, depositional, and production analyses.

Important structural detail was resolved during correlation of gamma radiation well logs. These details (1) show that structural influence is the prime factor in explaining the production phenomena observed in the Rulison field, (2) suggest structural reasons for the location of the Piceance Creek and White River Dome fields, and (3) suggest that a unique exploration strategy may exist for the northeast corner of the basin. Attendant isochore maps of the intervals between correlated horizons yield an indication of the relative time of activity for different structural features.

Depositional analysis provided several contributions towards better understanding sandstone reservoir geometry. In some intervals significant variation in reservoir rock content occurs as a function of location. Clusters of individual sand bodies form these reservoir trends. The shape, scale, orientation, and location of these trends are poorly resolved but agree well with previously published information. Better resolution could be achieved readily with additional, more detailed correlations and the computer codes from this study.

A significant data base has been assembled. Gas well production data and synthetic aperture radar imagery ^{was} assembled and reduced for analysis. The digitized data and successful correlations together form a comprehensive data base on the size distribution of lenticular sandstone reservoirs within the formations of interest. Future advances in understanding the reservoir rock's influence on production are planned and will benefit from the assembled data.

II. INTRODUCTION

Purpose

The purpose of this document is three-fold: (1) to present the results from a subsurface stratigraphic investigation, (2) to document the compilation of production data, geophysical well log data, and completion report data which was assembled as much for this study as it was for future work, and (3) to make recommendations for future research in the study area. This work is not intended as an end in itself but is rather meant to provide and document the geologic background necessary for a larger,

continuing effort.

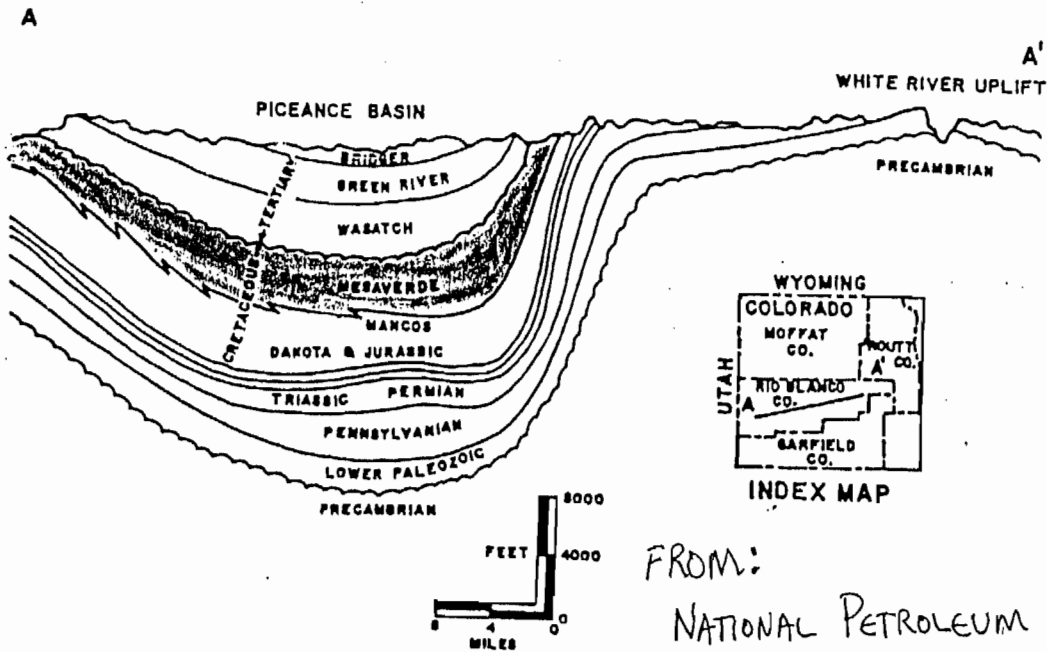
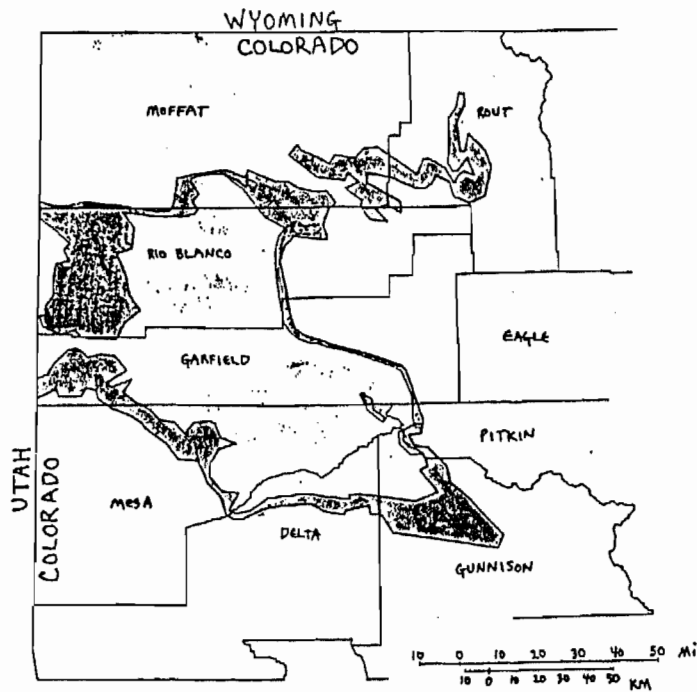
Study Area and Scope

The Piceance basin is a 600 square mile area of Garfield, RioBlanco, and Mesa counties located in the northwest corner of Colorado. Figure 1 shows the generalized geography and stratigraphy of the study area. The rock section of interest includes the Wasatch Formation (early Tertiary) and the Williams Fork Formation of the Mesaverde group (late Cretaceous). These sedimentary units constitute an 8000' vertical sequence of sandstones, shales and coals. The sandstones within the sequence are noted for being vertically and laterally discontinuous within the shale, and are often saturated with natural gas. The lack of horizontally traceable units, and the fact that the sands exhibit low permeabilities, make the entire section appear to be a homogeneous mixture of rocks wherein a vast resource of elusive reserves reside.

The sandstone reservoirs of interest were deposited as grains of sand within ancient river systems. The 8000' section represents accumulations over a long period of time by many different river systems. Analysis of sandstone content in the section as a whole does not show any trends in deposition, nor would it be expected to because the trends of different systems are superimposed and effectively hide one and other. The solution to this problem is to divide the section along natural divisions (stratigraphic correlation) forming smaller units. Analysis of these smaller sediment packages holds the potential for resolving reservoir properties, such as trends in reservoir rock thickness (sandstone isolith), which could not be resolved through analysis of the entire 8000' section of rock.

The probable reason that this type of analysis has not been done before lies in the fact that these formations are characterized by a lack of horizontally continuous beds, thus making stratigraphic correlations almost impossible. However, when the well logs of interest are displayed on an extremely condensed vertical scale (1 inch = 1200 feet) they reveal characteristics that can be correlated over large distances, in much the same way that a satellite photo reveals trends not recognizable from the earth's surface. Previously these well logs were displayed on paper with a vertical scale of 1 inch = 20 feet or 1 inch = 50 feet because they were created before digital data was an industry standard. The condensed vertical scale display of these well logs was made possible by manually digitizing the well log - a tedious task with advantageous results. Eleven horizons are identified and correlated throughout the basin where only two were previously documented by literature.

The gamma ray logs from 206 wells were digitized and analysed during this study. These wells were chosen by comparing information on commercially available logs (Petroleum Information Inc.'s well log locator) with USGS



FROM:
 NATIONAL PETROLEUM COUNCIL
 1980

FIGURE 1:

General geography and stratigraphy of the Piceance Basin. All of the Wasatch Formation and the upper part of the Mesaverde Group are of interest to this study. The Mesaverde rocks are shaded in both the plan view (top) and cross section view (bottom). Note that the shaded layer reveals the bowl shape of the basin.

maps (Granica, etal, 1980) which define the depth to the formations of interest at a particular location within the basin. An attempt was made to acquire log information for all wells producing from the formations of interest and also to acquire at least one log through the interval every six square miles. This distribution of well information was, however, not obtainable, and while there are additional logs pertinent to the study which could have been purchased they were not acquired because it was felt that they would not significantly add to the data base.

Of all the logs available for each well, the gamma-ray well logs were chosen for analysis not only because they are a fairly common log type but also because they serve as the single best indicator of reservoir rock. In a predominately sand and shale sequence, the level of natural gamma radiation (for the most part due to the radioactive isotope of potassium found in the mineral illite - the most common constituent in shale) serves as a good indicator of the "shaliness" of the rock units, so that sandstones can be differentiated from shaley sandstones which can be differentiated from shales. In general, the less "shaley" or "cleaner" a sandstone is the better the sandstone's reservoir properties will be.

Stratigraphic correlation of gamma radiation well logs offers improved knowledge of reservoir quality and distribution, yields information on the structural evolution of the basin, helps define the existance of trapping mechanisms, and can greatly improve our ability to determine how different reservoir properties affect the production behavior of wells in the formations of interest.

Background Geology

Two properties displayed by the sandstone reservoirs are responsible for making the exploitation of the hydrocarbon resources contained within them particularly difficult. First, these sandstones are plagued by extremely low matrix permeability (0.1 to 0.001 millidarcys) which dictates that a successful well be dependant on permeability provided by the existance of fracturing in the reservoir rock. Strongly developed folds and faults provide ideal places to explore for fractured reservoirs. Second, the sandstones have a strong geometric tendency to be horizontally discontinuous forming elongate lenticular bodies which extend several hundred feet horizontally and are up to a hundred feet thick. A lenticular sandbody geometry makes correlation and tracking of productive zones difficult or impossible, thus inhibiting a commonly successful exploration technique. Delineation of trapping mechanisms, folding, and faulting, is dependant on the existance of traceable horizons through the section.

Identifying and tracing continuous horizons through the rock section is seen to be an important step in developing the resources within the basin. An understanding of how stratigraphic horizons can be recognized within a section of discontinuous sandstones requires a knowledge of the history of

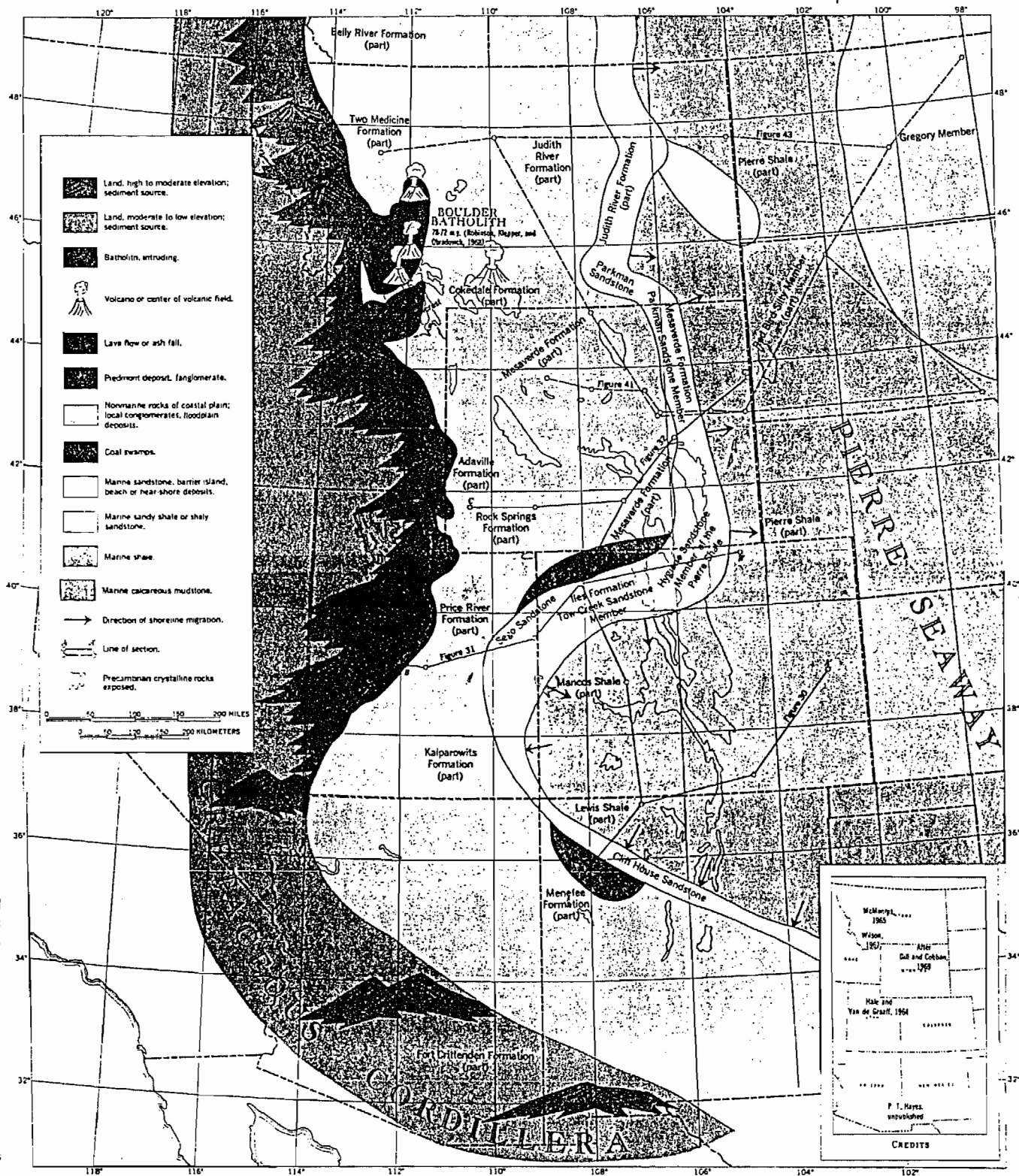
sediment accumulations in the area. Infact, a great deal can be surmised about the reservoir properties a rock will display given a working knowledge of its depositional history.

The rocks of the Williams Fork Formation (Mesaverde Group), the oldest rocks of interest, were deposited before the Piceance basin had significantly developed. They accumulated on a regionally large plain adjacent to a north-south trending coastline bordering a sea which covered much of the interior of North America. The rivers that flowed across this plain left deposits of sand and shale. These sediments accumulated as this plain and the middle of the North American continent imperceptibly subsided. Like rivers in similar situations today, viewed on a large scale they were most likely oriented perpendicular to the coastline. When viewed on a smaller scale (Lorentz, 1983), these rivers meandered significantly, and once near the ocean, in the delta environment, the river channels commonly split into a maze of distributary streams radiating through swamps which eventually terminated at the beach front.

The changes in river environments from fluvial plain, across the delta and swamps, out to the coast tend to be systematic as a river approaches its base level (in this case the ancient coastline). Thus, sediments deposited in these different environments form bands of similar deposits which parallel the coast. As the coastline shifts with geologic time the deposits associated with each of these environments shifts and accumulate on top of the deposits of the adjacent environment. The end result being that the deposits that are laterally adjacent at any one time become vertically adjacent over geologic time. This is the case in the Williams Fork, coastal deposits are overlain by swamp deposits, which are in turn overlain by the more upstream fluvial deposits. Lorenz (1983) studied the outcrops of the sand and shale deposits left behind by the Mesaverde Group rivers and was able to noticed distinct changes in the texture of the rock which were a direct result of accumulation in these different environments. It is this stacking of positionally unique packages of sediments which is responsible for the physical existance of correlatable horizons in the absence of single continuous sandstone layers.

Toward the end of Mesaverde Group deposition there was a drastic relative rise in sea level which unindated the study area with ocean. This was a much more sudden event than the previous seaward shifting of the shoreline associated with the stacking of sediment packages from different environments. Figures 2, 3, and 4 illustrate the regional change in shoreline during Mesaverde Group deposition. A pronounced period of erosion which unevenly removed some Meseverde sediments marked the end of Mesaverde Group deposition (Upper Cretaceous) and the start of Wasatch deposition (lower Tertiary - Eocene). Figure 5 illustrates the ancient geography of the lower Tertiary, note the drastic change in the ancient geography from what it was during the Upper Cretaceous.

In contrast to Mesaverde Group deposition, the rocks of the Wasatch



PALAEONVIRONMENT IN MIDDLE JUDITH RIVER TIME FROM: MCGOOKEY, ET AL, 1972.
 [During *Baculites scotti* range zone]

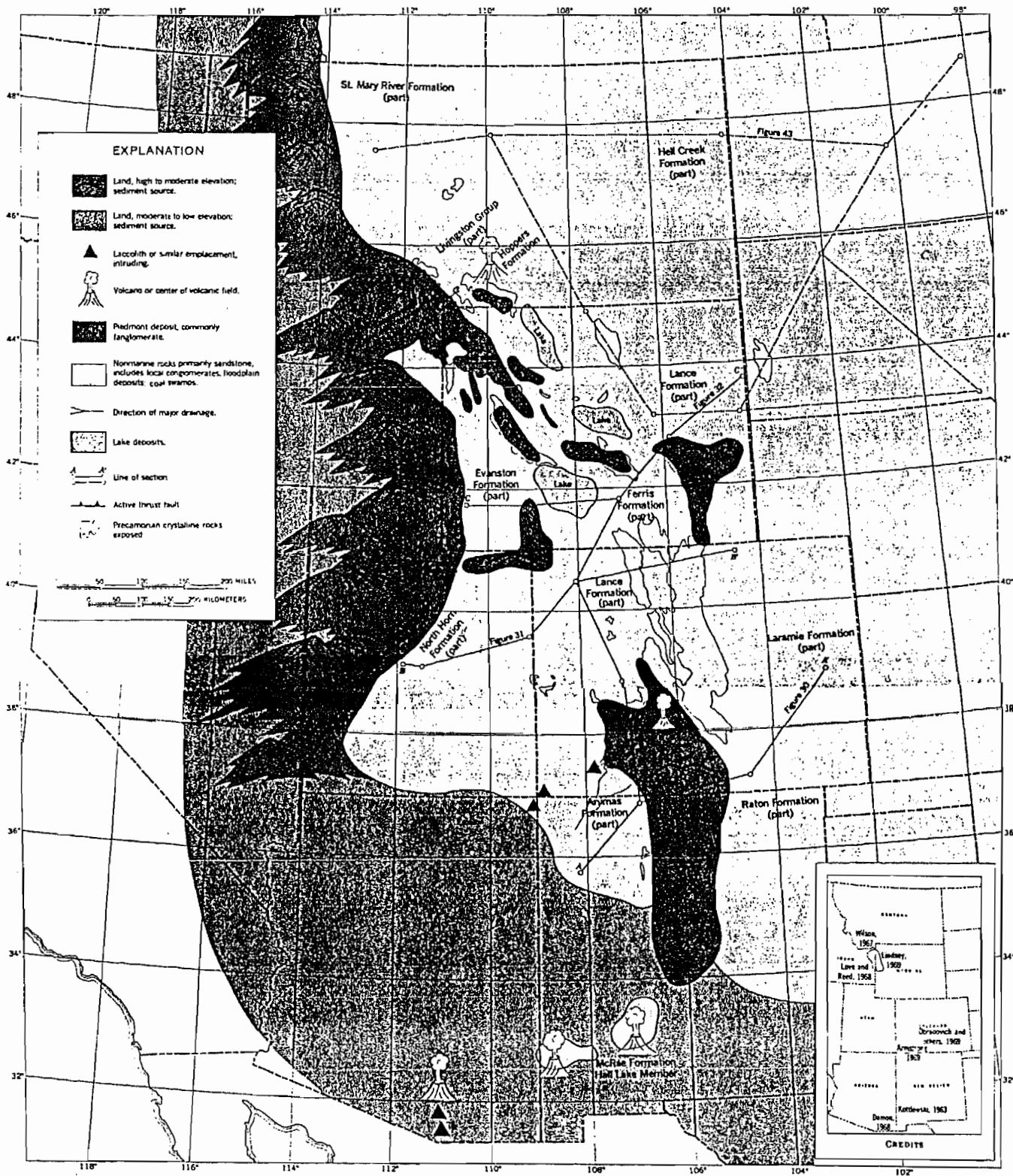
FIGURE 2:
 Geography during earliest Mesaverde deposition. Piceance basin is located in a marginally marine environment of deposition.



PALEOENVIRONMENT IN EARLY FOX HILLS TIME
 [During *Baculites clinolabatus* range zone]

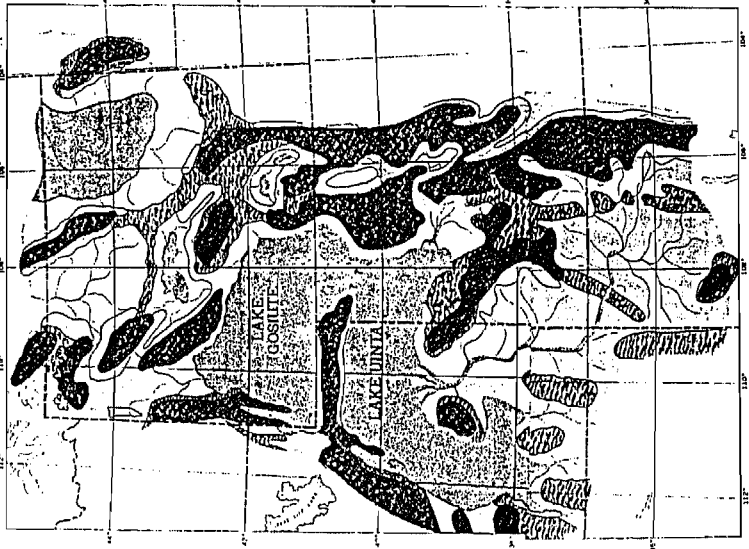
FROM:
 MCGOOKEY, ET AL, 1972.

FIGURE 3:
 Geography during middle Mesaverde deposition. Piceance basin is located within the delta plain and fluvial plain environments of deposition.

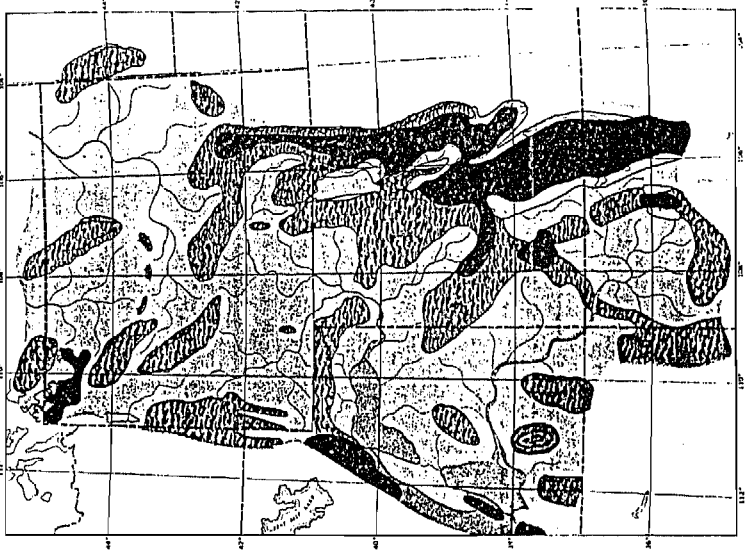


PALEOENVIRONMENT IN LATEST CRETACEOUS TIME FROM: M'GOOKEY, ET AL, 1972.

FIGURE 4:
 Geography before the end of Mesaverde deposition. The entire area is undated by the Cretaceous interior seaway.



PALEOGEOGRAPHY IN LATE EARLY TO MIDDLE EOCENE TIME



PALEOGEOGRAPHY IN LATE EOCENE TIME

FROM:
McGOOKY, ET AL, 1972.

EXPLANATION

Presambian crystalline rock exposed.

AREAS OF DEGRADATION

- High relief.
- Medium to low relief.

AREAS OF AGGRADATION

- Alluvial fans.
- Flood plains, mixed environments including fluvial, limited lacustrine, limited palustrine and peatland.
- Extensive swamps abundant thick coal beds.
- Extensive lakes, rivers (location conjectural).

0 50 100 150 200 MILES
0 50 100 150 200 KILOMETERS

FIGURE 5:

Geography during earliest Tertiary deposition. Note the major change between this illustration and figures 2,3, and 4. Rivers originate in Mountains to the east rather than to the west as before. The broad regional drainage pattern associated with an ocean in figures 2,3, and 4 are replaced by smaller independent drainage patterns associated with large lakes.

formation were deposited during Piceance basin development by river systems much different in extent and direction of drainage. However, the concept of systematic downstream change in depositional environments which was noted for the Mesaverde, is likewise applicable to Wasatch sedimentation. The differences in river character, the period of erosion marking the division between Cretaceous and Tertiary, and the delineation of the Piceance basin as an entity were all the result of upheavals associated with the initial stages of building the Rocky mountains. The direction of drainage had shifted 90 to 180 degrees during Wasatch deposition from what it was during Mesaverde Group deposition. Instead of the rivers originating in distant mountains as they did during Mesaverde deposition the mountainous origins were much more proximal to the area of sediment accumulation during Wasatch deposition. Instead of the regional swamps which existed during Mesaverde time (evident by the thick coals in the paludal zone) there were bogs developed during Wasatch time (evident by the discontinuous low grade coals). Instead of the ocean (adjacent to swamps) which acted as base level for Mesaverde rivers, large lakes (adjacent to bogs) acted as base level to Wasatch rivers.

Though the systematic downstream changes in Wasatch depositional environments were similar to those in the Mesaverde, the regionally uniform stacking of the sediment packages unique to those environments is probably not as well developed in the Wasatch because the lakes which act as base level of Wasatch rivers were not as prone to regional transgressions and regressions as were the oceans which acted as the base level of Mesaverde rivers. In other words, the Wasatch formation in the northern part of the basin is likely to be dominated by lacustrine and paludal deposits while the Wasatch formation in the southern part of the basin is likely to be dominated by fluvial and alluvial deposits. The physical nature of the correlated horizons and the regional extent of the intervals defined by them determine the meaning given to results of analysis.

III. METHODOLOGY

The procedure for data reduction and analysis followed three steps, (1) identification and correlation of arbitrary stratigraphic horizons within the formations of interest, (2) calculation of relative amounts of sand and shale for each well's gamma-ray log, (3) plan view and numeric summarization of the sand value data for different stratigraphic intervals. Additionally, structure contour maps and interval isochore maps were made to aid in checking the validity of the correlations and to provide basic data on sedimentation history.

Correlation of gamma-ray traces was best accomplished when logs were displayed on mylar drafting film with sufficient detail to distinguish sands of 20 feet or more in thickness. Transfer of sufficiently detailed condensed scale gamma-ray traces to paper was accomplished through Scott Cerullo's (E.G.G.) ingenious use of the Geosciences branch Log Analysis

System software and a tectronix rasterizer. Traces were then transferred to mylar by feeding a sheet of mylar through the bottom half of a zerox machine while the paper copy with trace data was on top. Using mylar copies for correlation allowed easy comparison of wells by overlaying the mylar sheets and were durable when mistakes in pencil were erased. About half of the wells in the study were suitably situated to be included in one of twenty two cross sections which served as a basis for the correlations. Wells not included on the cross sections were matched to the cross sections after the majority of correlating was finished. Some of these latter wells revealed mistakes in correlation or the existence of other equally likely correlations, which forced a re-evaluating of cross section correlations.

Determination of the relative sand and shale content from digitized gamma-ray log data was based on the assumption that sandstones emit less gamma radiation than shales. The gamma-ray values recorded for each well were subjected to statistical analysis and the value selected as the cutoff point between sand and shale was determined from the mean and standard deviation of the population. Values for clean -, 80 percent clean -, and 60 percent clean sandstones were calculated for analysis by the equations (mean - (std. dev. * 1.50)), (mean - (std. dev. * 0.90)), and (mean - (std. dev. * 0.20)), respectively. From comparative analysis of these values one can infer differences in reservoir quality and can better analyze reservoir distribution.

Analysis of reservoir distribution employed maps showing values of sandstone content between adjacent horizons (S1-S11) accompanied by histogram analysis of the sand body thicknesses within the same interval. For histogram analysis the study area was divided into six areas based on the extent of accurate stratigraphic correlation. These areas are defined as follows:

- 1) White River Dome Field | 108.15 > longitude > 108.39
40.07 > latitude > 40.19
- 2) Piceance Creek Field | 108.07 > longitude > 108.31
←40.82 > latitude > 40.94
- 3) Rulison Field | 107.78 > longitude > 107.94
└───39.44 > latitude > 39.56
- 4) Basin Southeast | 107.37 > longitude > 107.93
└───39.12 > latitude > 39.62
- 5) Basin Southwest | 107.93 > longitude > 108.50
└───39.12 > latitude > 39.62
- 6) Basin northwest | 108.32 > longitude > 108.62
└───39.62 > latitude > 40.12

IV. COMPILATION AND DOCUMENTATION OF DATA

During the course of the study a significant base of data has been compiled which includes production data, geophysical well log data, completion

report data, 1:250,000 scale topographic maps, and synthetic aperture radar (SAR) imagery of the area. The data comes from various sources at a cost of approximately one thousand dollars.

Production Data

Production data resides in three places; (1) on BM2352 which is the magnetic tape received from Dwights Energydata Inc., (2) in four data files FLDCHR1 - FLDCHR4, and (3) in a booklet with a blue cover containing production vs. time graphs for easy visual reference. Dwights data is comprehensive for the years 1970 through 1985. There are 210 wells listed in the data set, about half of which produce from zones within the Wasatch or Williams Fork formations. When the original Dwights data is dumped to file at 90 characters per record the fortran program PREDEC.FOR reads and reformats this data for graphing, decline curve analysis, listing well header information, etc. The well name assigned to the output produced by this program consists of a letter (N or S) and the record number in the data file where that well's information starts. These names are cross referenced with well API numbers in the data file API.DAT.

Because of data oddities, production data have been prepared for analysis in four different ways, and the data files FLDCHR1-4 contain these different versions. Each record in these files contains a well name, an observation number, a monthly production value, and a field horizon identifier. The observation number indicates months since the well was first put into service. The field horizon identifier represents an early attempt at grouping wells by location and stratigraphy, and should be replaced with an identifier indicating production zone based on the intervals formed by the correlated horizons S1-S11. FLDCHR.DAT contains production data as reported by dwights. The remaining files contain altered or synthetic production data in an attempt to represent actual well performance unaffected by flow restrictions caused by the gas gatherer and pipeline system. These effects are obvious in the raw data where nearby wells all show months of reduced flow which coincide with each other. FLDCHR2.DAT contains reported production data with all zero production figures removed, and the observation numbers adjusted to be continuous so as not to reflect the removed values. FLDCHR3.DAT contains decline curve data from the 'best fit' decline curves thought the production data. Observation numbers have been adjusted to reflect the alternate time that the decline analysis used for a starting point. FLDCHR4.DAT contains decline curve data which was fit using an alternate time of 1 for decline analysis. The observation number in this file are identical to those found in FLDCHR.DAT. Personally, I favor FLDCHR3.DAT as the source of production data to be used in subsequent analysis.

Geophysical Well Log Data

Microfiche of geophysical well logs were purchased from M.J. Systems

Inc., They have been cross referenced with well API number, and are cataloged in a 8 by 5 wooden reference card box by API number. Gamma ray well logs used in this study were digitized using the "Log Analysis System" (Geosciences Branch, B-2). Condensed scale displays of the gamma ray logs are visually cataloged in Appendix B and organized by well API number. This data has been transferred to magnetic tape in three forms. First, well logs on the Log Analysis system have been transferred to tape (BM) by that system's archive utility. Second, data files (names reflecting well API number) for each well have been assembled so that the main VAX computers at METC have access to digitized gamma ray log data. These data were stored on magnetic tapes (BM2668, BM8049, BM8308, BM2694, BM2664, BM2669) using the DCL backup utility. Third, summary data files for each well have been assembled and contain the results of gamma ray log analysis, general well information, and stratigraphic correlation data for that well. Summary data file names are identical to those containing raw data on magnetic tape, except that the version specification number on these files is 2.

Completion Report Data

General well information used during the study is contained in the data file WHCSPCB.DAT, and includes API number, location, elevation, and assorted perforation information which comes largely from Petroleum Information's Well History Control System (WHCS). This information has been, and needs to be updated and corrected continuously. Microfiche duplications of Colorado State well completion reports were purchased from M.J. Systems, Inc. specifically for this purpose. At present perforation interval data from these reports are being used by Jason Nye, ORAU, to update that information. Ten percent of the well elevations in the WHCS data were found to be significantly different from that recorded on microfiche. Therefore all elevation data in the WHCSPCB.DAT file now reflects the more accurate elevation data from the well logs. Additionally, some wells have been added to the list, and some locational information upgraded.

The Fortran program LOG7.FOR combines the gamma-ray data, general well information data, and the stratigraphic correlation data found in STRAT.DAT in analysis of gamma ray logs and produces a summary file for each well along with a suite of map files containing information on reservoir distribution for the individual horizons. If a more detailed correlation of one of the stratigraphic horizons is attempted by expanding the vertical scale display of that interval and subsequently dividing the interval by correlation, this program could be used for detailed analysis of those intervals. The Fortran program LOG8.FOR retrieves information from each well's summary file and reformats it for statistical analysis.

Synthetic aperture Radar (SAR) Imagery

SAR data (8 strips of 70mm film) were purchased from the N.O.A.A.'s

National Climatic Center, satellite Data Services Division. Mosaics of the portions covering the Piceance basin were constructed and photographed (see Appendix D) for each of two illumination directions. The images of a single area taken at different angles of illumination differ significantly with respect to observable lineaments. The SAR data was acquired by a SEASAT satellite (June 26, 1978 to October 10, 1978) at an altitude of 790 kilometers, it has a spatial resolution of 25 meters, and operated at 23 cm wavelength and 1.275 gigahertz with illumination angle at 70 degrees off horizontal.

V. DISCUSSION OF RESULTS

Correlation of Stratigraphic Horizons

Twenty-two cross sections were constructed (Figure 7, and Appendix A) showing the position of eleven stratigraphic horizons across the basin. As mentioned earlier (see Background Geology) these horizons are probably related to similarities in the depositional environment of the rocks. Figure 6 illustrates how these eleven horizons correspond to available information on the stratigraphic nomenclature of the area. The positioning of each of the horizons (S1-S11) was chosen because they showed promise of being accurately traceable over long distances not because of relationships to existence nomenclature. The base of the formations of interest (S11, the top of the Iles Formation, Mesaverde Group) was continuously the most easily recognizable horizon because of its characteristic "coarsening upward" gamma ray signature. The top of the formations of interest (approximately at S1), by contrast, is a very gradational contact. Its position was approximated in the southern half of the basin by locating its elevation from detailed geologic maps of the area (Roehler, 1973; Yeend, etal, 1968), and in the northern half of the basin by the location of a marker bed (Orange marker, see Figure 6) in the bottom part of the Green River Formation. The correlated horizons within Mesaverde rocks (S6-S11) show a similarity to the divisions of that section made by Lorentz (1983) based on depositional environment. In contrast, the horizons within Wasatch rocks (S1-S6) could not be related to the formation/member nomenclature presented by Donnell (1961) because of sparse data around the area of his outcrop description.

It is important to note that the correlations are not absolute, that is, that the S4 horizon on the northern most cross section may not be in the same stratigraphic position as the S4 horizon on the southern most cross section. Even though an absolute relationship is implied by the name, and should physically exist in Mesaverde Group rocks and to a lesser extent in the Wasatch formation (see background geology), it has not been pinned down because of areas with scarce data between places where log character changes significantly. However, considering the accuracy of the correlations within groups of intersecting cross sections is thought to be good, and that the length of some cross sections is up to one-third the

0510307550
4s- 97w- 7
elev: 7157

0510307040
2s- 98w- 3
elev: 6732

0504206325
6s- 94w-25
elev: 5355

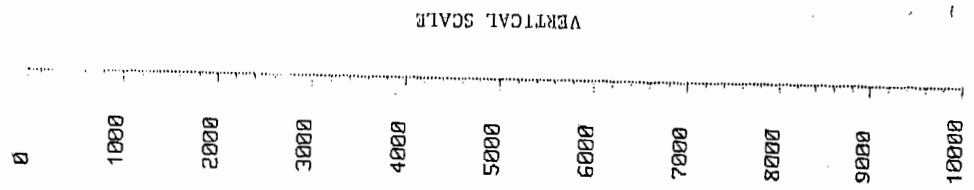
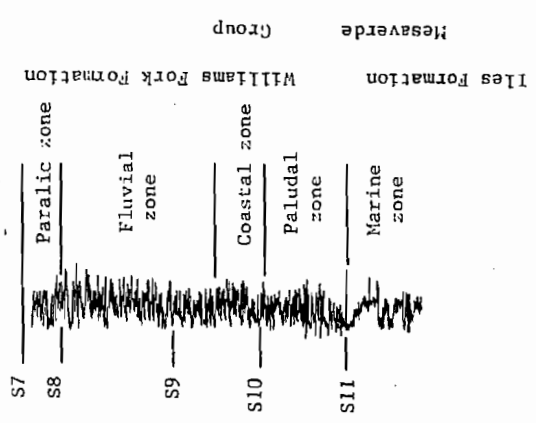
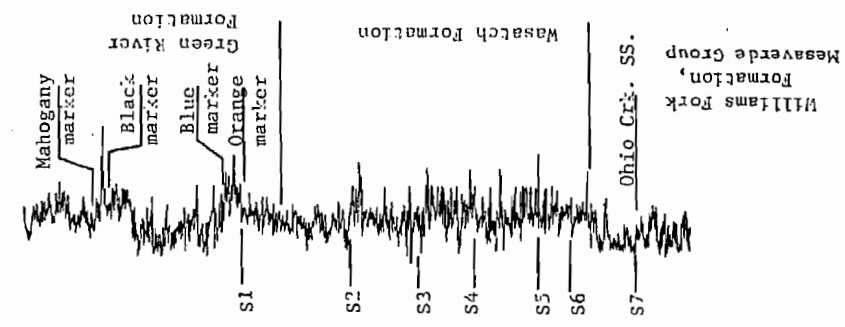
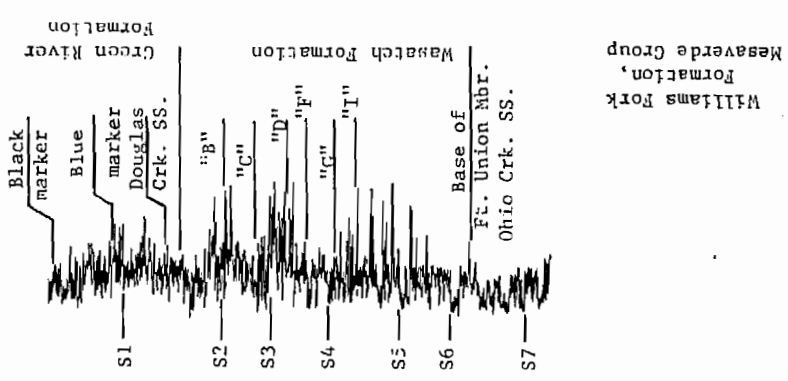


FIGURE 6:

Relationship between existing stratigraphic nomenclature and the correlated horizons S1 through S11. Vertical scale is in feet. Note the positioning of horizons S7 through S11 with respect to the Paralic, Fluvial, Coastal, Paludal, and Marine depositional zones (Lorenz, 1983).

total length across the basin, the correlations as they exist are accurate enough to draw sound conclusions during subsequent analysis provided we keep their short-comings in mind.

Horizons S1 through S11 divide the rock section along natural breaks within the reservoir rock. Within Mesaverde rocks these divisions appear in every case to be related to differences in environment of deposition. In this case the gamma radiation signature of each interval maintains a unique character over long distances. This is also true for some Wasatch rocks in the southern part of the basin. In the northern part of the basin however, some of the divisions in Wasatch rocks appear to divide the section along large scale "cyclothem". This suggests the influence of a single re-occurring process. In this case the gamma ray signatures of different intervals are similar to one and another and described as "fining upward" sequences.

Structural Features and Basin Evolution

Figure 7 shows the location of cross sections, detailed maps, and well data points. Basinwide structure contour maps and interval isochore maps were drawn for each of the eleven horizons and ten intervals, respectively. Detailed sections were constructed for the major gas fields. The overall structure of the basin shown in Figures 8 and 9 is in good agreement with previously published data by Granica (1980, see Figure 10). The structural maps drawn for the White River Dome, Piceance Creek, and Rulison fields show details important to hydrocarbon exploration which are not included in previous work.

Maps showing elevation differences between two given stratigraphic horizons (isochore maps) are useful for showing a geologic feature's effect on contemporaneous deposition. Figures 11 and 12 show the interval thickness between the S1-S6 horizons (Wasatch Formation) and the S6-S11 horizons (Williams Fork Formation) respectively. Note that Wasatch formation (Figure 11) is restricted along the western and southern borders of the basin much more so than the Williams Fork formation (Figure 12), reflecting the fact that the basin was formed prior to or during Wasatch deposition and after Mesaverde deposition. Figure 13 shows the S9-S10 interval thickness. Note that there is a pronounced thinning of sediments in the White River Dome area (north central) indicating that the structure was growing and affecting sedimentation during Mesaverde time. The map of S3-S4 interval thickness (Figure 14) shows sediment thinning over both the White River Dome and the Piceance Creek (center) structures, indicating that both were active during wasatch deposition. When searching for productive hydrocarbon traps, the timing of structure formation can be an important parameter to consider in respect to the timing of hydrocarbon generation and migration.

The prevalent structure in the White River Dome field is a graben feature

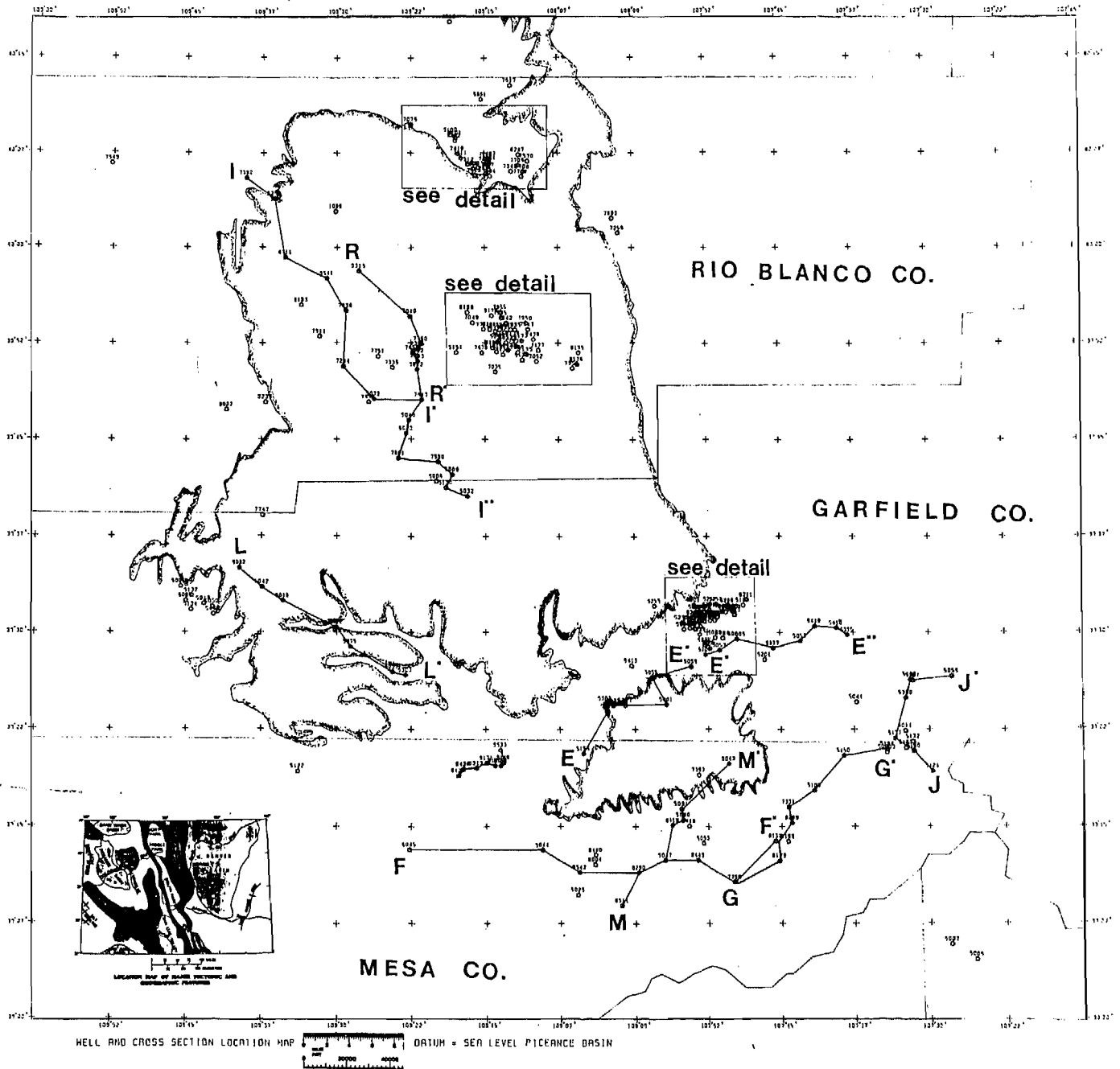
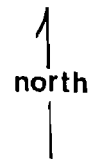


FIGURE 7:

Well and Cross section location map showing the top of the Wasatch Formation outcrop for reference. Detailed sections are available for the White River Dome (top center), Piceance Creek (center), and Rulison (lower right) fields where an abundance of data exists.

LEGEND

-  Fault - ticks on down-thrown side
-  1234 Data location w/ API number



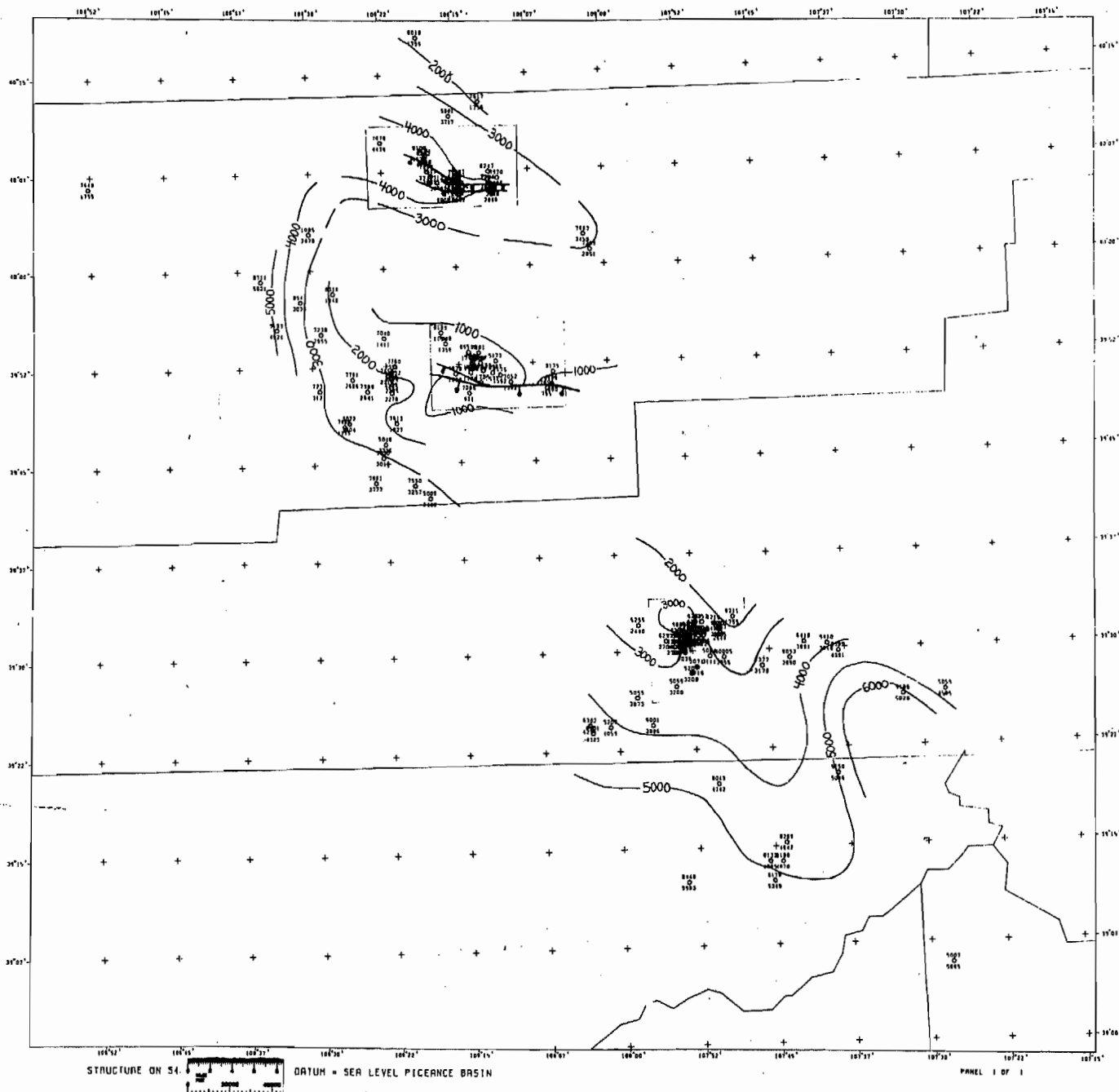
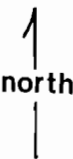


FIGURE 8:

Structure on the S4 horizon. Contours show elevation (feet) above mean sea level. Note that the fault in the Piceance Creek field cuts across the curved hinge of the antiform.

L E G E N D

-  Fault - ticks on down-thrown side
-  1234
Data location w/ API number
-  north

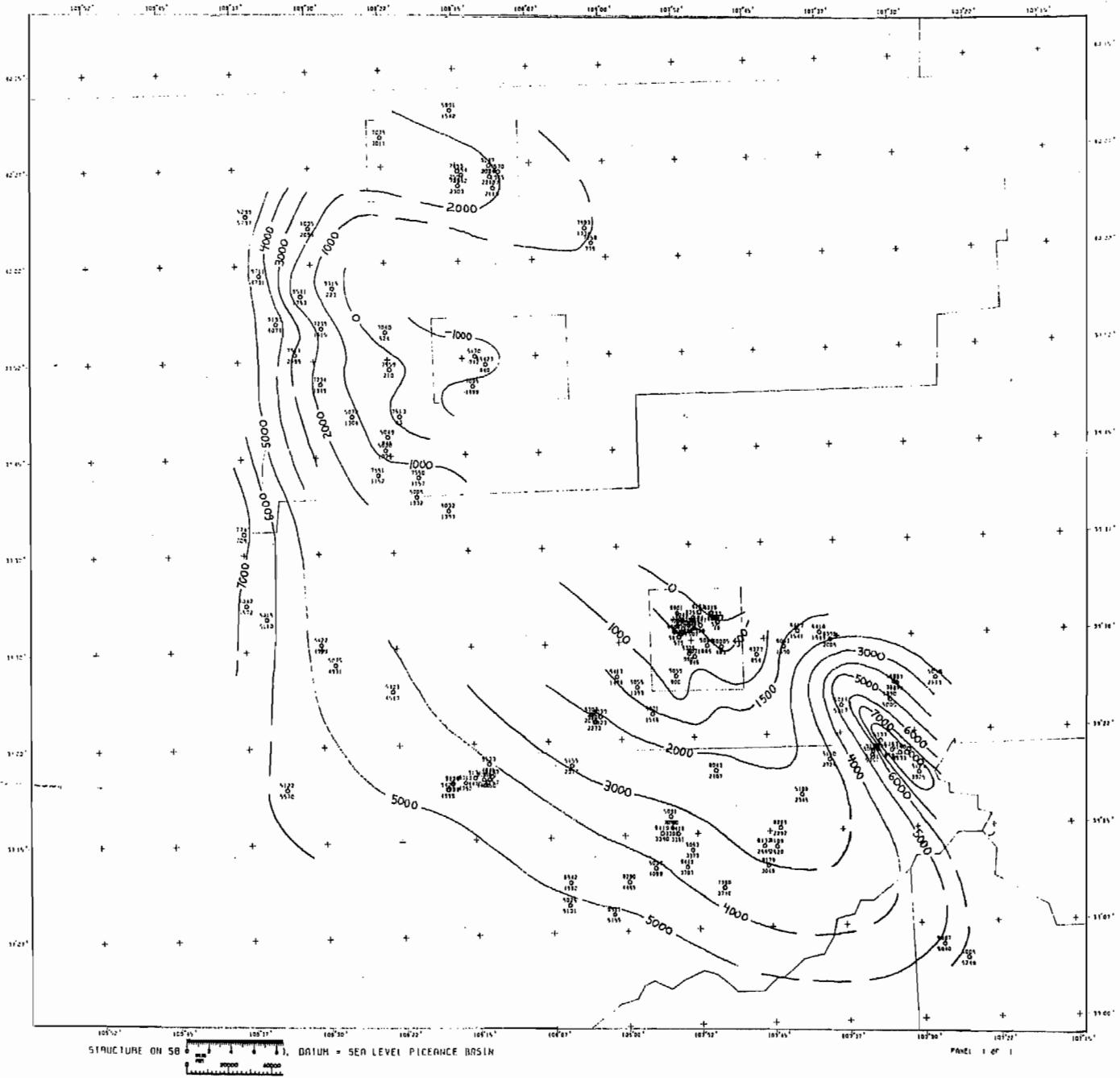
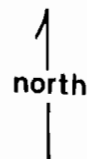


FIGURE 9:
 Structure on the S8 horizon. Contours show elevation (feet) above mean sea level.

L E G E N D



Fault - ticks on down-thrown side



Data location w/ API number

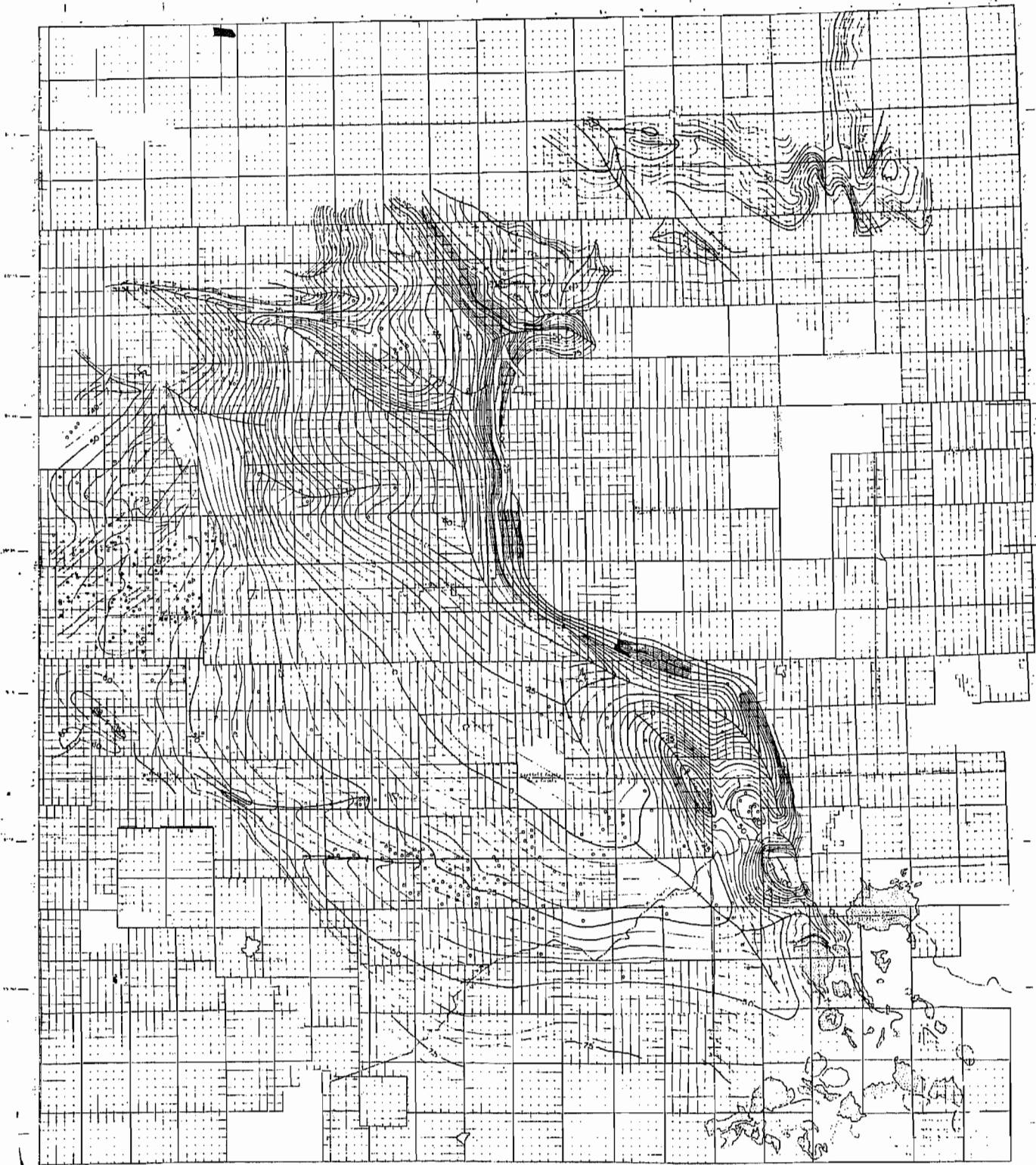
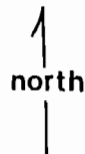


FIGURE 10:

Structure on top of the Rollins sandstone (?), base of the Williams Fork formation, Mesaverde Group. Contours show elevation (feet) above mean sea level.

L E G E N D

-  Fault - ticks on down-thrown side
-  1234 Data location w/ API number



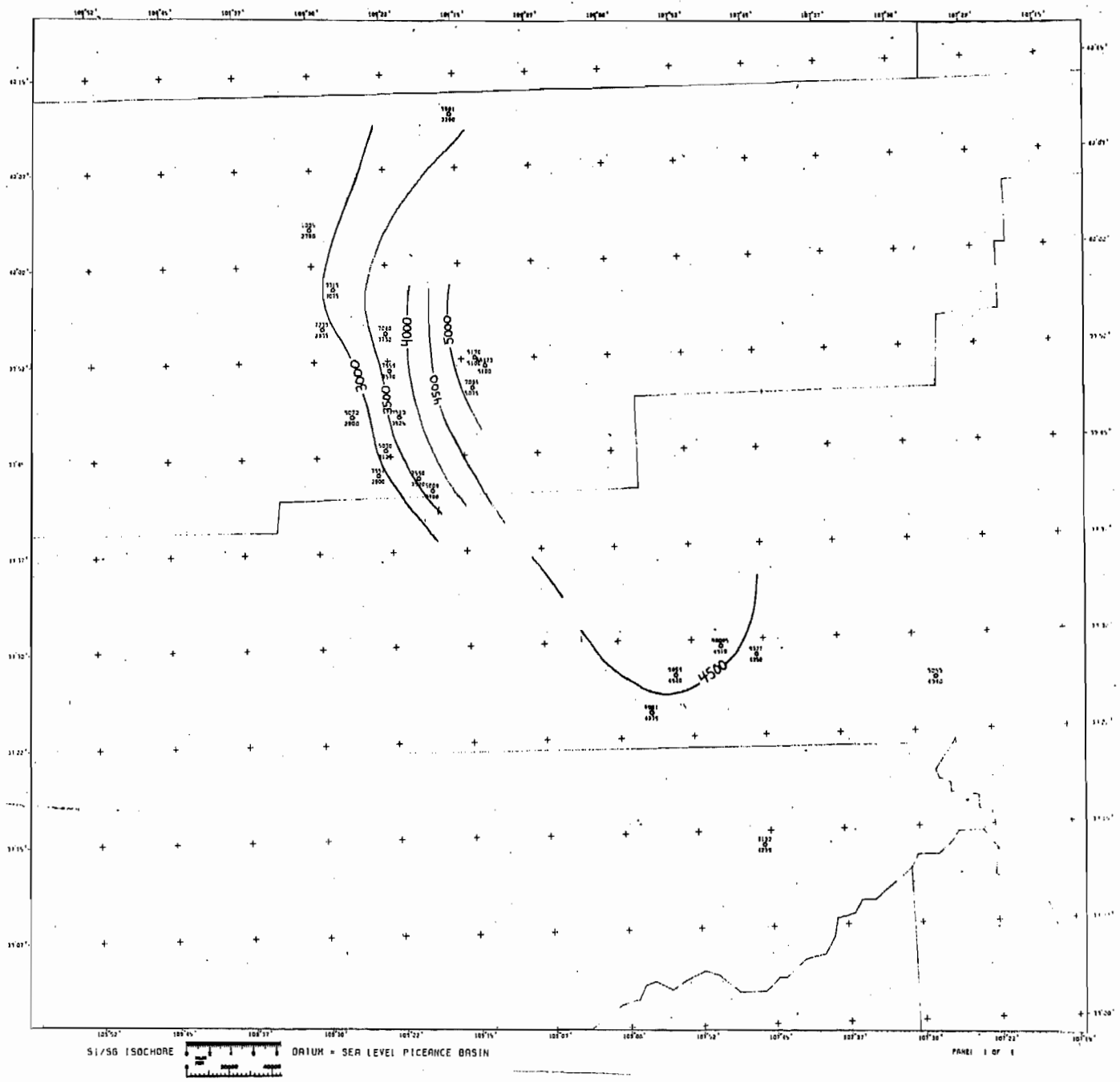
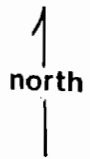


FIGURE 11:

Thickness of the S1/S6 interval (approximately the Wasatch formation). Contours show thickness (feet). Note that the deposits are more areally confined than those in figure 12.

L E G E N D



Fault - ticks on down-thrown side



1234
Data location w/ API number

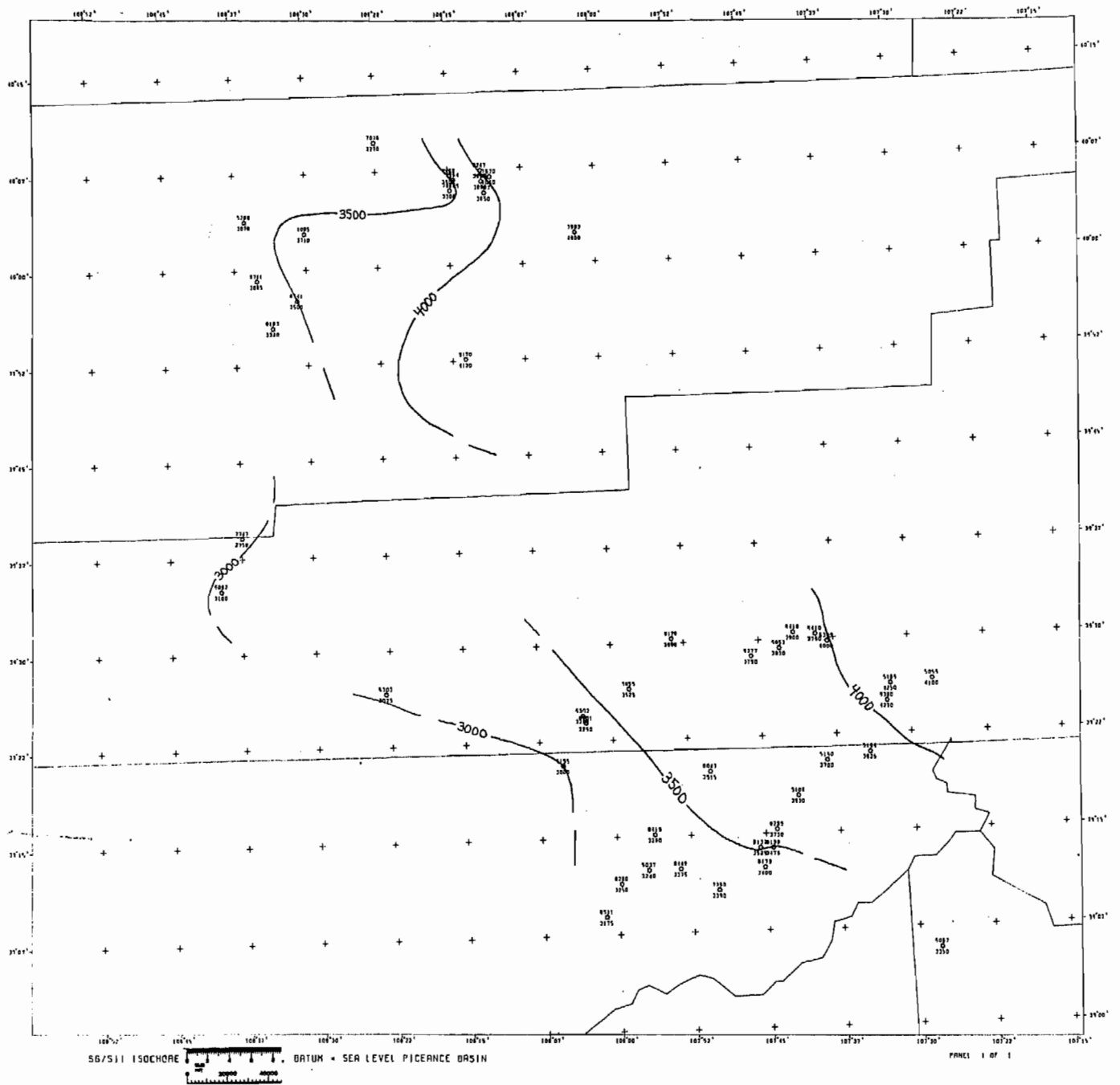
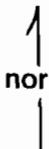


FIGURE 12:

Thickness of the S6/S11 interval (approximately the Williams Fork formation). Contours show thickness (feet). Note that the accumulations do not reflect present day basin shape.

L E G E N D

-  Fault - ticks on down-thrown side
-  1234 Data location w/ API number
-  north

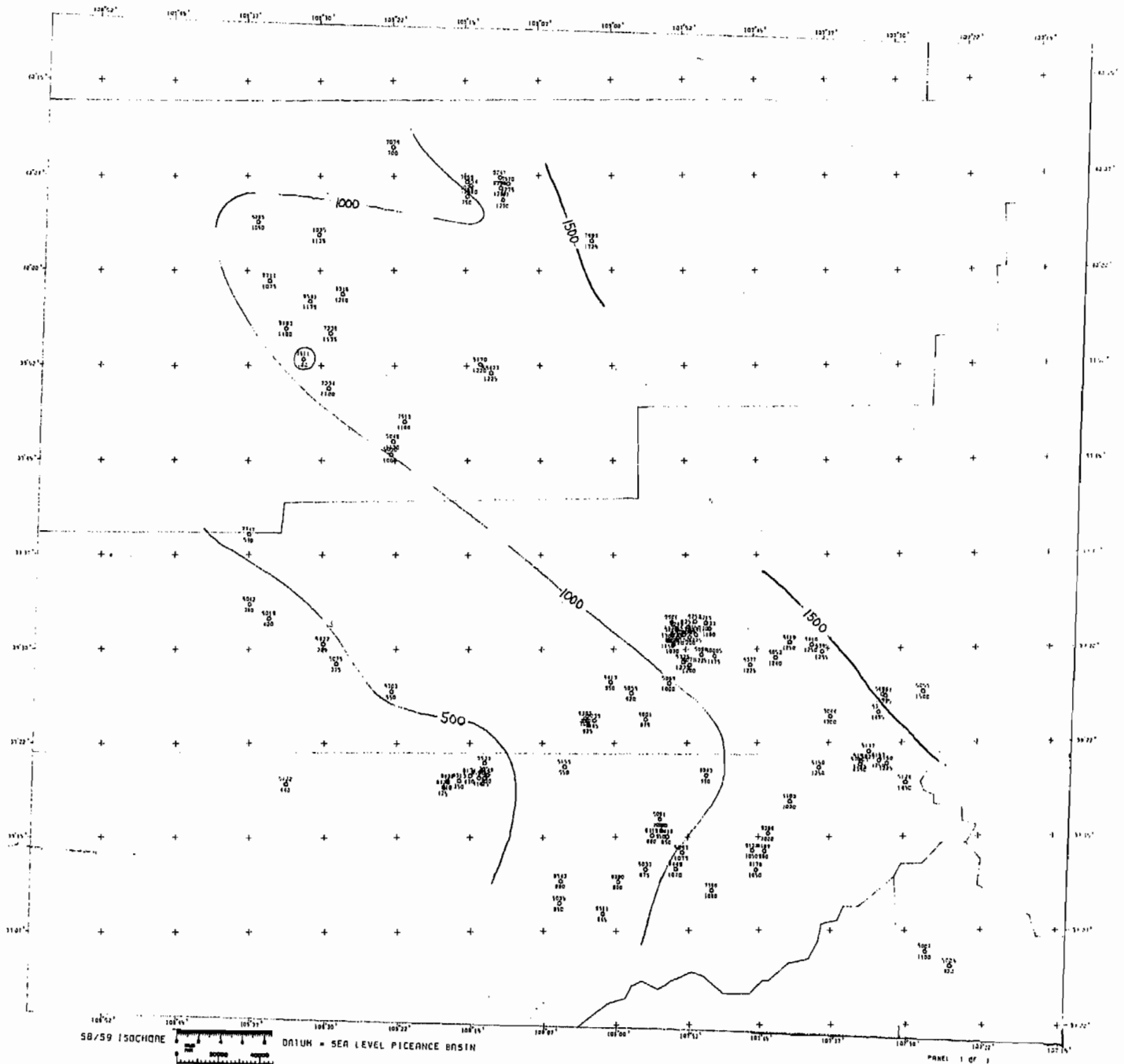
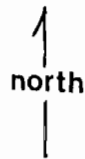


FIGURE 13:

Thickness of the S8/S9 interval.
 Contours show thickness (feet). Note
 the anomalous thinning over the White
 River Dome area (north center) which is
 indicative of structural activity during
 deposition of this interval.

L E G E N D



Fault - ticks on
 down-thrown side



1234
 Data location
 w/ API number

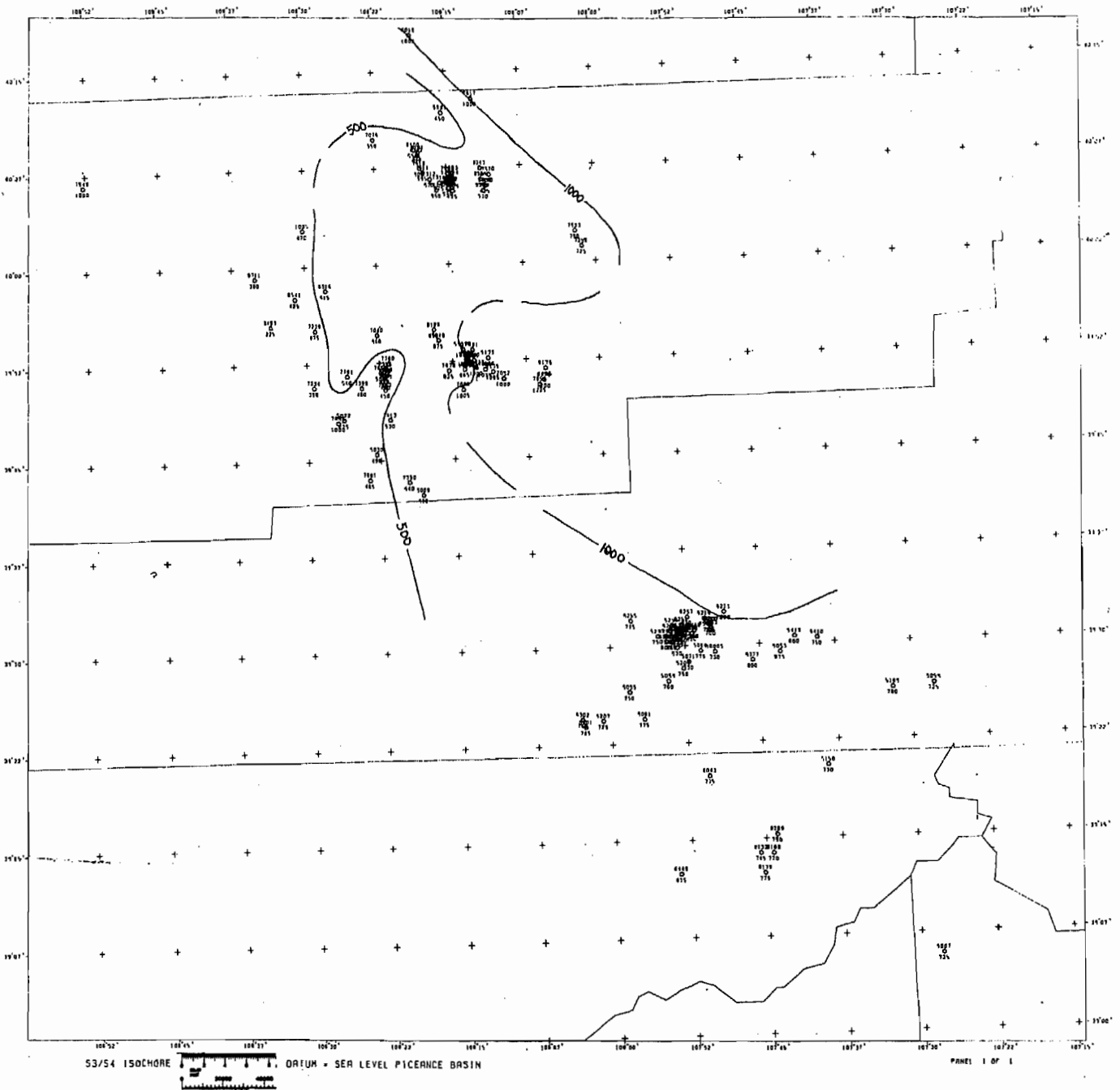


FIGURE 14:

Thickness of the S3/S4 interval. Contours show thickness (feet). The anomalous thing over the Piceance Creek area (center) and the White River Dome area (north center) is indicative of structural activity during deposition.

L E G E N D

-  Fault - ticks on down-thrown side
-  1234 Data location w/ API number
-  north

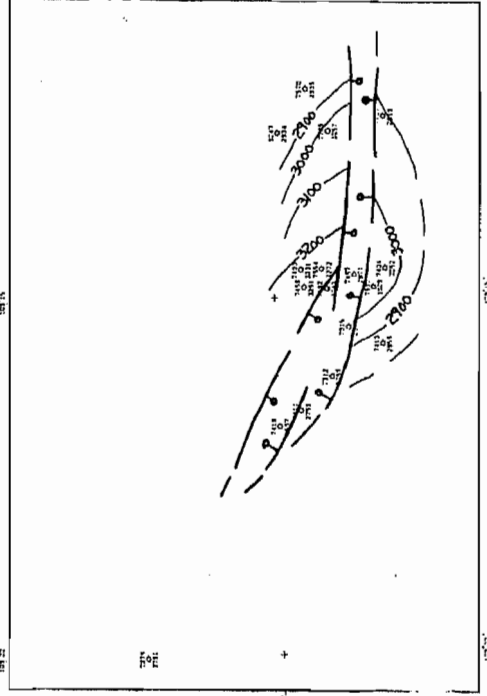
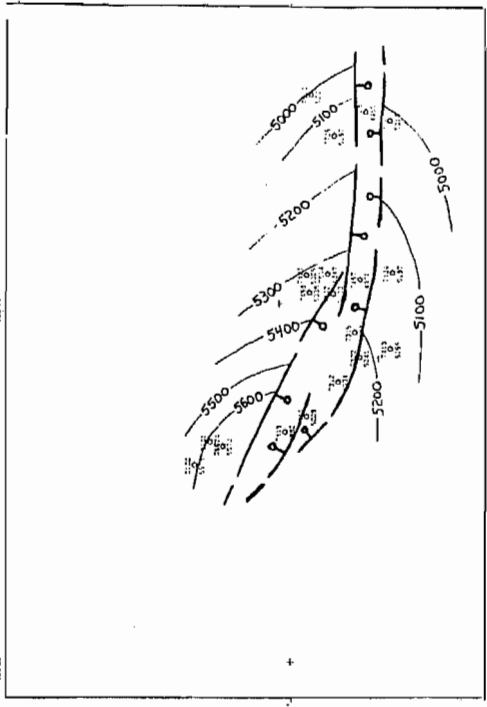
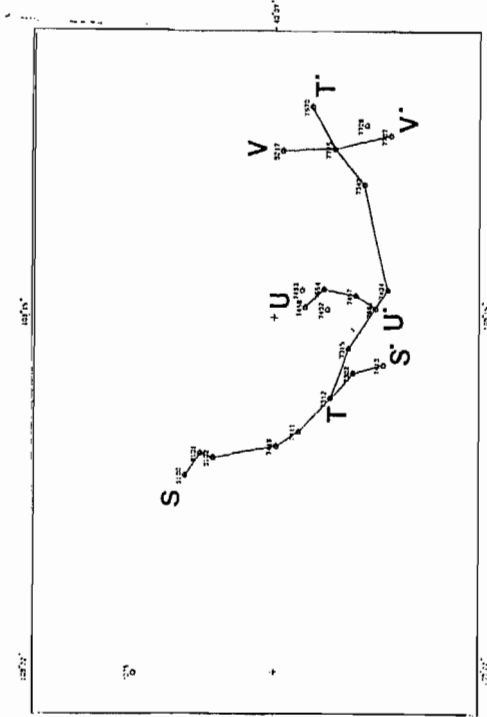


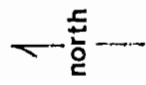
FIGURE 15:

Detail of White River Dome area. Contours show elevation (feet) above mean sea level. "A" shows the location of cross section through the field. "B" shows the structure on the S2 horizon. A graben feature dominates the area and is probably more complex than shown. "C" shows the structure on the S4 horizon. Note the closure on the southern most block which was not evident in "B".

L E G E N D

Fault - ticks on down-thrown side

1234 Data location w/ API number



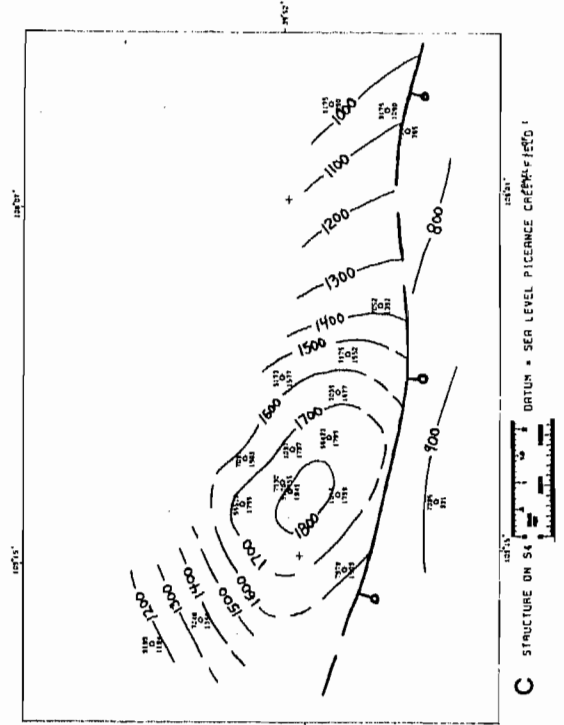
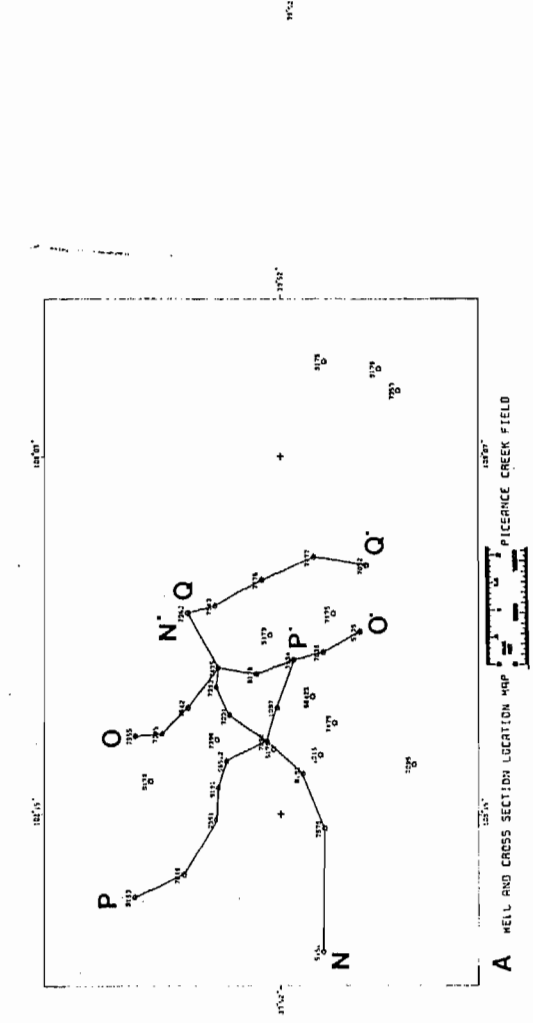
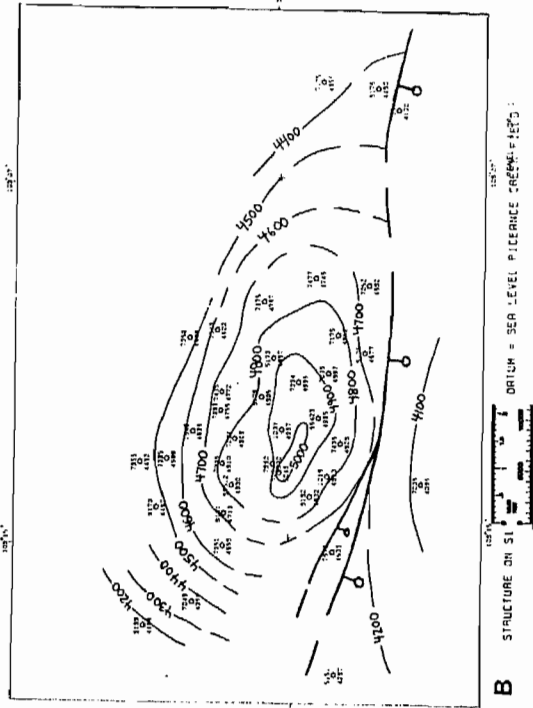
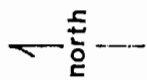


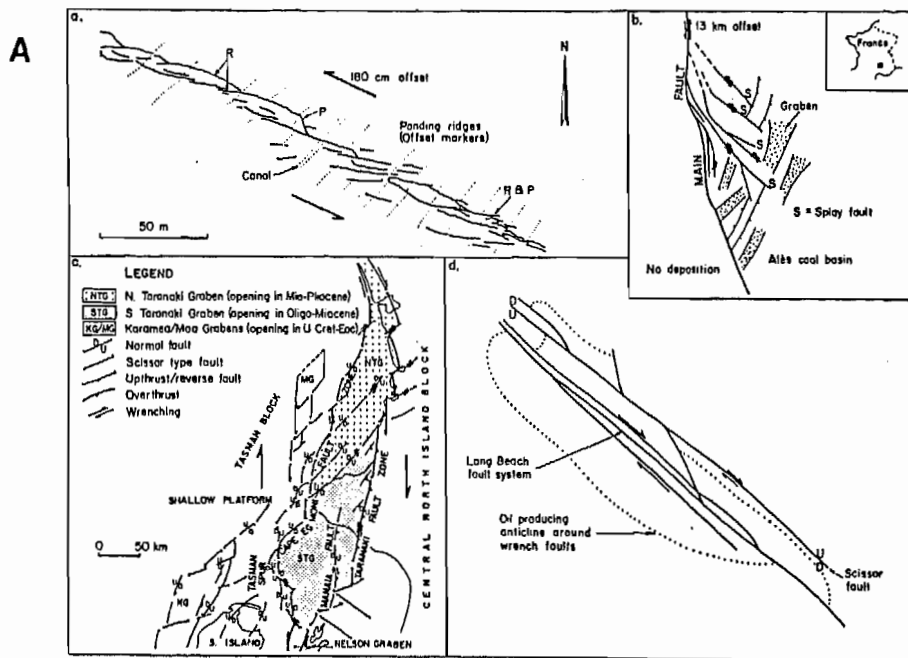
FIGURE 16:

Detail of the Piceance Creek area. Contours show elevation (feet) above mean sea level. "A" shows the location of cross sections constructed through the area. "B" shows the structure on the S1 horizon. This geometry is similar to a "trap door" structure and implies the existence of deep seated strike-slip faulting. "C" shows the position of the fault at the far right in both "B" and "C" is locked between two wells indicating that the fault is nearly vertical through the 3000' section between horizons S1 and S4.

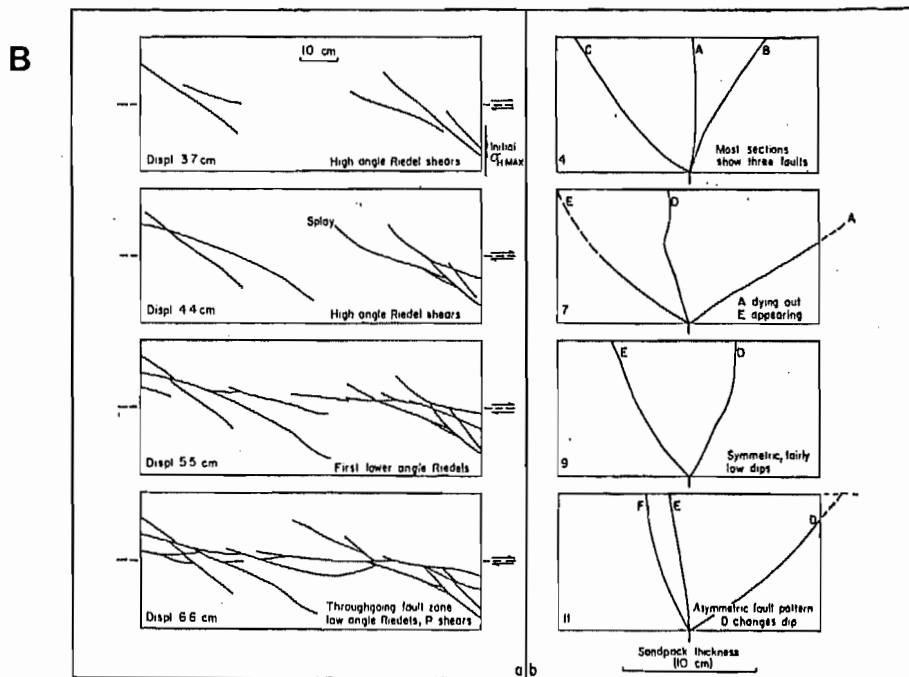
L E G E N D

-  Fault - ticks on down-thrown side
-  1234 Data location w/ API number





Natural examples of wrench fault patterns. (a) Riedel and P shears in the Dasht-e-Dayaz fault zone, Iran (after Tchalenko 1970). (b) Splay faults in the Alès coal basin, France (after Arthaud & Matte 1977). (c) En échelon shears showing characteristic scissor faulting in the Taranaki graben, New Zealand, where wrenching post-dated graben formation (after Pilon & Wakefield 1978). (d) Seal Beach oilfield, on the Newport-Inglewood trend, California (after California Division of Oil and Gas 1960).



Experimental results in Case C, pre-stressed with σ_1 perpendicular to the basement fault. (a) Evolution of the fault zone. (b) Series of sections from a separate experiment; sections are 10 cm apart.

FROM: NAYLOR, M.A., ET AL, 1986.

FIGURE 17:

Anatomy of a flower structure. "A" shows the plan view of actual fault zones associated with strike-slip displacement. "B" shows both plan and associated cross section views of a modeled flower structure. The term flower structure is descriptive of the near surface bifurcation of the fault apparent in cross section.

which is situated along the crest of the dome (see Figure 15). This implies the formation of the graben is directly related to tensional forces created at the crest during the formation of the dome structure. In Figure 15 note that the western half of the graben trends NW-SE while the eastern half trends E-W. The structure is probably considerably more complicated than is shown, and may be only a part of a much larger feature. For instance, Granica (1980, see Figure 10) illustrates a similar feature oriented NW-SE just to the south of the one shown in Figure 15. Also the structure appears to change with depth: Figure 15b shows the structure on S4 (which is within the Wasatch Formation), and in Figure 15c (which is within the Williams Fork Formation) a pronounced doming on the southern most block (south central) appears near well 7404 which was not present in Figure 15b. The time of formation of this dome was in part during Mesaverde Group time as is evident by the rapid thinning of the S8/S9 interval as shown on cross section T-T' (see Appendix A). This thinning appears not to be just truncation of the top of the S8/S9 interval but rather a relative lack of deposition during the entire interval.

Figure 16 shows that the prevalent structure of the Piceance Creek field is also a dome, or antiform, and is bound on the south by a single normal fault. The geometry of this structure is commonly referred to as a "trap door" structure, and is usually associated with strike-slip displacement in a basement fault. If indeed this feature is related to basement faulting then the potential for the existence of several similarly productive traps in the area significantly increases.

There are several lines of evidence to suggest that the structure shown in Figure 16 is associated with a much larger fault system along which a significant amount of strike-slip fault movement has taken place. First, the way the fault changes dip with depth suggests that it is not merely a normal fault but part of a "flower structure" which is the term used to describe the vertical profile of the large strike-slip fault systems associated with trap door structures (see Figure 17). The Geologic Map of Colorado (Tweto, 1975, see Appendix C) shows the existence of an antiform bound on the south by a large normal fault which is parallel to, and located approximately 1 to 2 miles north of the similar configuration shown in Figure 16b. Assuming that the two are related, the fault trace at the surface (Tweto, 1975) is displaced southward 1 to 2 miles during a vertical descent of 3000 feet to its new position shown in Figure 16b. This is similar to what might be expected of a normal fault. However the fault trace then appears to become nearly vertical during an additional 3000 foot vertical drop. Figure 16c shows the structure on a horizon which is, 3000 feet below the horizon in Figure 16b, and 6000 feet below the surface. The location of the fault in Figures 16b and 16c locked between the wells 4190 and 4480 (lower right hand corner), attesting to the near vertical attitude of the fault trace between these two horizons. A simple normal fault which is unrelated to a flower structure should show a continuous decrease in dip with depth rather than an decreasing dip changing to an increasing dip as is indicated here. The fault trace shown in Figure 16 is located directly

below, and is coincident with a semi-linear portion of Piceance Creek. It is suggested that a vertical element of the flower structure proceeds from its location in Figure 16 directly to the surface. Figure 17b shows cross section and plan views of flower structure geometry.

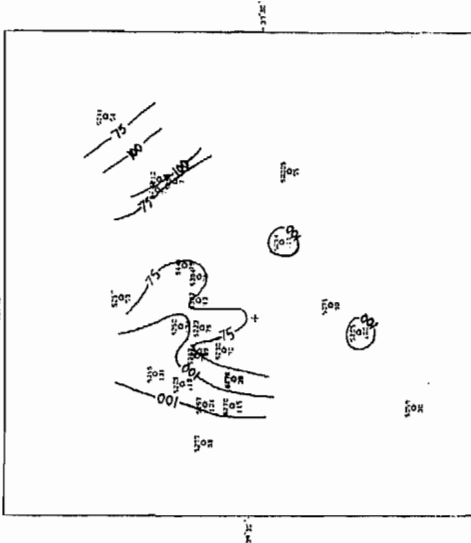
Second, the fault trace and the hinge of the antiform cross each other in a weaving fashion (see Figure 8). The trap door geometry, along with the interweaving of the antiform hinge and the fault trace are indicative of lateral displacement fault systems. In these systems movement along the fault causes opposite sides of the fault to alternately form dome like structures or en echelon antiforms.

Third, the orientation of the fault in Figure 16 is conspicuously parallel and in line with the WNW-ESE trending section of the Grand Hogback (see Appendix C). Flower structures represent surface layer reactions to deep basement strike-slip fault movement, and the Grand Hogback does represent a very definite basement feature. The alignment of the features suggest a common origin.

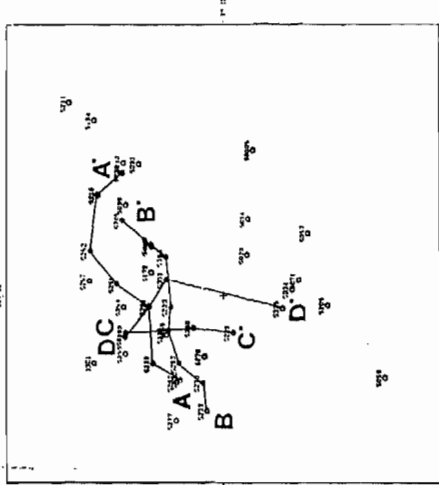
Finally, interpretation of synthetic aperture radar imagery of the area (Appendix C) implies the existence of a continuous zone of faulting between Grand Hogback and the fault shown in Figure 16. The Geologic Map of Colorado (Tweto, 1974) suggest that the antiform in Figure 16 is part of a longer anticlinal structure which is bound on its southern margin by two separate normal faults near either end. This suggests that the antiform and the fault(s) are only coincidentally parallel and proximal to each other because the antiform is indicated to exist were faulting does not. However, radar imagery suggest the the fault trace is continuous along the length of the indicated fold (the trace does however fade slightly in the middle). These facts suggest a direct association between faulting and the antiform even though the fault dips away from the antiform.

While the presents of strike slip faulting in the Piceance Creek area is at this point totally hypothetical, the implications of this theory are far reaching. Immediately northward of this area there are several faults shown on the Geologic Map of Colorado (Tweto, 1975) which parallel and appear to be related to the faulting shown in Figure 16. Under normal circumstances these faults are of potentially little importance, but considering that strike slip movement may be involved then each of those fault traces could be associated with a trap door structure like the one responsible for the existence of the Piceance Creek field.

Figure 18d shows the structure on a horizon within the Williams Fork formation and indicates that the Rulison field is located on the nose of a northward plunging anticline. This broad and gentle structure, which is not likely to be associated with significant amounts of fracturing, changes significantly at shallower depths. Figure 18c shows the structure on a horizon within the Wasatch Formation. Note the development of the second order folds on the northwest flank of the nose. These compressed,



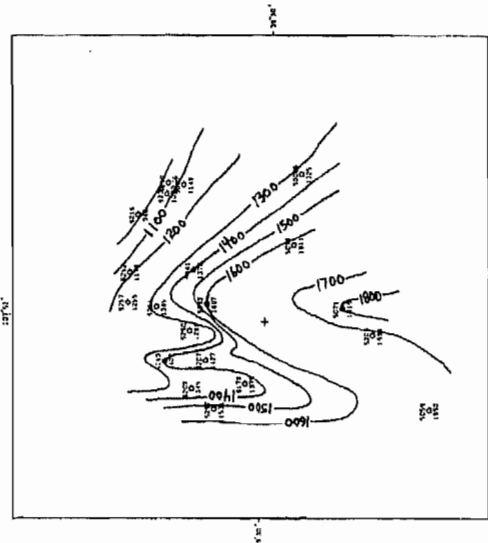
A 8D% CLEAN NET SAND S3/S4 ORTUM - SEA LEVEL RULISON FIELD



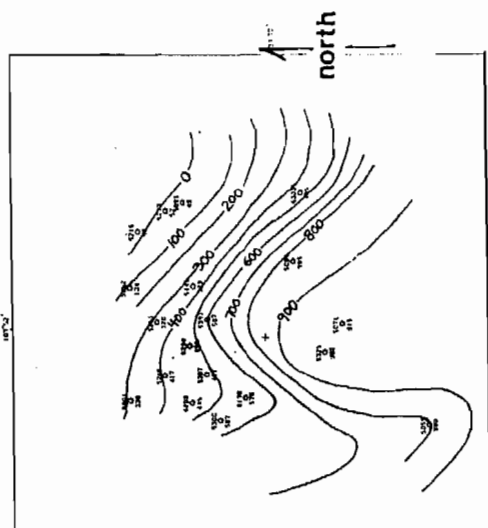
B WELL AND CROSS SECTION LOCATION MAP

FIGURE 18:

Detail of Rulison field area. "A" shows the summed thickness of sand in the S3/S4 interval. The bifurcation and curvilinear trends of thick sand are characteristic of fluvial deposition. "B" shows the location of cross sections constructed through the area. "C" shows the structure on the S6 horizon. Note the second order "kink" folds developed on the northwest flank of the north-south trending anticline. "D" shows the structure on the S8 horizon. Notice that the northwest flank of the anticline is not kink folded at this depth, but is anonymously shaped.



C STRUCTURE ON S8 ORTUM - SEA LEVEL RULISON FIELD



D STRUCTURE ON S6 ORTUM - SEA LEVEL RULISON FIELD

LEGEND

- Fault - ticks on down-thrown side
- 1234 Data location w/ API number

parasitic folds are much more likely to be fractured than the broader, first order anticlinal nose. The conclusions drawn from a reservoir modeling study by Mercer, et al (1986) concur with these results in that gas migration from the Navy Oil Shale Reserve no. 3 (located immediately to the north and west of Rulison Field) southwest into the producing Rulison field was noticed to occur for Wasatch reservoirs but not for Williams Fork reservoirs. Also of note is that the wells with the most favorable production character in the Rulison field are located in the Northwest corner of the field (personal commun. J.C. Mercer, 1986).

Reservoir Distribution

Data on reservoir distribution for each well consists of sand body thicknesses found in the intervals formed by adjacent pairs of the horizons (S1-S11). These data serve as a basis for identifying which intervals contain the most reservoir rock. The abundance of reservoir rock in turn gives us an idea of the extent of possible in situ resources, but no indication of total producible reserves or production characteristics. Reservoir distribution data was mapped to check for patterned reservoir variations within the intervals. The results suggest (1) that large scale depositional trends do exist in some intervals but cannot be accurately located because of sparse data, and (2) that the average interval thickness between adjacent horizons is too large to resolve individual sandbody/reservoir geometry.

Maps of reservoir distribution data show significant variation of sandbody content over short distances within intervals, and only vaguely locates general directional trends of ancient river systems. Figure 18a shows the total sand thickness (sand isolith) for the interval between the S3 and S4 horizons in the Rulison field area. The pattern of thick sand (shaded) can be thought of as indicating the shape and location of an ancient river channel. Its geometry is exactly the pattern one would expect to find in fluvial deposits. Note the scale of the curvature, bifurcation, and width features of the thick sand. In areas where data points are considerably more scarce these variations would not be discernable. Also note that a general orientation of ancient river trend is indicated as being from the south to the north, which is in agreement with the reconstruction of ancient Wasatch geography shown in Figure 5 (McGookey, et al, 1975). The fact that a thousand foot section of rock (S3/S4 interval) reveals depositional trends suggests that clusters of individual sandbodies form these trends, and sand bodies may intercommunicate to form a large reservoir. In other areas where data is abundant, reservoir patterns in map view are much more complex, and it appears that thinner intervals of analysis would more accurately resolve individual reservoir geometries there.

Of interest is that the depositional trends coincident with the the graben feature in the White River Dome area are notable absent. This suggests

faulting occurred after deposition even though uplift was contemporaneous with deposition (see Figures 13, and 14).

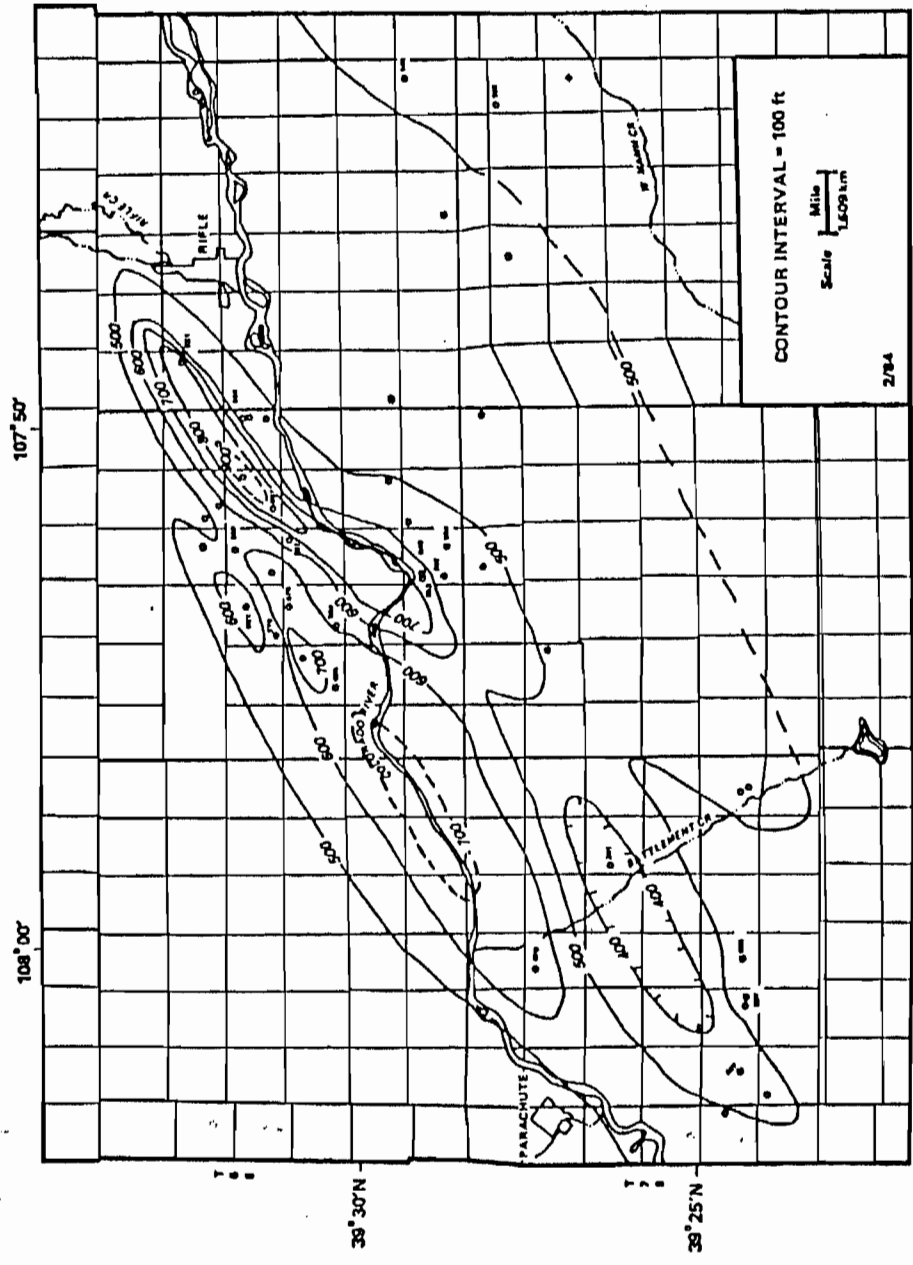
Large scale depositional trends were noticed to exist in Williams Fork rocks. The sand isolith maps of the intervals S9 to S10 and S10 to S11 can be contoured to be in good agreement with ancient Mesaverde geography shown in Figure 3. The 200 foot isolith on these maps defines a cobweb pattern of thick sand trends spread over the basin. At the center of the basin the trends are oriented E-W (east to west). This orientation swings to ENE-WSW (east-northeast to west-southwest) in the southeast part of the basin, and to WNW-ESE in the northwest part of the basin. These results agree with the results presented by Peterson (1984). Figure 19 shows the sand isolith map compiled by Peterson (1984) over an interval roughly equivalent to the S9/S10. A large scale WSW-ENE depositional trend is seen to intersect the Rulison field.

Additional isolith maps are not presented because they can be contoured a lot of different ways. Isolith maps are inherently subjective requiring interpretation during contouring because the contours are not on a tangible "surface" but along a statistical boundary. Additionally, the data points locating these trends becomes widely spaced revealing only a very general picture compared with the detail suggested by Figure 18a. The values on all isolith maps show a wide range within each horizon suggesting that there are areas of thick, clean reservoir rock adjacent to areas of very poor reservoir rock within each horizon.

Numeric summary of mapped data helps to better picture actual reservoir properties. Tables 1 and 2 give an indication of the variability of reservoir rock distribution. Table 1 shows some descriptive statistics of the wells' sand content for each interval in the Rulison area. Comparison of the maximum and minimum observed values shows a large difference in the amount of sand a well can intersect. Table 2 shows the distribution of individual sand body thicknesses for each interval in the Rulison field area. Note that the standard deviation of each distribution is usually greater than the mean sand thickness, indicating a skewed distribution with its tail in the thick sand region (compare the average sand body thickness with the maximum sandbody thickness for each interval). The slightly different procedures of analysis responsible for the data in Tables 1 and 2 are instrumental in determining the meaning of conclusions drawn from the data.

VI. CONCLUSIONS

1) The correlations (S1-S11) trace differences in the rock inherent to the depositional processes active during sediment accumulation. This implies that different, and somewhat unique, reservoir properties exist within each interval.



Total "cleaner" sandstone isopach map in the fluvial zone of the Mesaverde group.

FROM: PETERSON, 1984.

FIGURE 19:

Sand isolith map of the "Fluvial Interval", Mesaverde Group rocks, Rulison field. Contours show thickness (feet). A regional trend of thick reservoir rock trending WSW-ESE intersects the Rulison field confirming similar independent results.

Table 1

NET SAND VALUES (> 80% CLEAN) OF EACH WELL IN RULISON FIELD AREA

INTERVAL	MEAN	SIGMA	MAX.	MIN.	N
S1/S2	46	34	71	22	2
S2/S3	89	54	359	17	40
S3/S4	80	34	148	7	26
S4/S5	78	32	156	17	22
S5/S6	181	79	418	52	21
S6/S7	137	57	236	48	15
S7/S8	118	62	237	16	20
S8/S9	214	82	385	20	18
S9/S10	288	83	454	187	9
S10/S11	146	65	210	79	3
S1/S6	332	.	332	332	1
S6/S11	923	65	970	877	2

Table 2

THICKNESS (FEET) OF SAND BODIES > 80% CLEAN IN RULISON FIELD AREA WELLS

INTERVAL	MEAN	SIGMA	MAX.	MIN.	N
S2/S3	4.4	3.2	12	1	29
S3/S4	6.5	6.9	46	1	558
S4/S5	6.7	18.3	311	1	300
S5/S6	7.6	15.7	311	1	446
S6/S7	7.2	8.2	70	1	294
S7/S8	11.3	12.5	72	1	202
S8/S9	9.5	9.4	52	1	390
S9/S10	6.5	16.9	308	1	369
S10/S11	5.7	10.1	72	1	66

- 2) significant changes occur in the volume of reservoir rock within an interval as a function of location.
- 3) Large scale reservoir trends appear to exist in some intervals but can only vaguely be outlined because of sparse data and the highly variable nature of the trend.
- 4) Clusters of sand bodies are responsible for the observed reservoir trends. This suggest that some prolific reservoir could actually be clusters of intercommunicating sand bodies.
- 5) Better resolution of sand body cluster geometry could be attained with relatively little effort by expanding the gamma ray traces of a chosen interval, performing a more detailed correlation, and then using the methods and computer codes developed in this study for analysis.
- 6) There is a strong structural influence on production phenomena in the Rulison Field.
- 7) Each of three major gas fields is associated with the occurrence of natural fracturing near structural highs.
- 8) Changes in structural geometry with depth are important within the formations of interest.
- 9) During the coarse of the study a significant base of data has been compiled which includes production data, geophysical well log data, completion report data, 1:250,000 scale topographic maps, and synthetic aperture radar imagery of the area.
- 10) The digital gamma radiation logs and the defined stratigraphy combine to form a useful data set on reservoir distribution.
- 11) SAR imagery is a potentially useful tool for the generation of prospects in the sediments of interest. Some of the lineaments observed on the imagery coincide with faults mapped on the Geologic Map of Colorado. Others are extensions of indicated faults or parallel them.
- 12) Several potential prospects could be generated from the assembled information, the details of which are beyond the scope of this paper.

VII. SUGGESTIONS FOR FUTURE WORK

Considering the assembled data, and what is known about the inherent difficulties involved in exploitation of the resource, several research projects are suggested which will meet with Western Gas Sands project goals to varying degrees. These suggestions are as follows:

- 1) Data on sand body distribution should be input to the LENDA computer code for estimation of reservoir rock volume, and to determine the location of sand body clusters most likely to form intercommunicating packages. A statistical approach to reservoir distribution analysis is recommended considering what is known about the reservoir variability within each interval. Geologically, the assembled base of data is particularly well suited for use in these calculations.
- 2) Detailed depositional analysis for the most productive intervals should be completed as part of a study on reservoir effects on production. Limiting this analysis to the major gas files may be a mistake considering that these fields are not separate from trends that extent across the basin.
- 3) Synthetic aperture radar imagery of the basin should be interpreted and field checked in a study of its usefulness as a prospect generation tool.
- 4) Future Extraction Section efforts should concentrate as much on reservoir modeling as on production modeling.
- 5) A field study of reservoir properties is warranted. The nature of potentially unique properties within in each intervals, and the internal geometry of sand body clusters should be investigated.
- 6) Considering the modeling capabilities available, an estimate of natural gas reserve is possible Any attempt at reserve potential estimations must necessarily include sound assumptions of geologic variables such as undiscovered structural features, basinwide overpressuring phenomena, etc. To reduce the scale of either a resource or reserve evaluation, the study could include a limited number of stratigraphic intervals, perhaps the two most productive intervals would be selected.
- 7) Continued upgrade of the existing data base could provide the public with a very useful tool for unconventional gas exploitation.

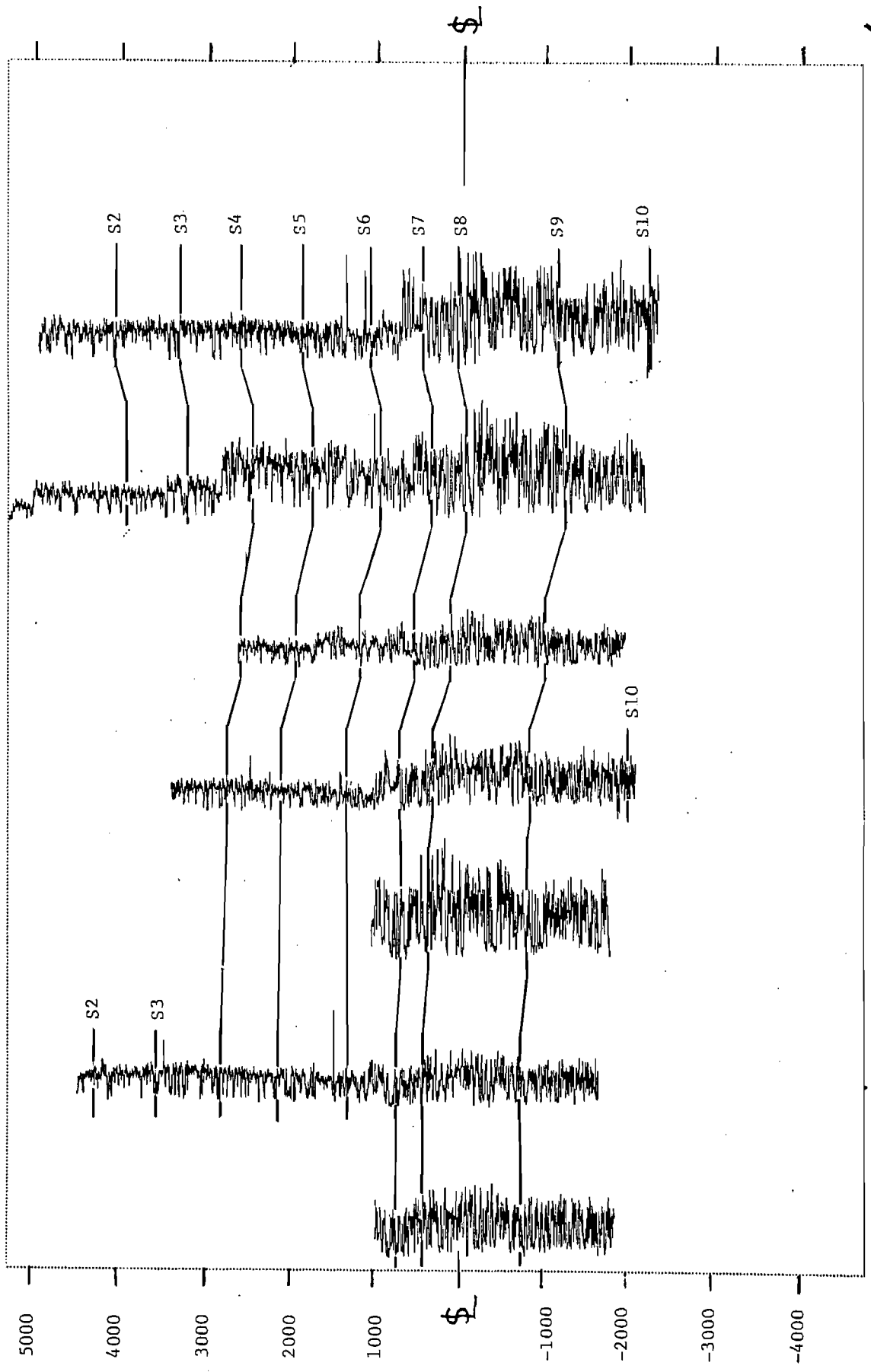
VIII. BIBLIOGRAPHY

- Donnell, J.R., 1961. "Tripartition of the Wasatch Formation Near DeBeque in N.W. Colorado", USGS Professional Paper No. 424B.
- Granica, M.P., and R.C. Johnson, 1980. "Structure Contour and Isochore Maps of the Non-marine Part of the Mesaverde Formation/Group, Piceance Creek Basin, Colorado", USGS Miscellaneous Field Investigations Map MF-1189, 1 sheet, scale 1:250,000, 10 page pamphlet.
- Lorenz, J.C., 1983. "Reservoir Sedimentology in Mesaverde Rocks at the Multiwell Experiment Site". Report to DOE/METC by Sandia National Laboratories under DOE contract No. DE-AC04-76DP00789.
- Mercer, J.C., J.R. Ammer, R.A. Moore, A.W. Layne, K-H. Frohne, 1985. "Study of Gas Migration from Naval Oil Shale Reserve No. 3 to the Rulison Field", U.S. Dept. of Energy Technical Note, DOE/METC/TN-85/3.
- McGookey, D.P., J.D. Haun, L. Attole, H.G. Goodell, D.C. McCubbin, R.J. Weimer, and G.R. Wolf, 1972. "Geologic Atlas of the Rocky Mountain Region", Rocky Mountain Association of Geologists, Denver, Colorado, pp 190-228.
- National Petroleum Council, 1980. "The Piceance Basin"; in Tight Gas Reservoirs, Part II: Unconventional Gas Sources, pp 1-65.
- Naylor, M.A., G. Mandl, C.H.K. Sijpesteijn, 1986. "Fault Geometries in Basement-induced Wrench Faulting Under Different Initial Stress States", Journ. of Structural Geology, Vol.8, No. 7, pp 737-752.
- Peterson, R.E., 1984. "Geological and Production Characteristics of the Nonmarine Part of the Mesaverde Group, Rulison Field Area, Piceance Basin, Colorado. SPE/DOE/GRI 12835. Presented at the Society of Petroleum Engineers/Department of Energy/Gas Research Institute Unconventional Gas Recovery Symposium, Pittsburgh, PA., 1984.
- Roehler, H.W., 1973. "Geologic Map of the Calf Canyon Quadrangle, Garfield County, Colorado", U.S.G.S. Geologic Quadrangle Map, GQ-1086.
- Yeend, W.E., and J.R. Donnel, 1968. "Geologic Map of Rulison Quadrangle, Garfield County, Colorado, U.S.G.S. Open File Map.

IX. APPENDIX A

Cross sections A-A' through V-V' constructed for correlation purposes. Plan view of cross section locations is shown in figures 7,15,16, and 18. Well traces are adjusted to sea level elevations, and the vertical scale is in feet relative to sea level. The API number and township, section, and range location is indicated for each well.

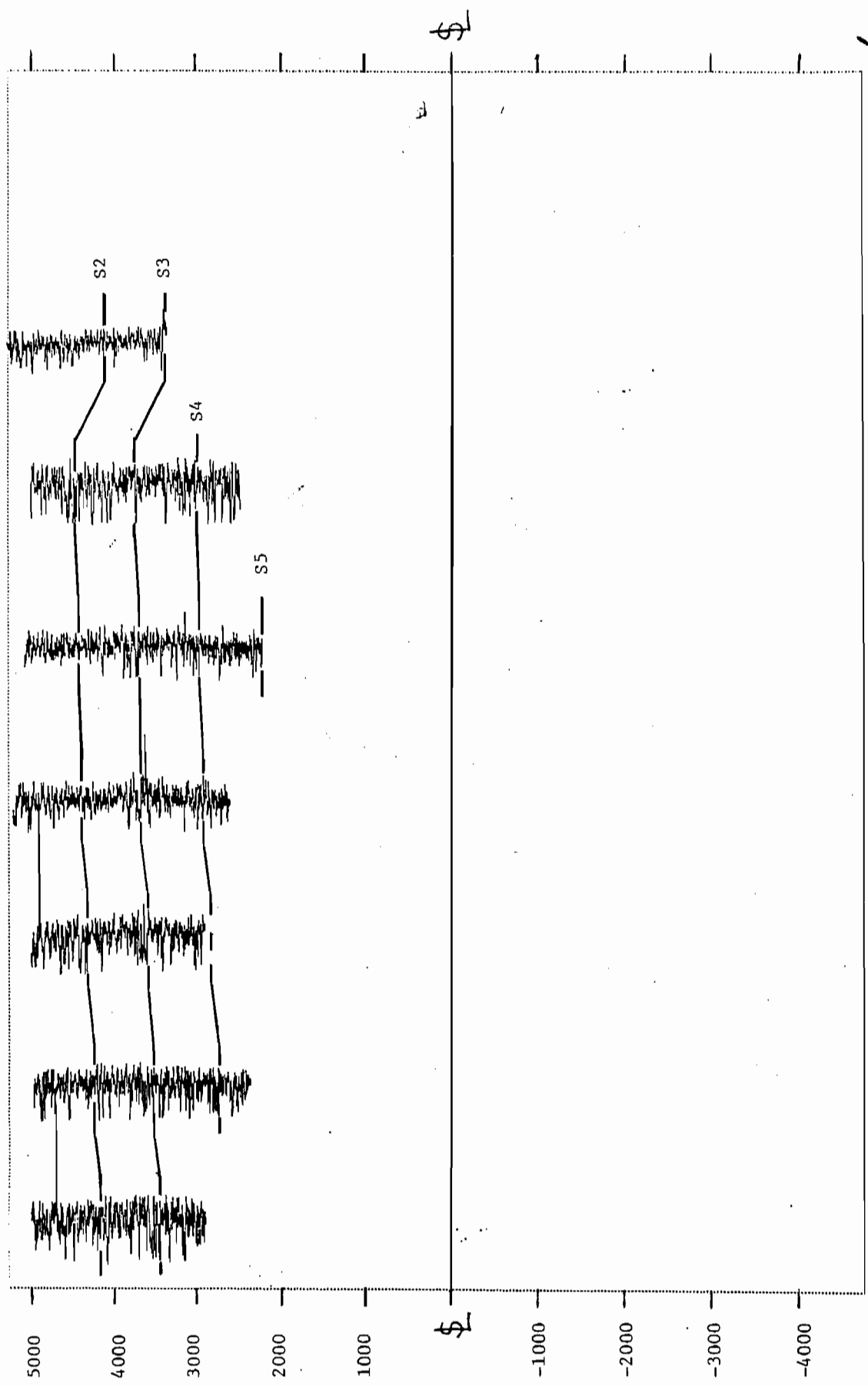
0504506300 S6/W94/20 0504506208 S6/W94/16 0504506231 S6/W94/15 0504506251 S6/W94/15 0504506252 S6/W94/11 0504506216 S5/W94/12 0504506233 S6/W94/13



A

A

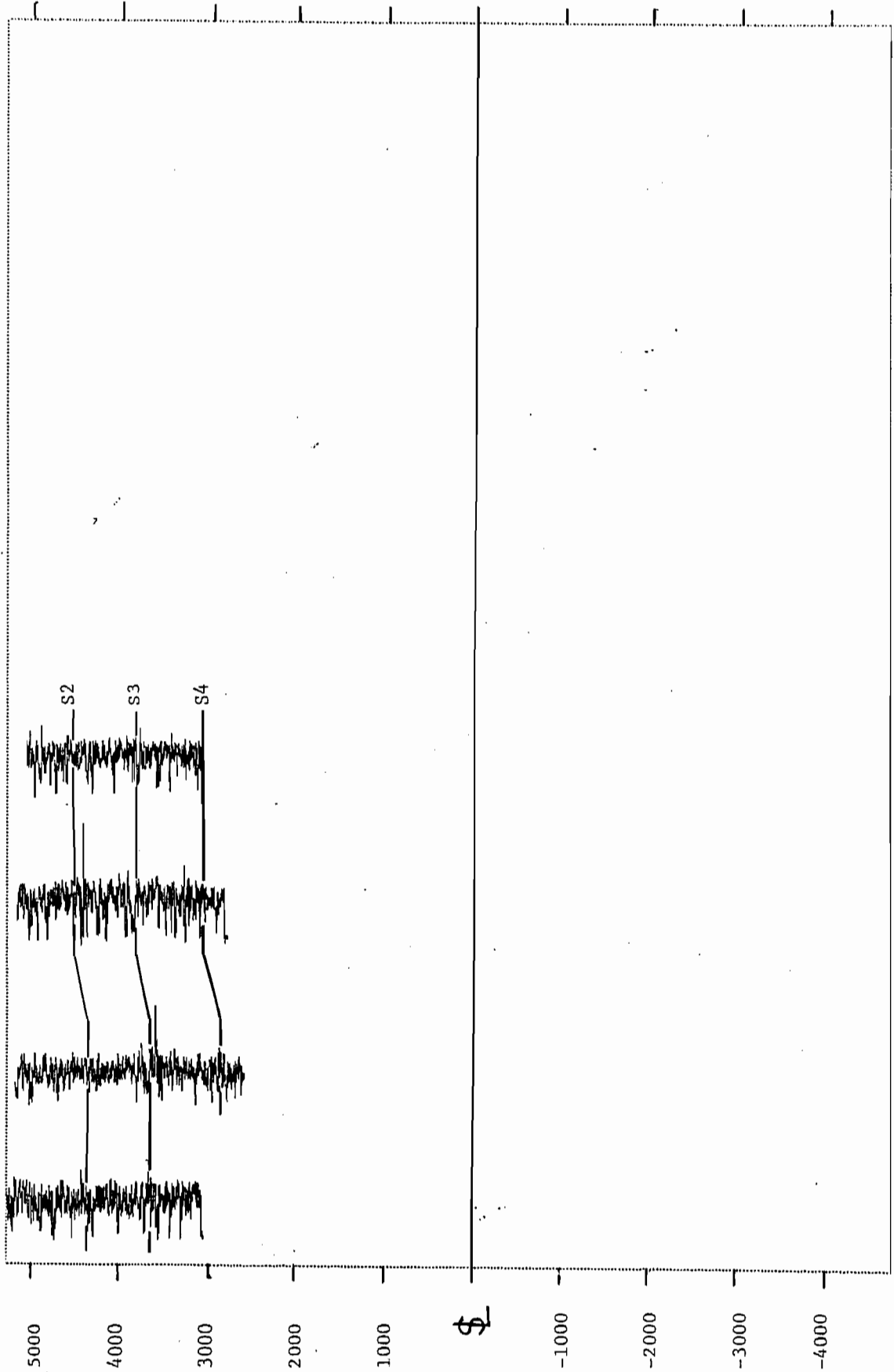
0504506298	0504506270	0504506283	0504506266	0504506229	0504506384	0504506206
S6/W94/20	S6/W94/20	S6/W94/21	S6/W94/21	S6/W94/22	S6/W94/23	S6/W94/14



B

B

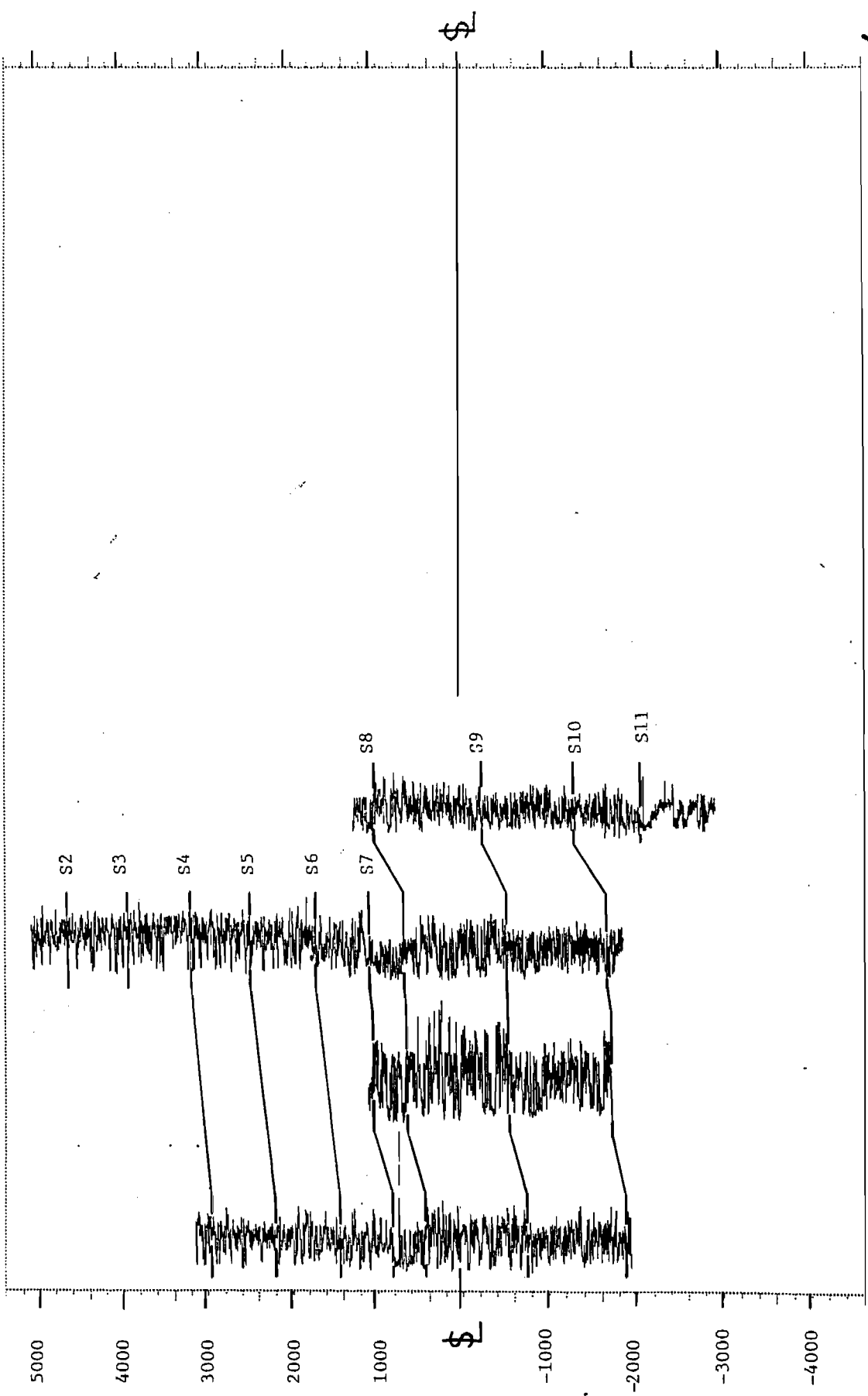
0504 506268 S6/W94/16 0504 506266 S6/W94/21 0504 506230 S6/W94/21 0504 506228 S6/W94/28



C

C

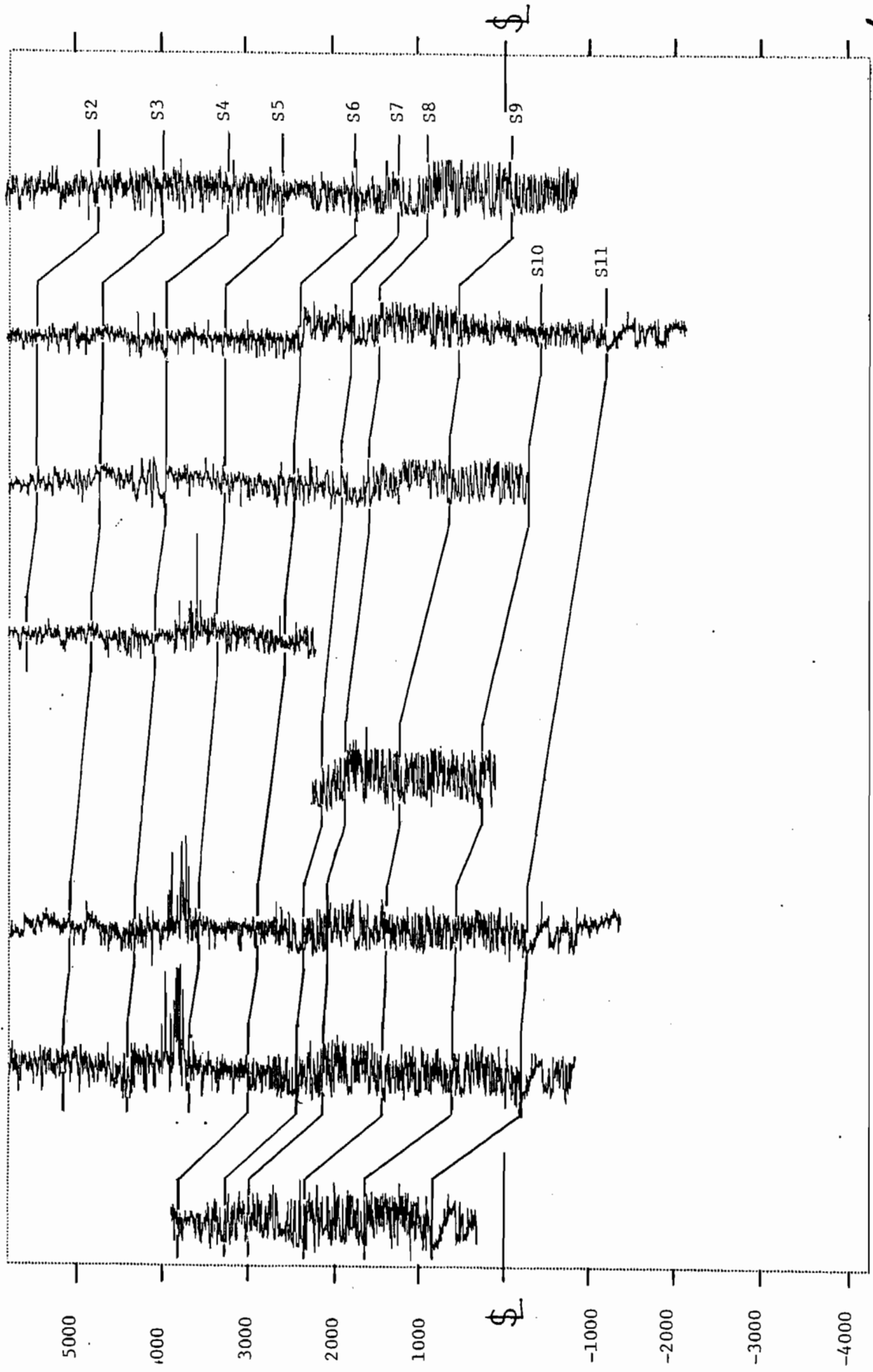
0504506249 0504506231 0504506393 0504506325
S6/W94/16 S6/W94/15 S6/W94/22 S6/W94/22



D

D

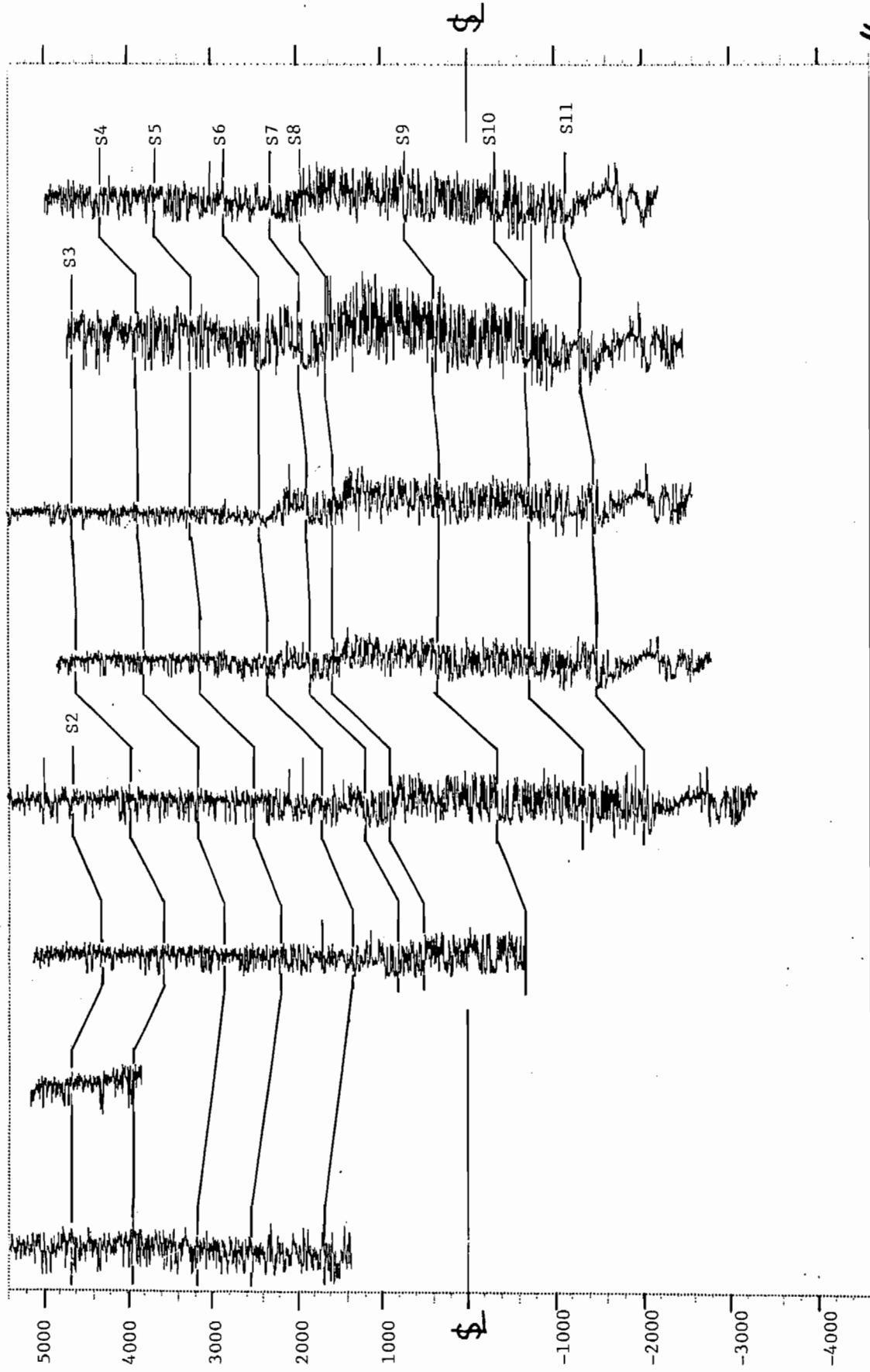
0507705155 S8/M96/15 0504506301 S7/M95/31 0504506302 S7/M96/25 0504505039 S7/M95/30 0504505207 S7/M95/29 0504506001 S7/M95/25 0504505055 S7/M95/14 0504505059 S7/M94/8



E

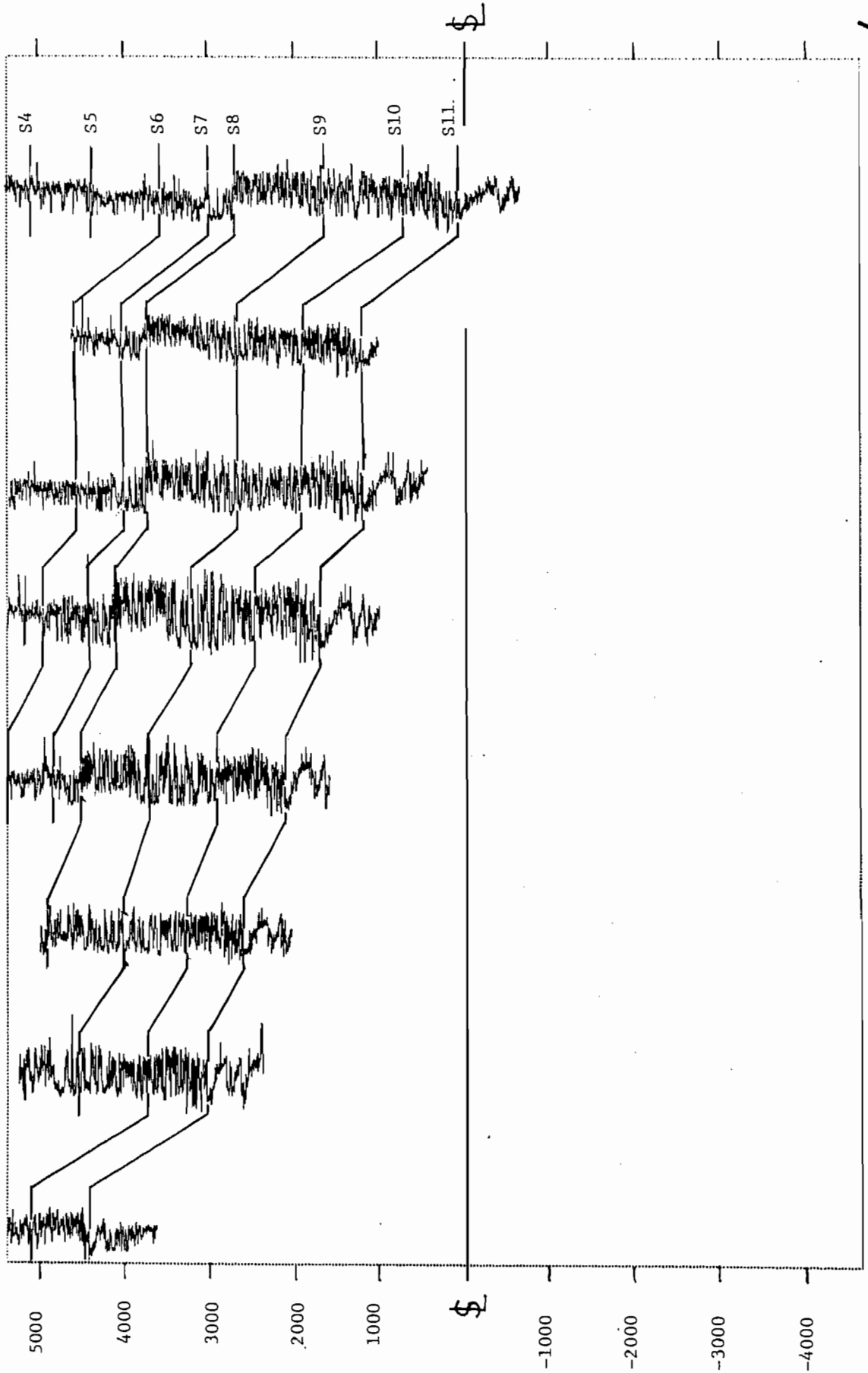
E

0504505206 S7/W94/3
0504506057 S6/W94/35
0504560005 S6/W93/30
0504506377 S6/W93/34
0504506053 S6/W93/36
0504506419 S6/W92/20
0504506410 S6/W92/22
0504506395 S6/W92/26



E " E

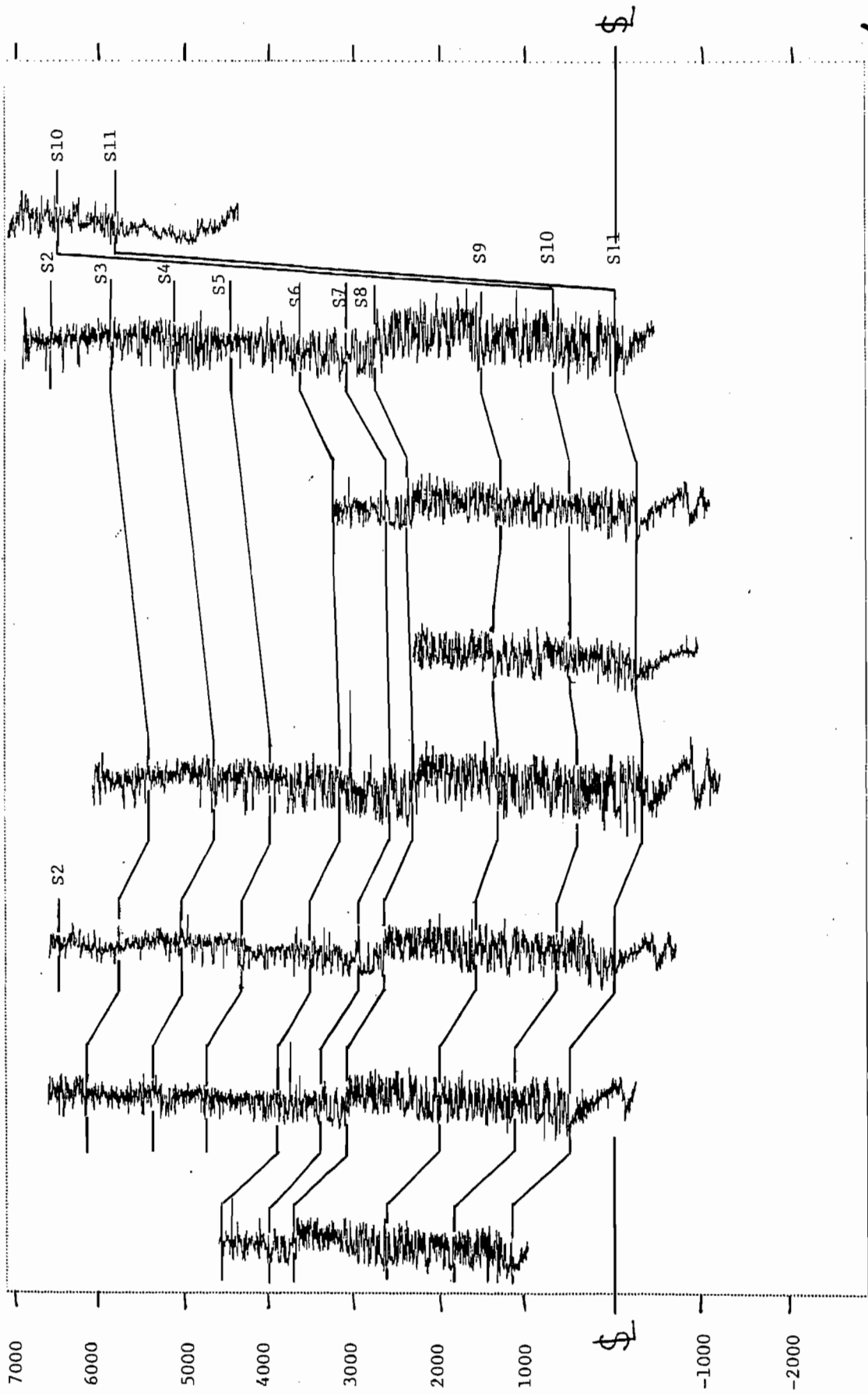
0507705045 S10/W98/6 0507705044 S10/W96/6 0507708542 S10/W96/15 0507708290 S10/W95/16 0507705037 S10/W95/12 0507708449 S10/W94/9 0507707360 S10/W94/24 0507708132 S9/W93/34



F

F

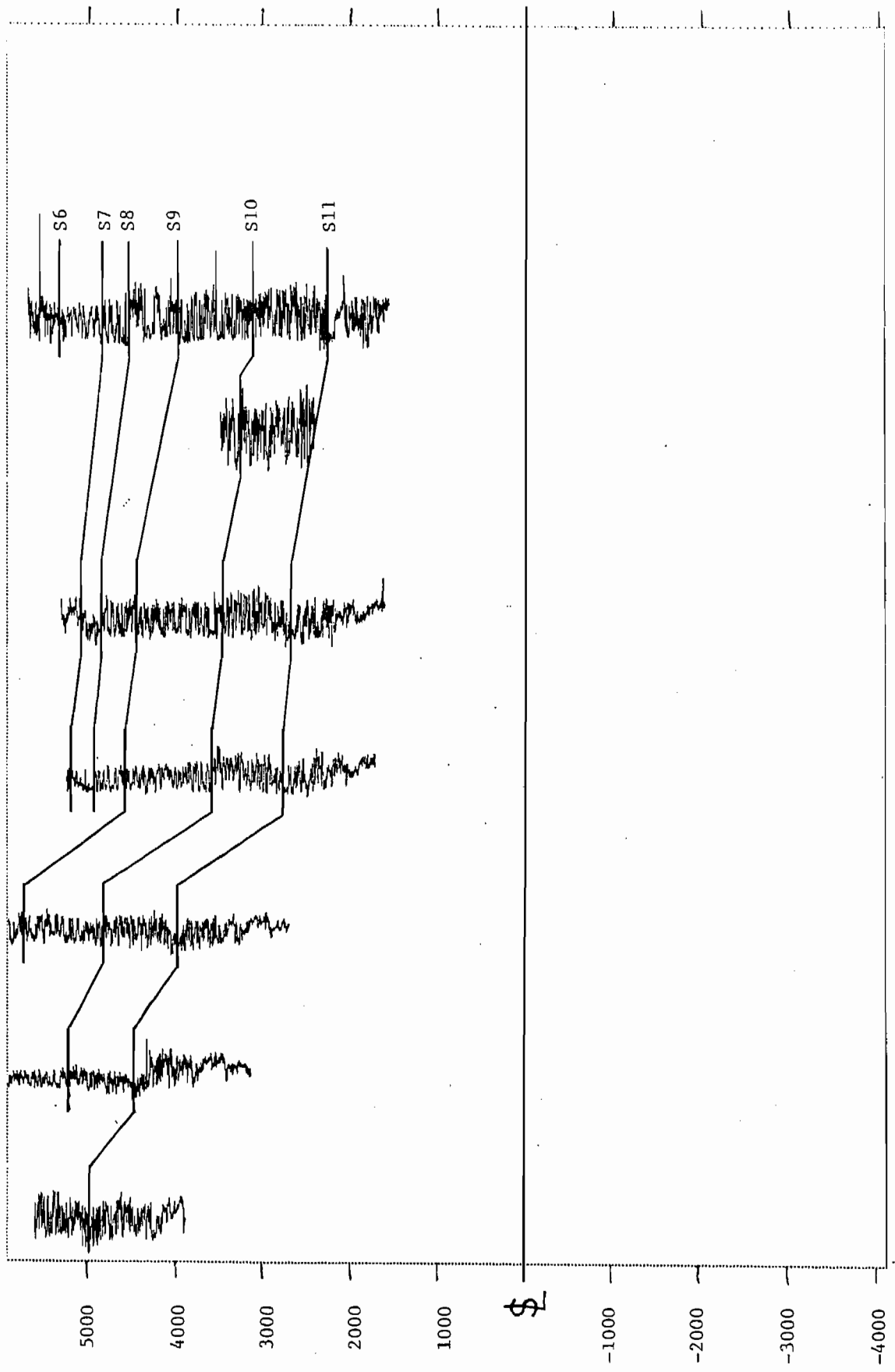
0507707360 0507708179 0507708132 0507708289 0507707331 0507705108 0507705150 0507705167
 S10/W94/24 S S10/W93/10 S9/W93/34 S9/W93/23 S9/W93/14 S9/W92/5 S8/W92/22 S8/W91/22



G

G

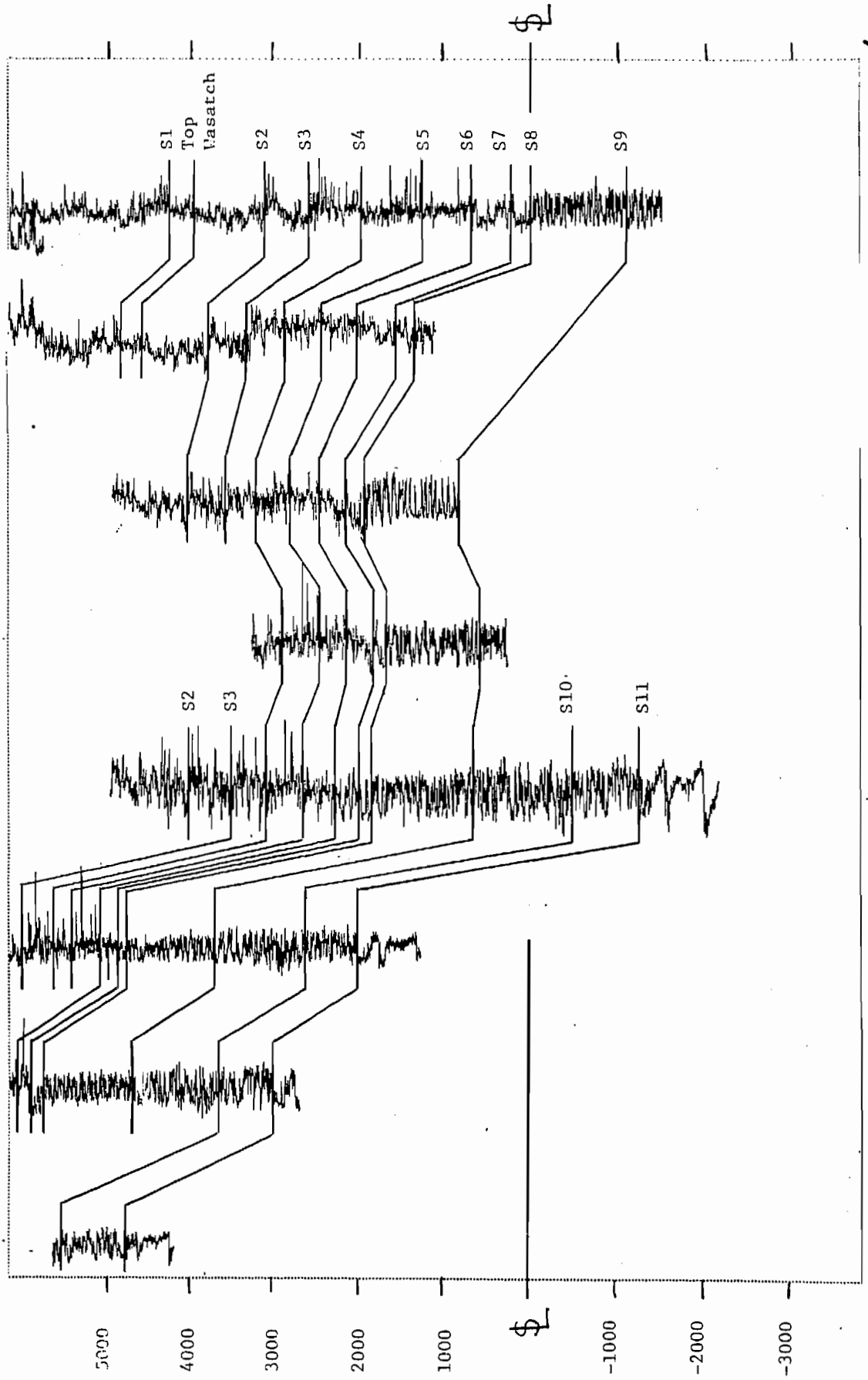
0504506092 S5/W100/30 0504506042 S6/W101/2 0504506016 S6/W100/7 0504506422 S6/W100/25 0504505075 S7/W99/6 0504505057 S7/W99/14 0504506303 S7/W99/13



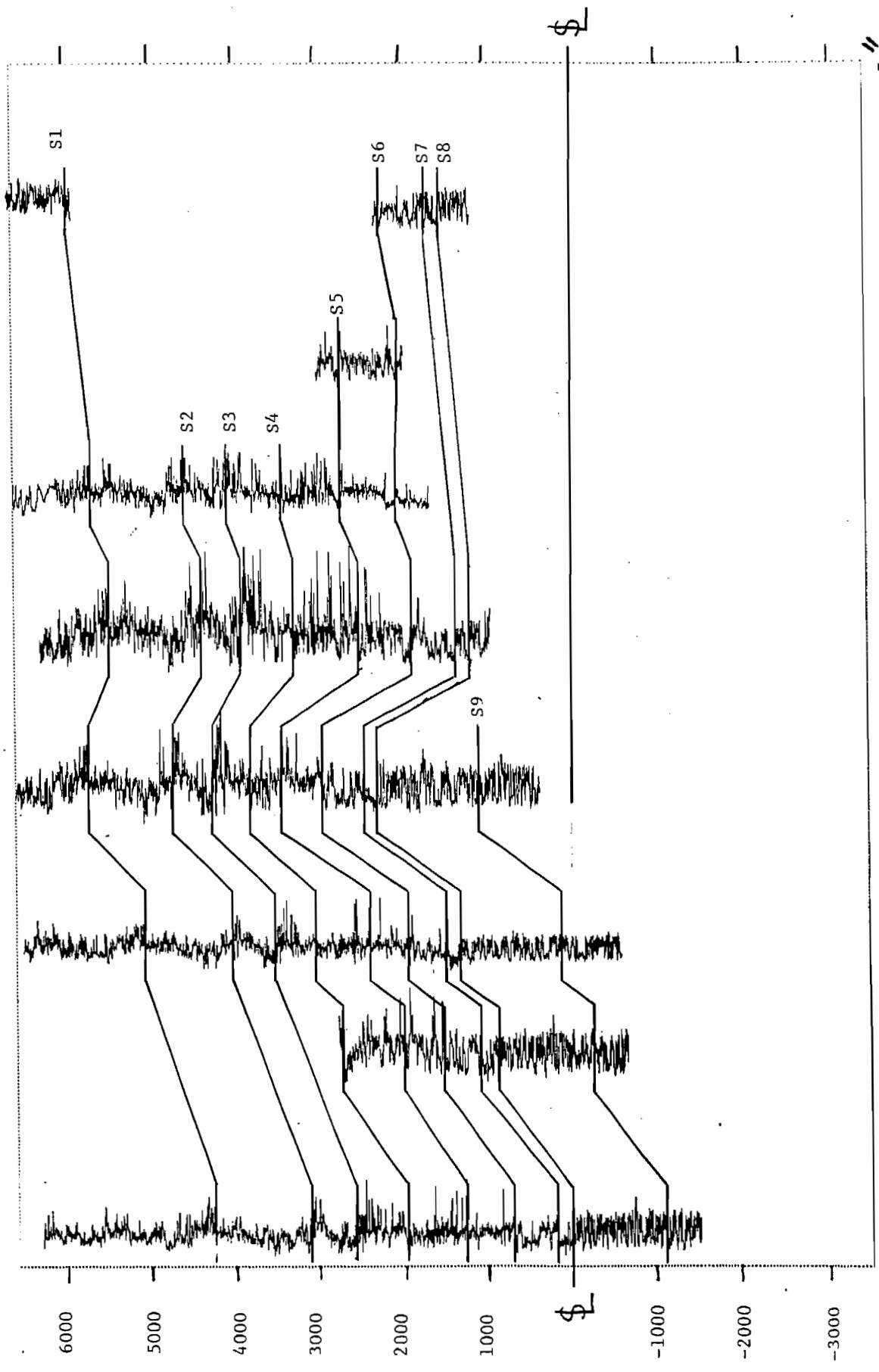
H

H

0510307382 N1/W100/6
 0510305288 N1/W100/10 S1/W100/2
 0510308541 S1/W99/16
 0510307238 S1/W99/34 S2/W99/27
 0510305072 S3/W98/7
 0510307613 S3/W98/11



0510307613 S3/W98/11 0510305048 S3/W98/22 0510305030 S3/W98/27 0510307661 S4/W98/4 0510307550 S4/W97/7 0510305009 S4/W97/17 0504505130 S4/W97/19 0504506032 S4/W97/28



S1

S2

S3

S4

S5

S6

S7

S8

S9

\$

\$

6000

5000

4000

3000

2000

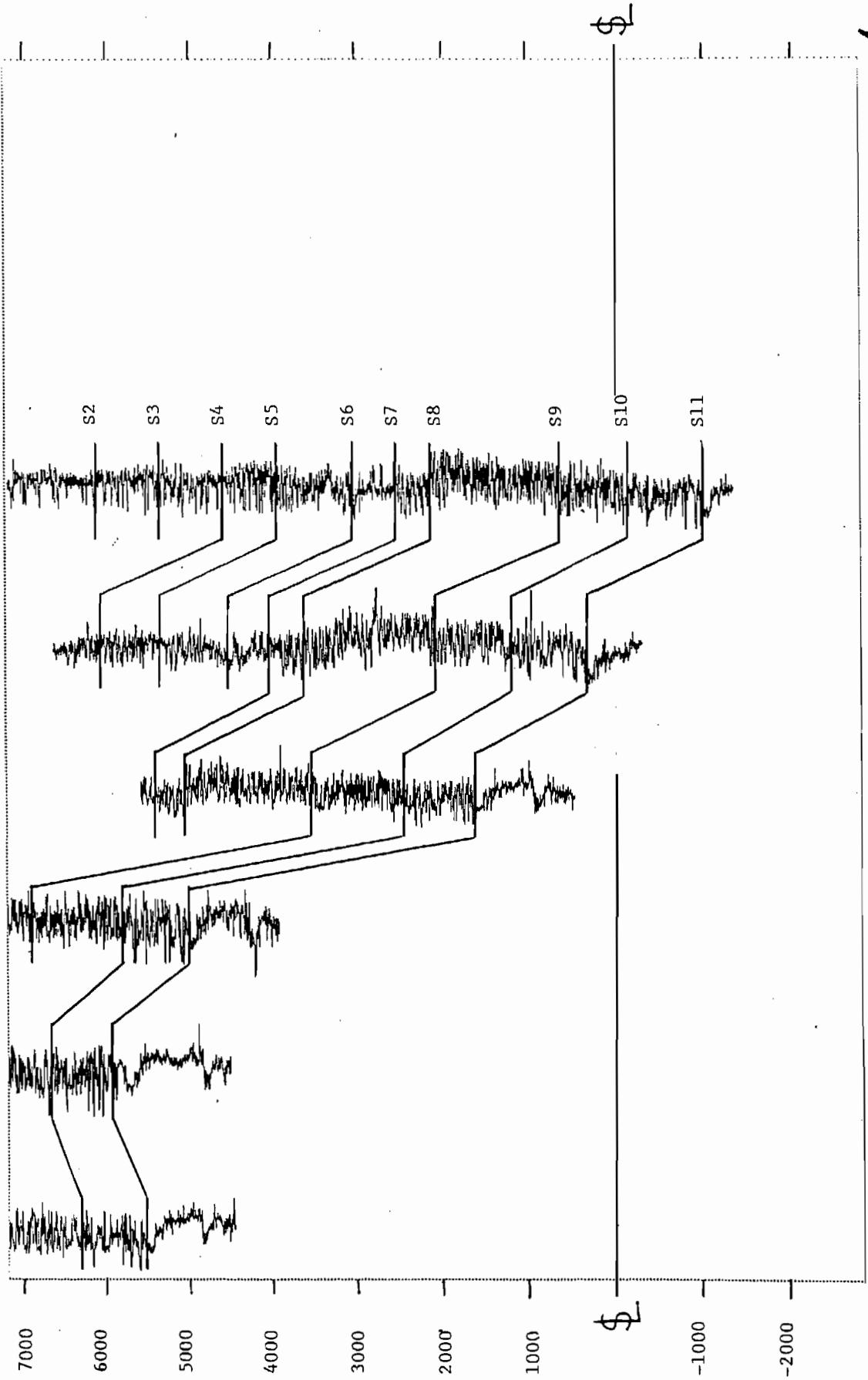
1000

-1000

-2000

-3000

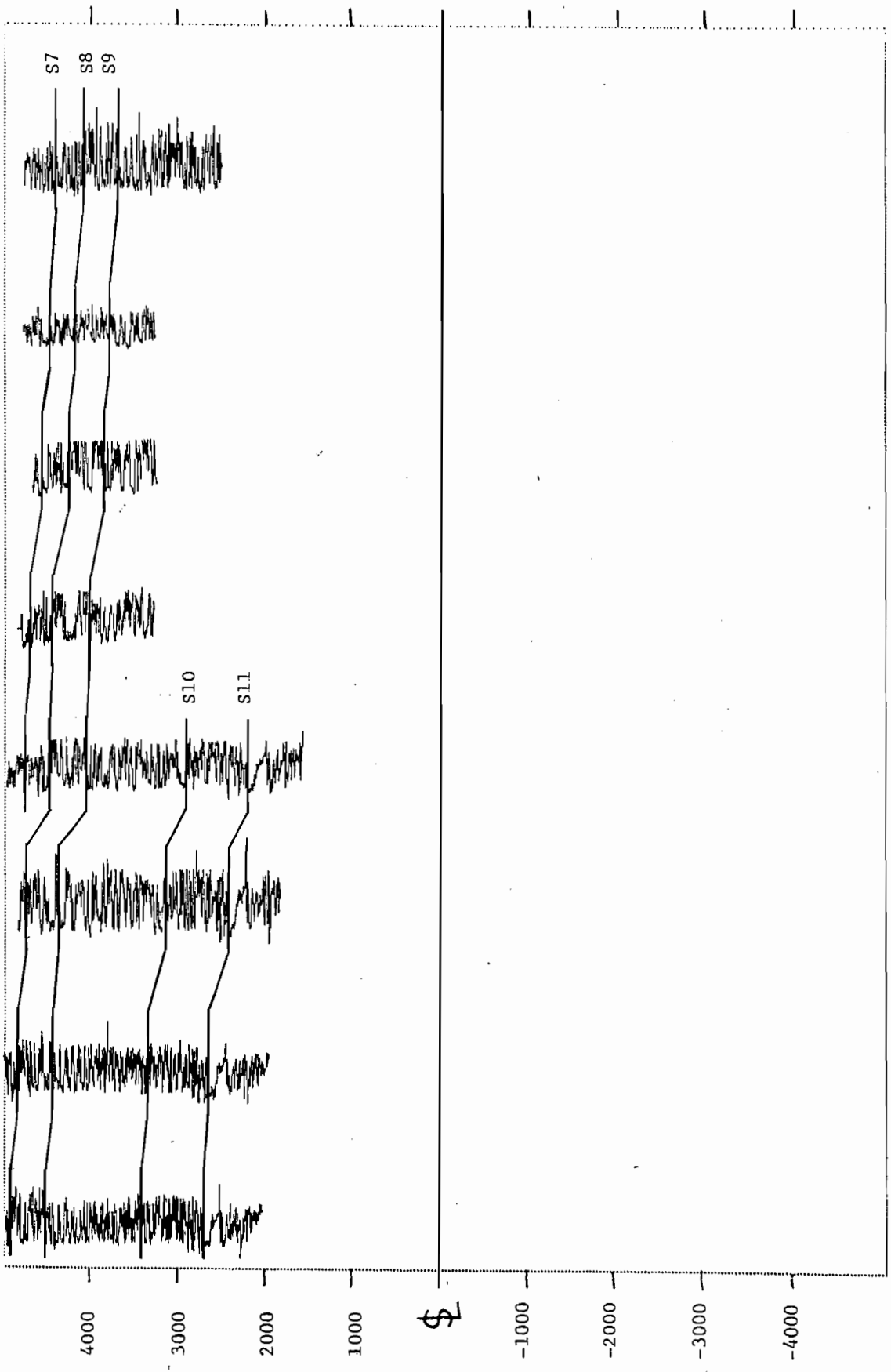
0507705124 S8/W91/36
0507705160 S8/W91/23
0507705177 S8/W91/16
0504506390 S7/W91/27
0504505186 S7/W91/22
0504505056 S7/W90/17



J

J

0507708420 S8/W98/35 0507708432 S8/W98/26 0507708313 S8/W97/30 0507708171 S8/W97/29 0507708149 S8/W97/29 0507708150 S8/W97/28 0507708148 S8/W97/28 0507708533 S8/W97/21



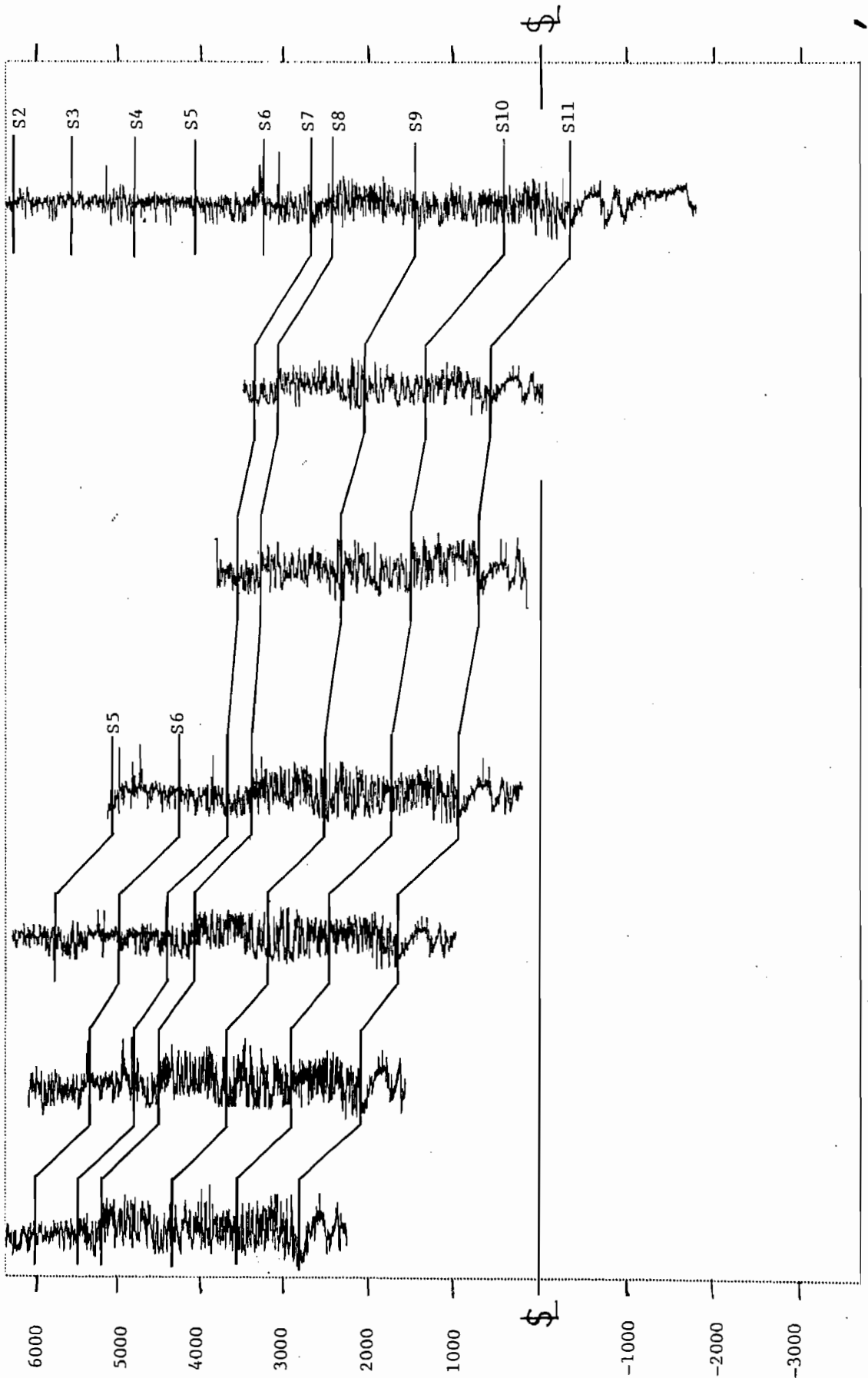
\$

\$

L

L

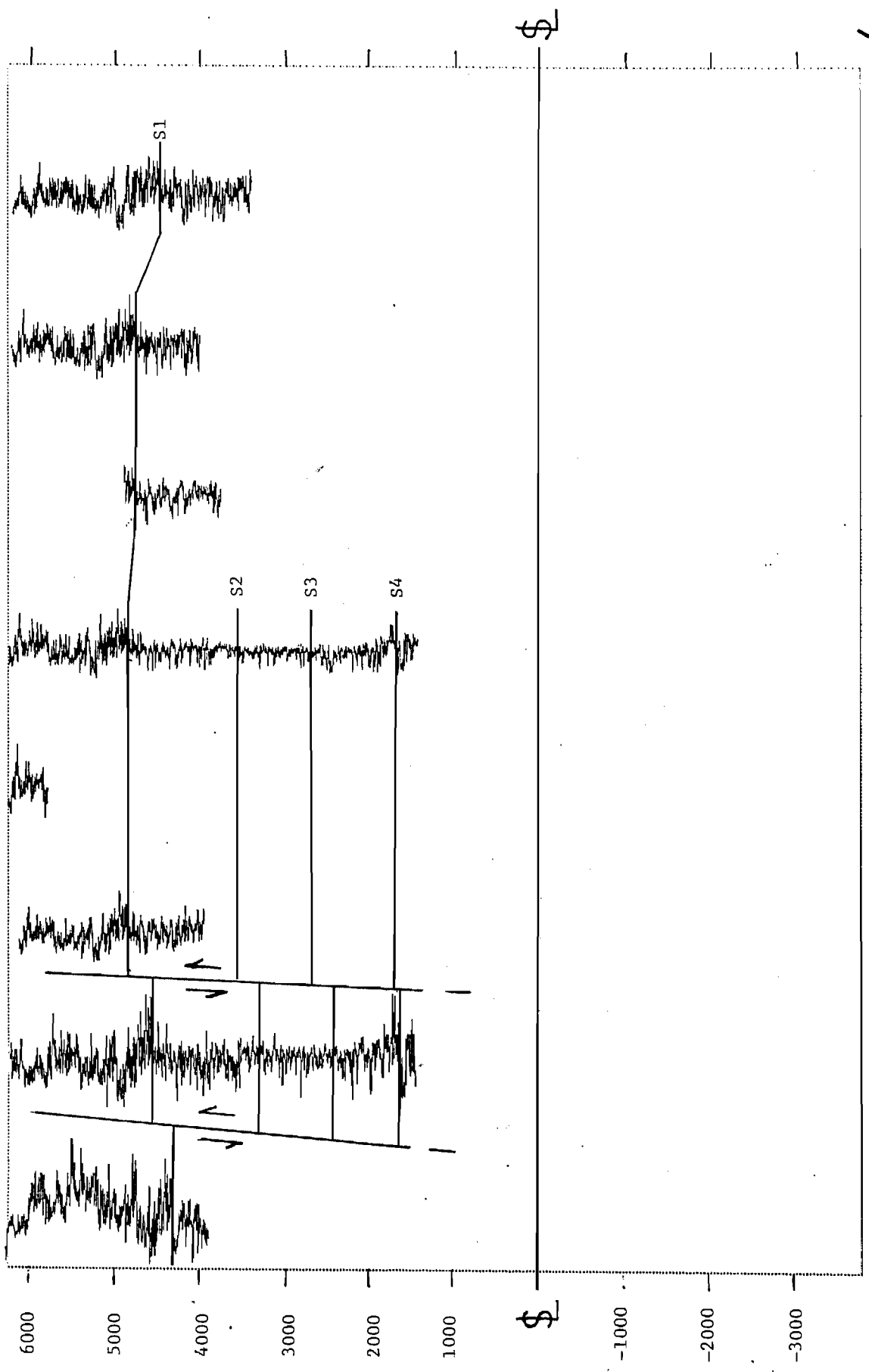
0507708511 S10/W95/32
0507708290 S10/W95/16
0507705037 S10/W95/12
0507708419 S9/W95/25
0507705080 S9/W94/19
0507705091 S9/W94/18
0507708043 S8/W94/25



M

M

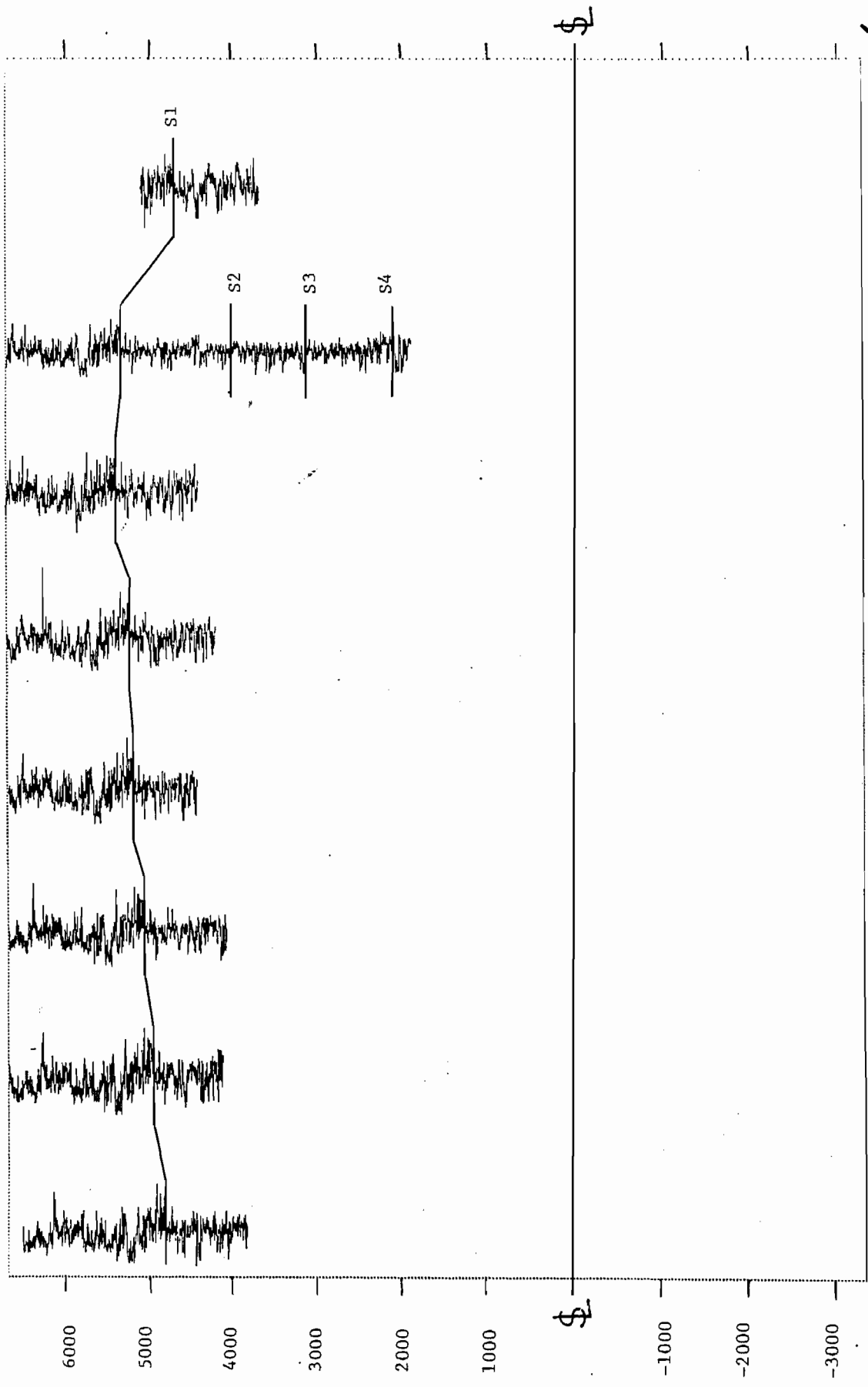
0510305151 S2/W97/20
 0510307678 S2/W97/23
 0510308182 S2/W97/13
 0510307890 S2/W97/13
 0510307091 S2/W96/7
 0510307993 S2/W96/7
 0510307435 S2/W96/8
 0510307960 S2/W96/4



N

N

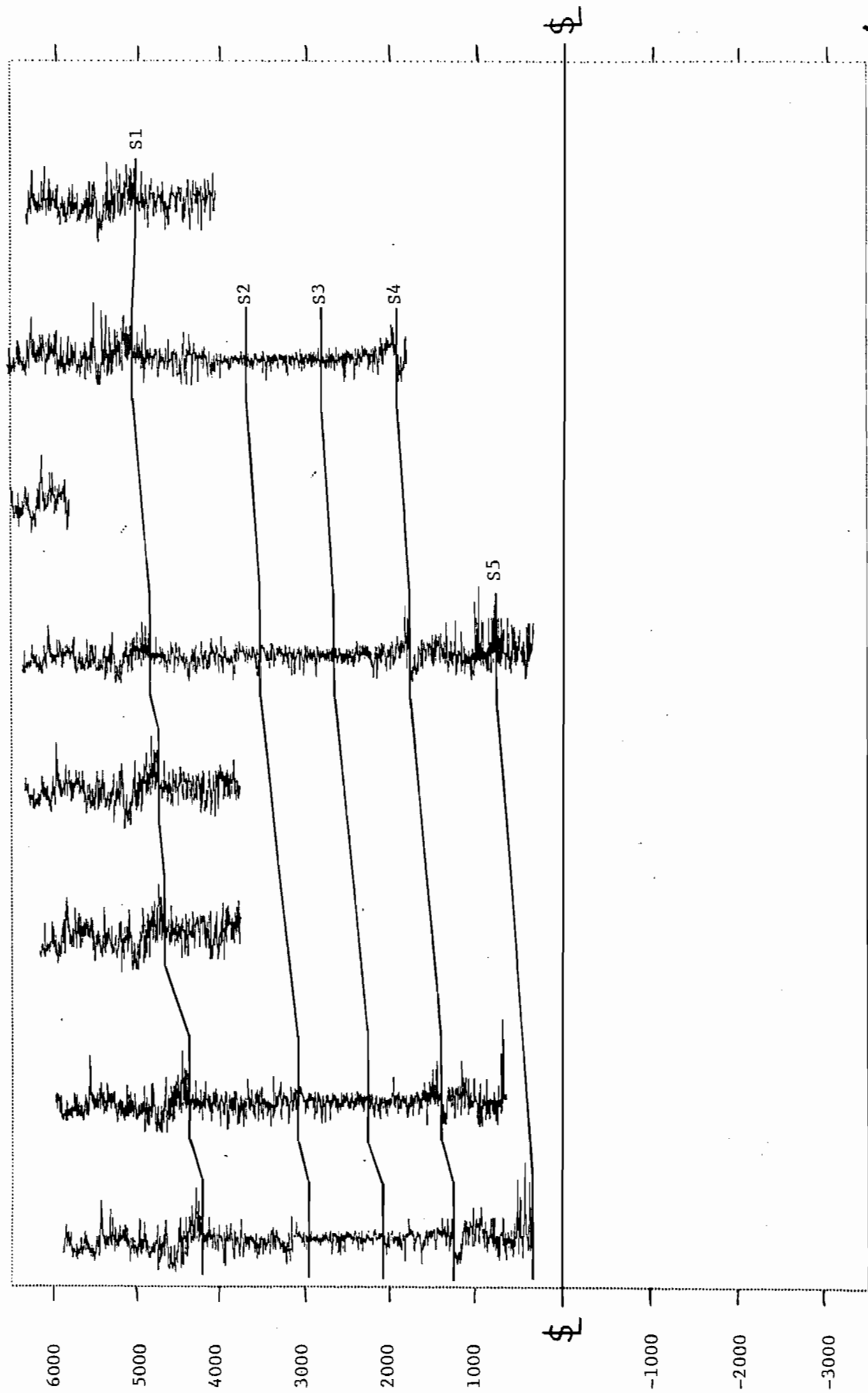
0510307955 S1/W97/36
0510307995 S2/W97/1
0510307542 S2/W96/6
0510307435 S2/W96/8
0510308178 S2/W96/18
0510307994 S2/W96/17
0510307036 S2/W96/20
0510305136 S2/W96/26



O

O

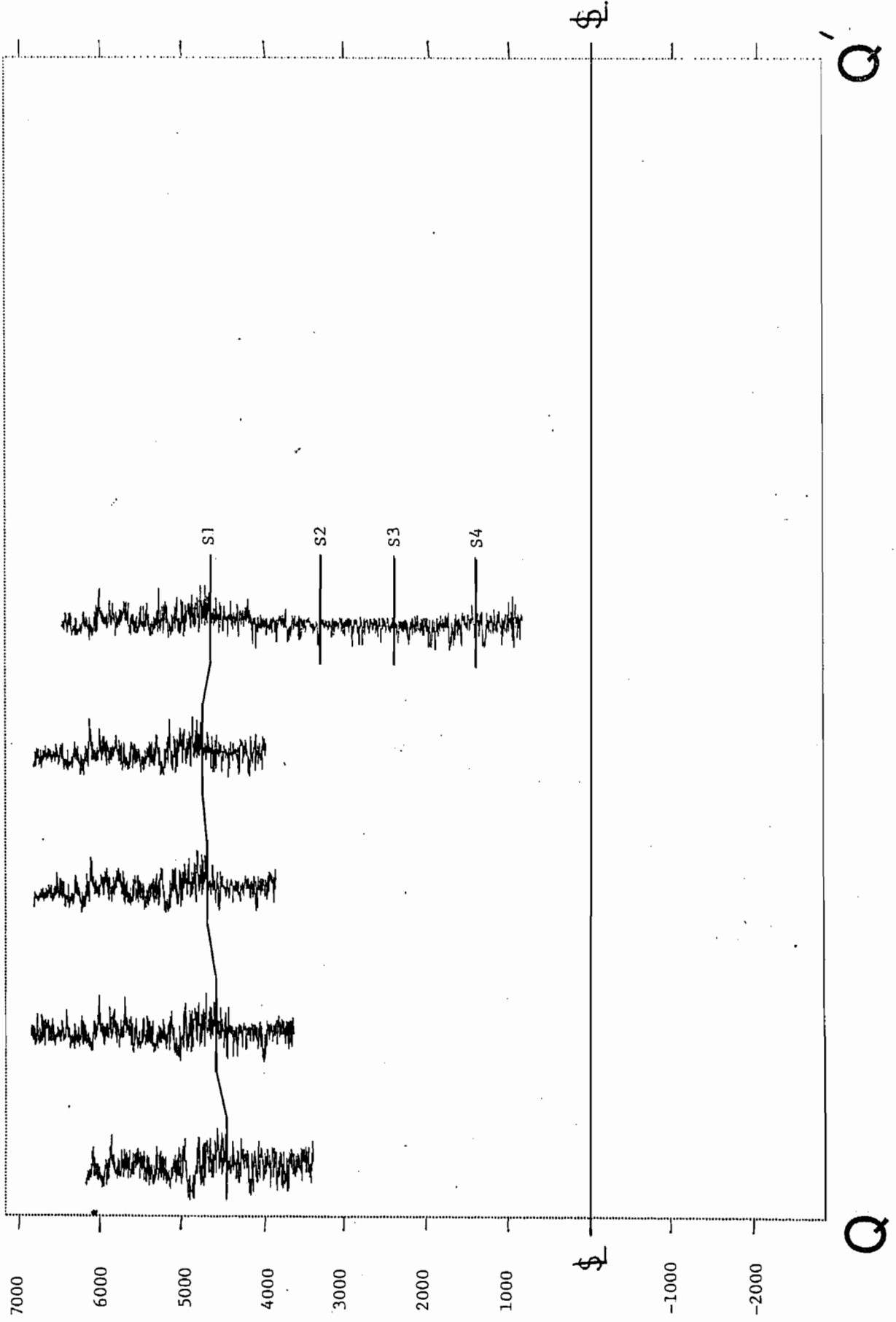
0510308189 S1/W97/33 0510307048 S2/W97/3 0510307961 S2/W97/11 0510308181 S2/W97/11 0510366512 S2/W97/12 0510307890 S2/W97/13 0510301097 S2/W96/18 0510307994 S2/W96/17



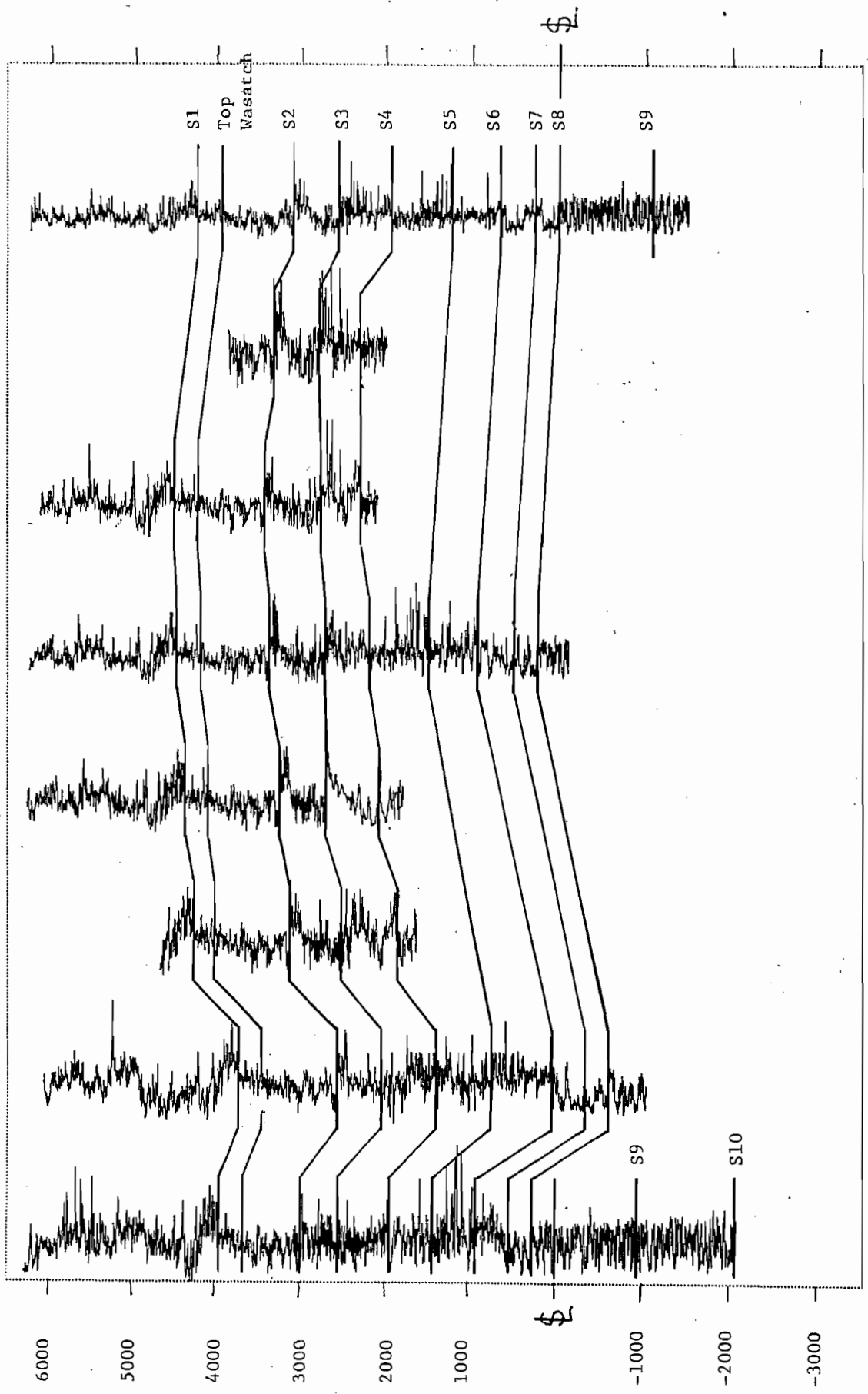
P

P

0510307960 S2/W96/4 0510307543 S2/W96/9 0510307476 S2/W96/16 0510307477 S2/W96/22 0510307052 S2/W96/27



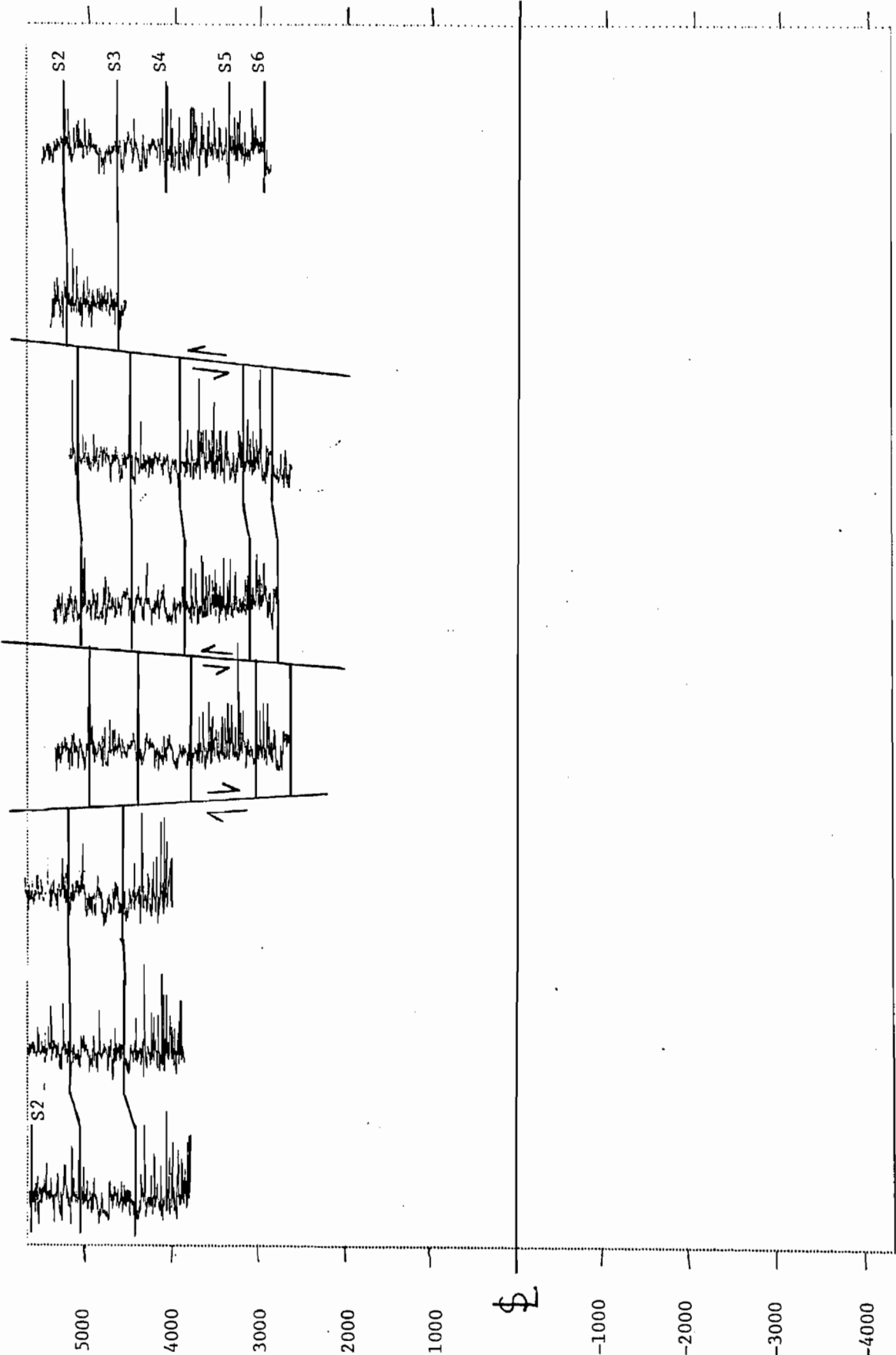
0510308316 S1/W99/14 0510307040 S2/W98/3 0510307760 S2/W98/14 0510307355 S2/W98/23 0510307659 S2/W98/22 0510307563 S2/W98/26 0510307662 S2/W98/26 0510307613 S3/W98/11



R

R

0510308100 0510308101 0510308102 0510307418 0510307411 0510307312 0510307302 0510307413
 N2/W97/17 N2/W97/17 N2/W97/17 N2/W97/20 N2/W97/28 N2/W97/28 N2/W97/34 N2/W97/34



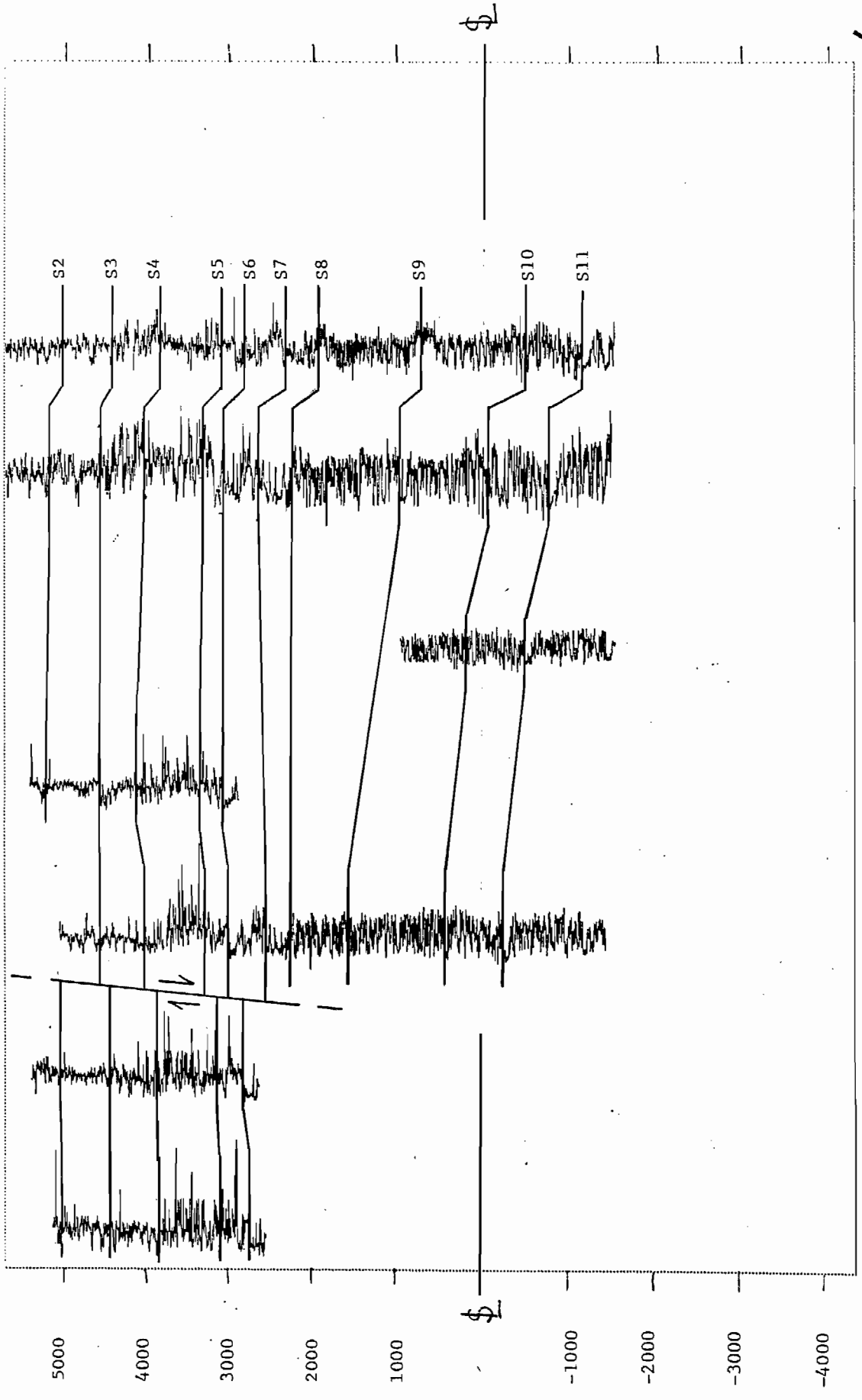
\$

S

\$

S

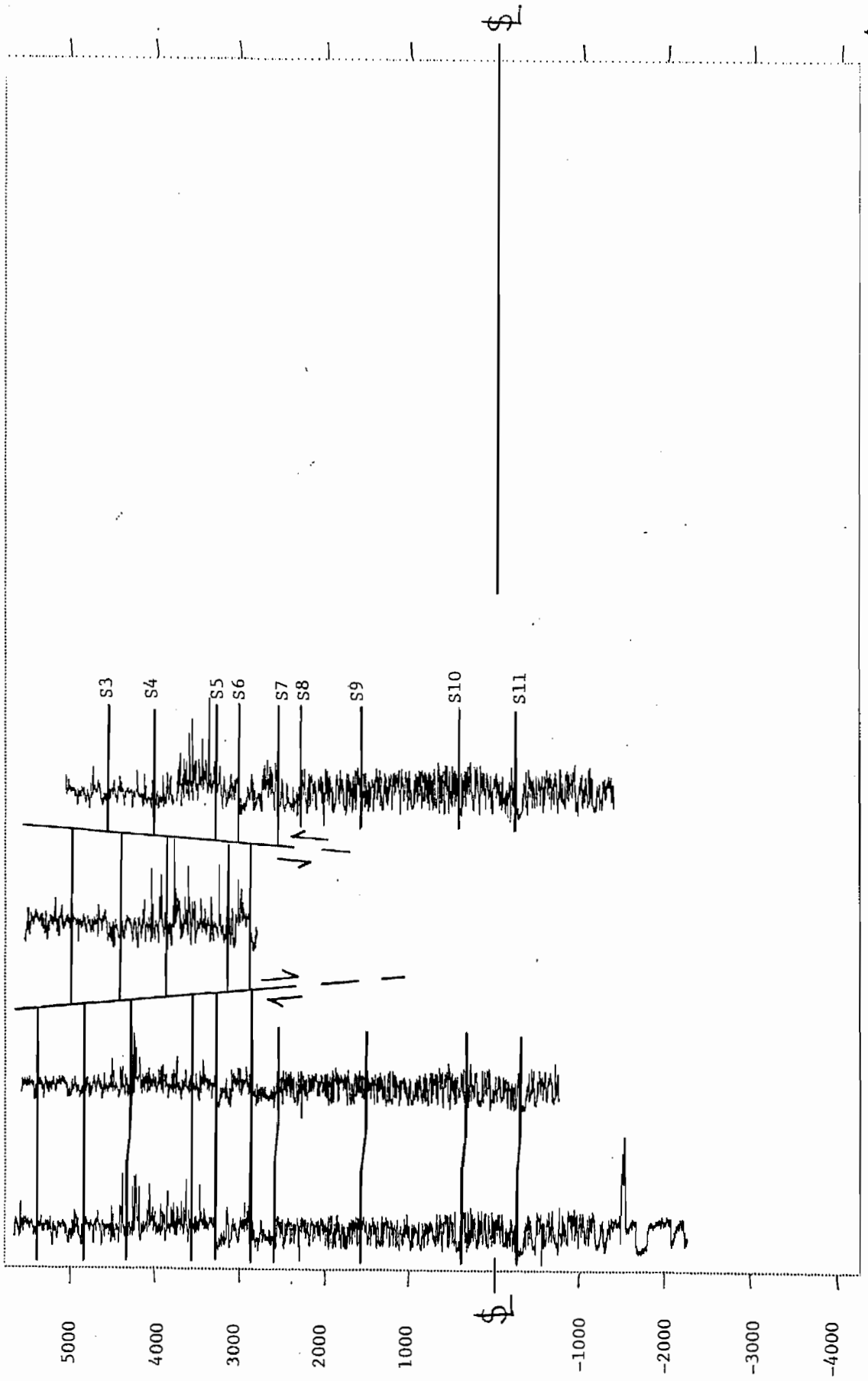
0510307312 N2/W97/28
 0510307315 N2/W97/34
 0510307681 N2/W97/35
 0510307404 N2/W97/35
 0510307349 N2/W96/31
 0510307706 N2/W96/29
 0510307570 N2/W96/28



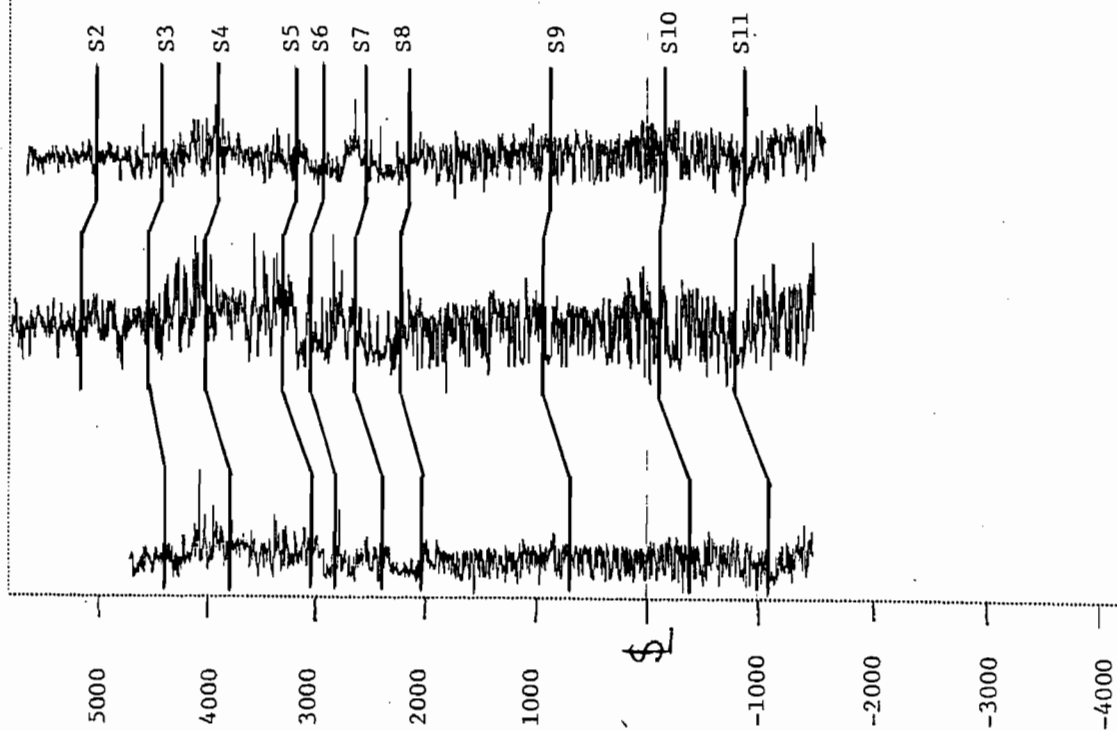
T

T

0510307468 0510307564 0510307467 0510307681
N2/W97/26 N2/W97/26 N2/W97/35 N2/W97/35



0510308247 N2/W96/20
0510307706 N2/W96/29
0510307707 N2/W96/32



S2
S3
S4
S5
S6
S7
S8
S9
S10
S11

V

V

X. APPENDIX B

Condensed vertical scale displays of all gamma radiation logs used in the study. These traces are organized by well API number and show intersections with correlated horizons S1-S11. Vertical scale is feet below surface elevation.

28-JAN-87 14:31
57/W99/14
GAR05057
GR
0

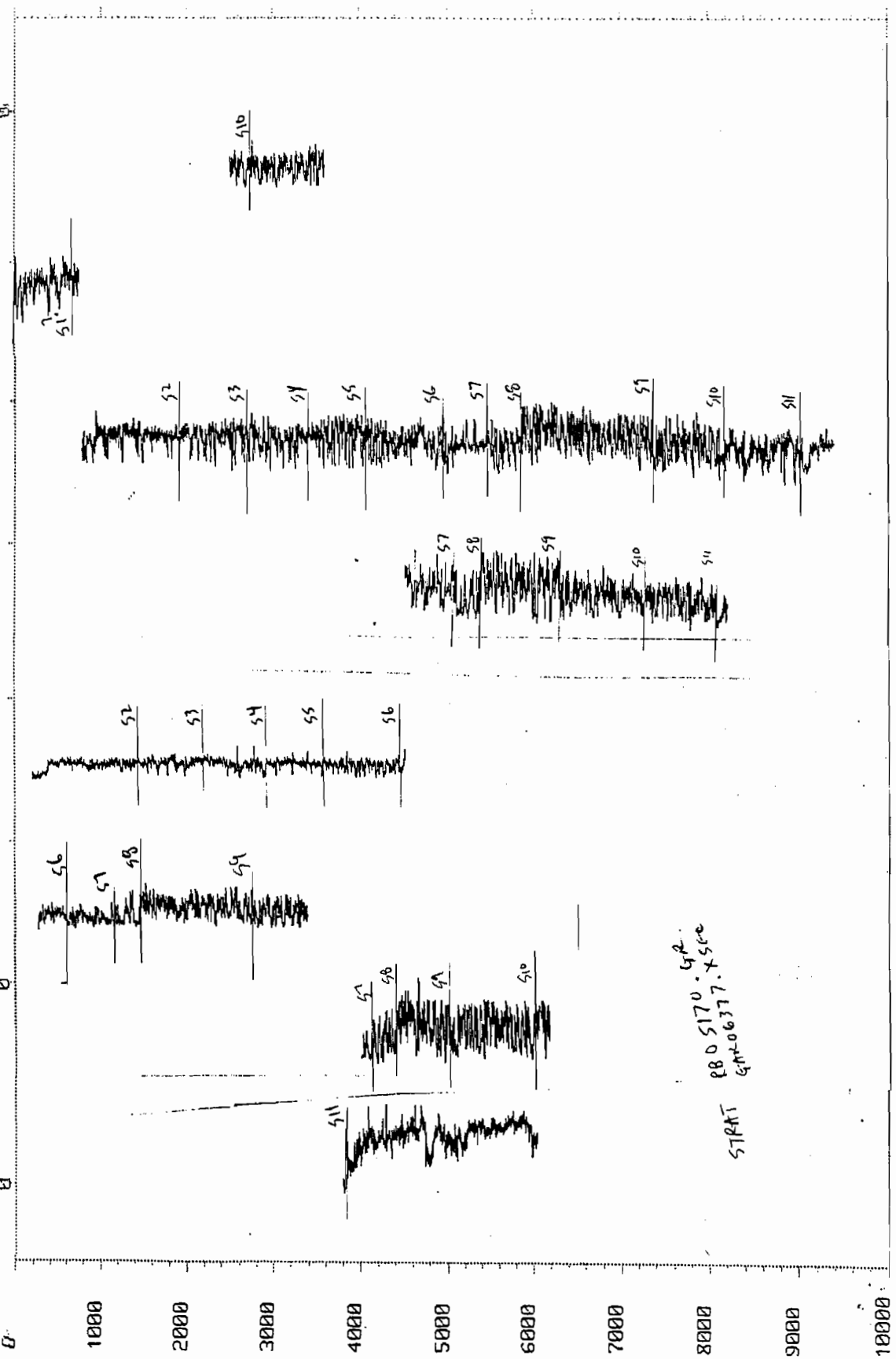
57/W90/17
GAR05056
GRC
0

57/W95/14
GAR05055
GRC
0

57/W92/36
GAR05044
GR
0

57/W95/30
GAR05039
GR
0

58/W91/10
GAR05011
GR
0



START
880 5170 - 4P.
5-M-06377.X 500

14

GAR05096
GR
0

GAR05093
GR
0

5386
GAR05024
GR
0

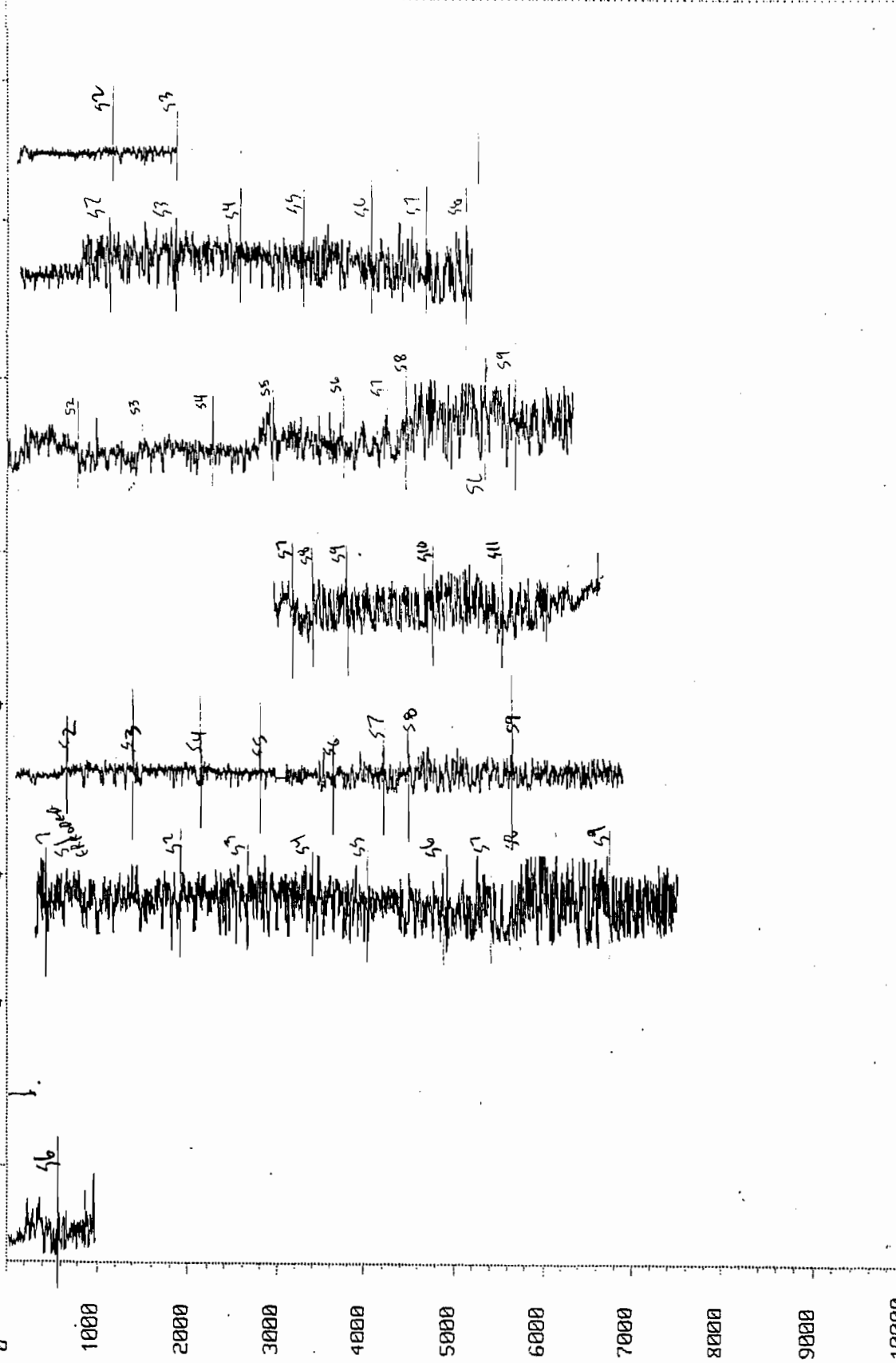
GAR05075
GR
0

GAR05071
GR
0

GAR05059
GR
0

GAR05059
GRC
0

GAR05057
GRC
0



1:23

2 GAR05207
GR
0

GAR05206
GR
0

GAR05204
GR
0

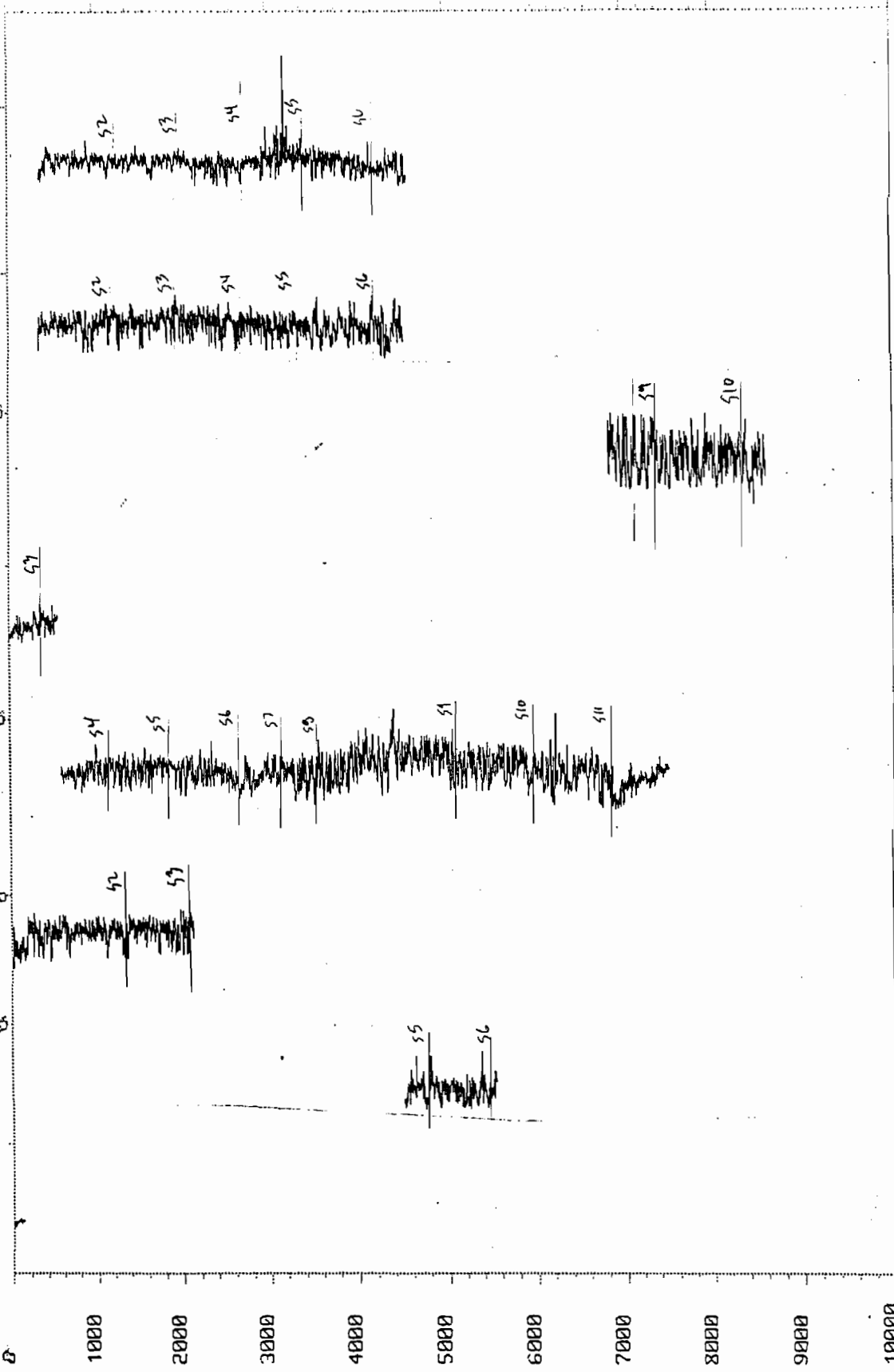
GAR05186
GRC
0

GAR05186
GR
0

GAR05130
GR
0

GAR05184
GR
0

GAR05096
GRC
0



28-JAN-87 15:30

GAR06042
GR
0

GAR06034
GR
0

GAR06032
GR
0

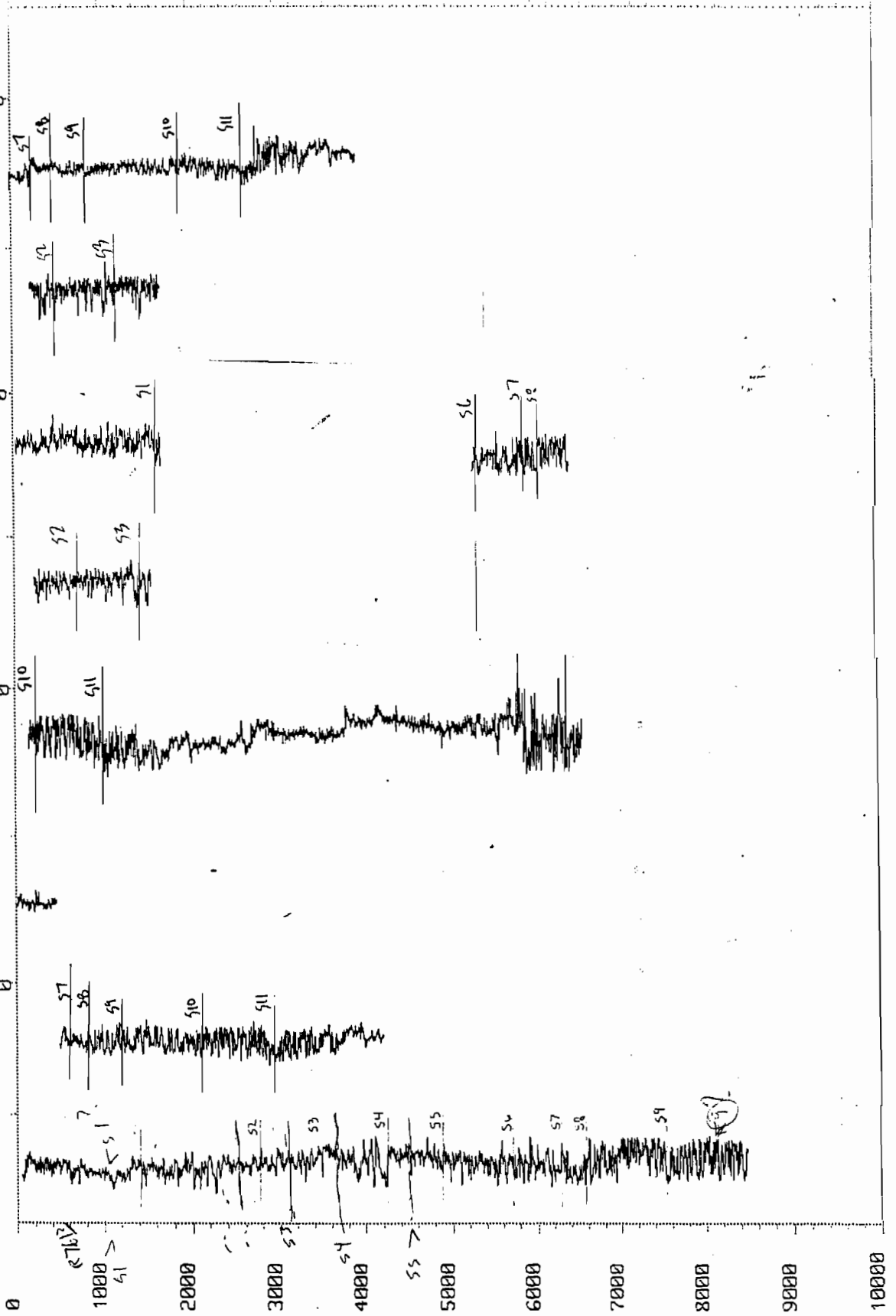
GAR06023
GR
0

GAR06018
GR
0

GAR06016
GRC
0

GAR06016
GR
0

GAR06001
GR
0



9-JAN-87 08:03

GAR06050
GR
0

GAR06053
GR
0

GAR06057
GR
0

GAR06085
GRC
0

GAR06092
GRC
0

GAR06127
GR
0

GAR06050
GR
0

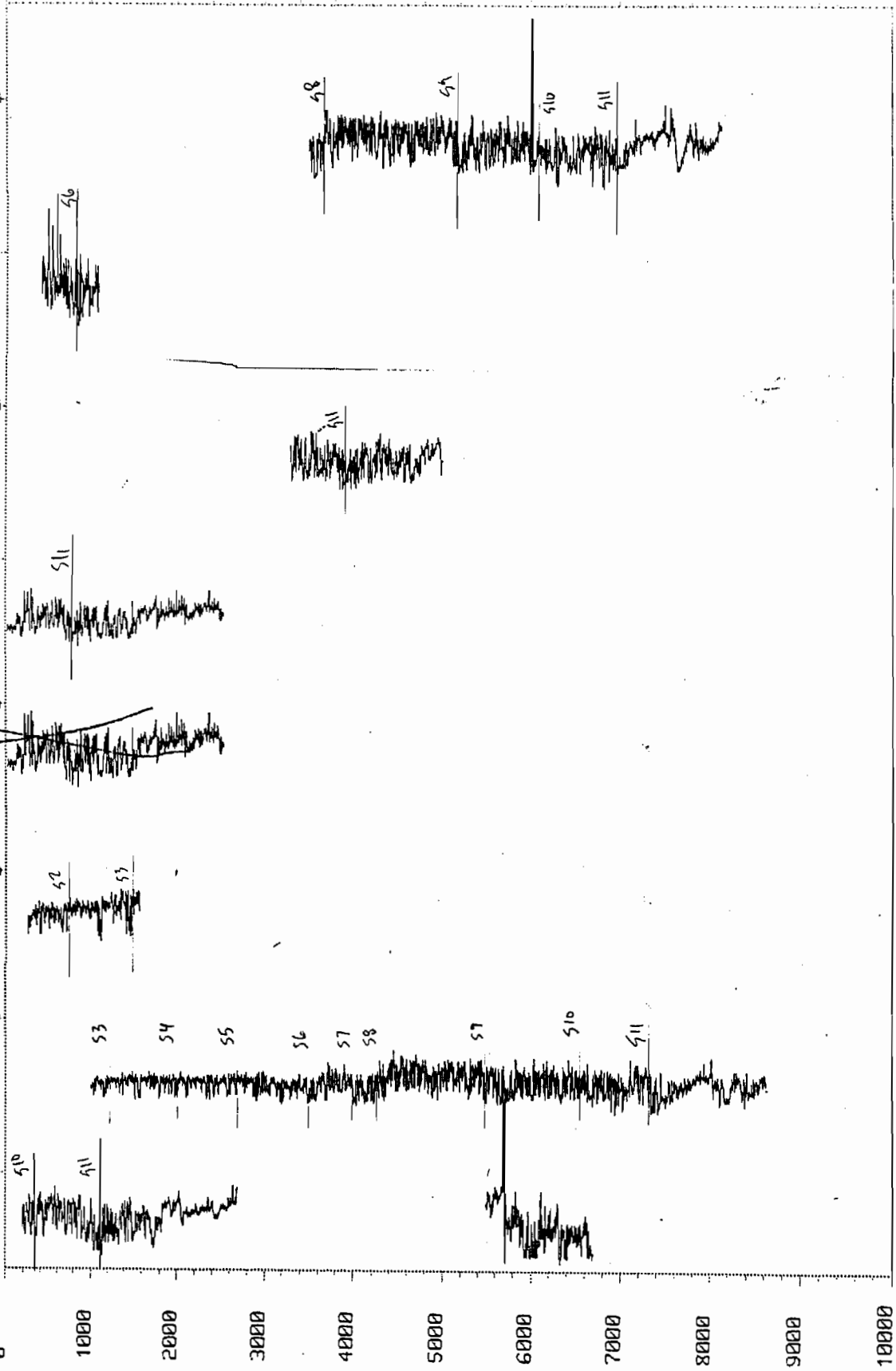
GAR06053
GR
0

GAR06057
GR
0

GAR06085
GRC
0

GAR06092
GRC
0

GAR06127
GR
0



24

GAR06207
GR
0

GAR06206
GR
0

GAR06179
GRC
0

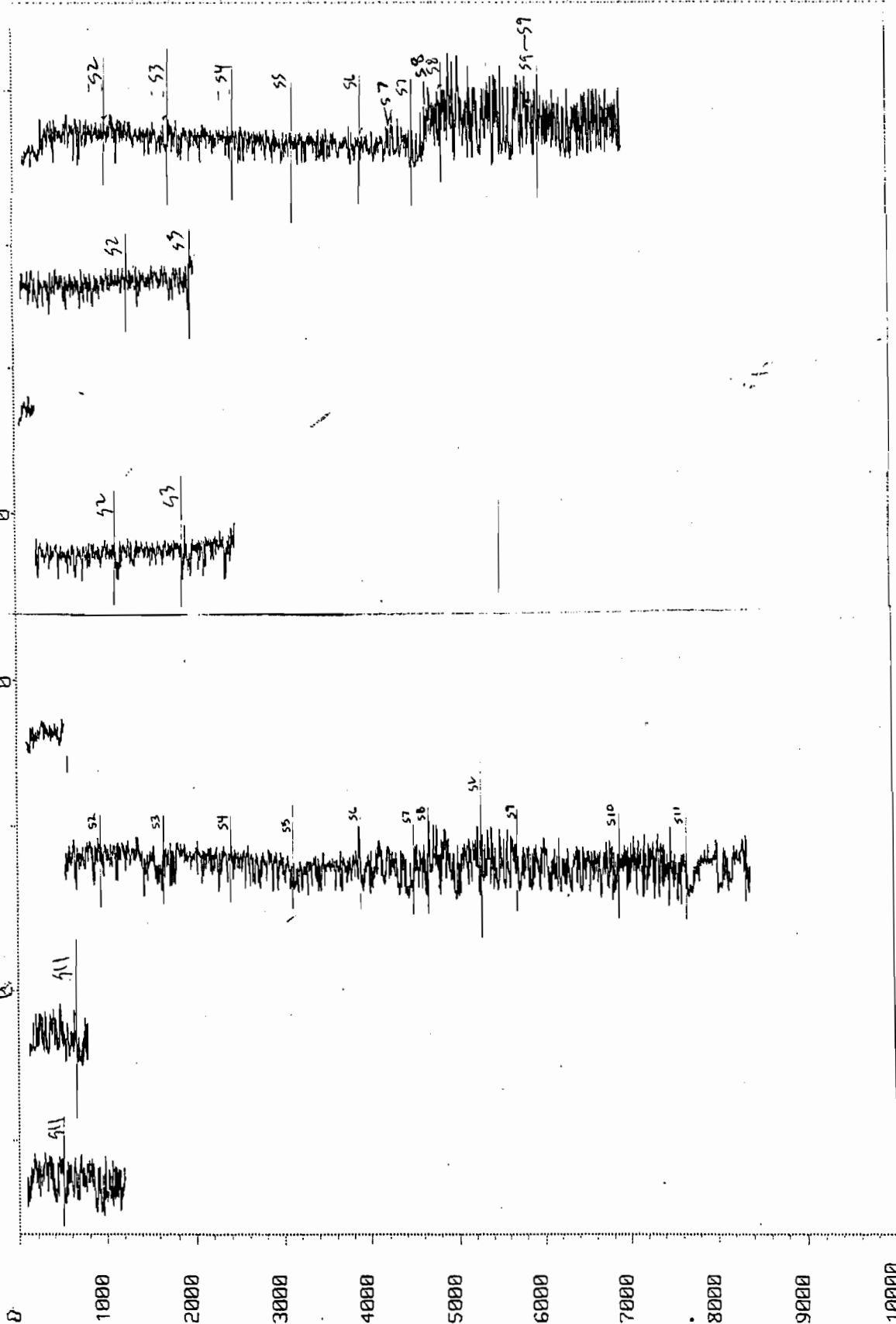
GAR06179
GR
0

GAR06178
GRC
0

5275
GAR06178
GR
0

GAR06134
GR
0

GAR06132
GR
0



29-JAN-87 08:42

GAR06224
GR
0

GAR06222
GR
0

GAR06216
GRC
0

C

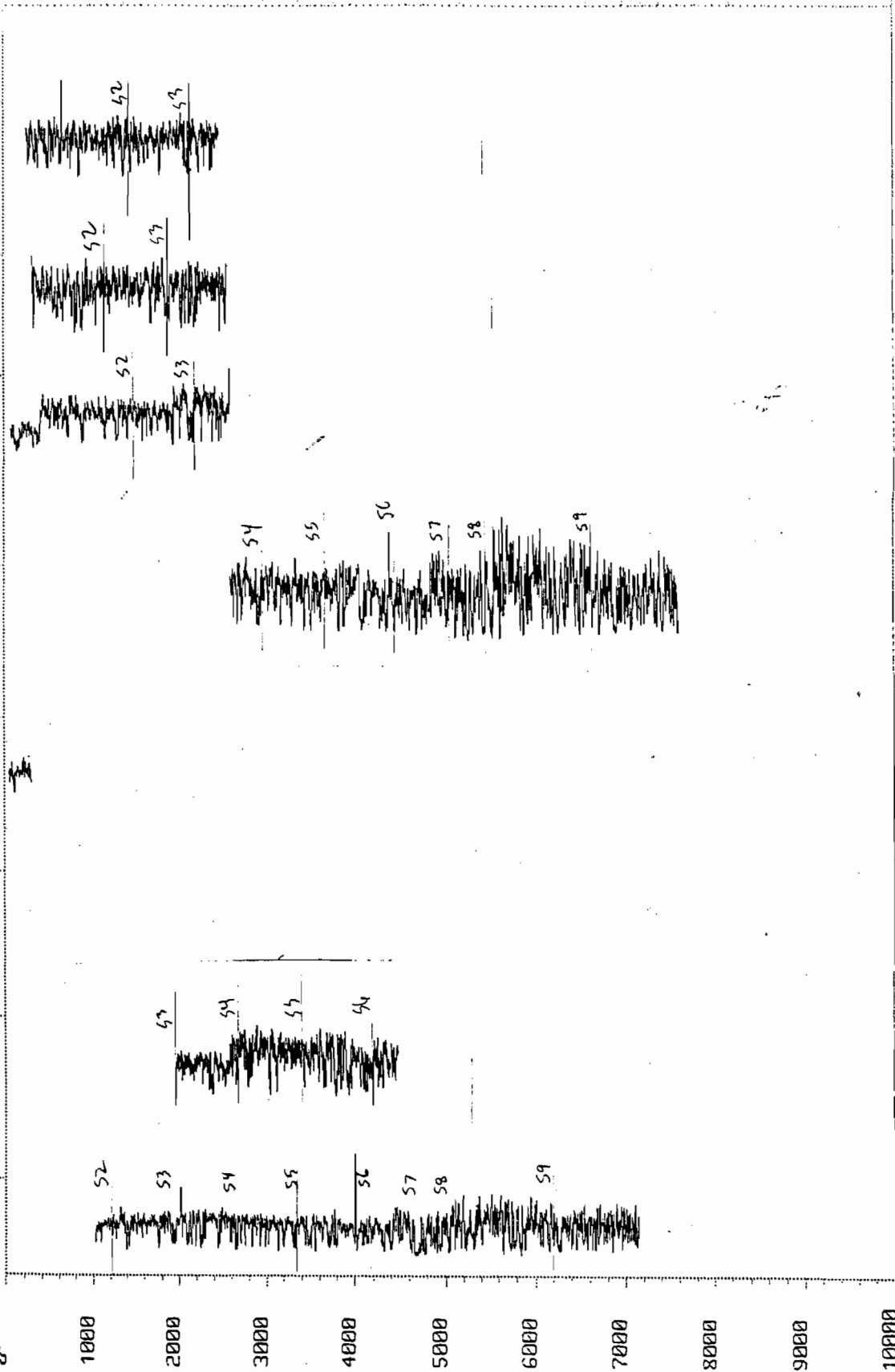
GAR06216
GR
0

GAR06211
GR
0

GAR06211
GR
10000

GAR06210
GRC
0

GAR06208
GR
0



29-JAN-87 09:03

GAR06249
GR
0

5307

GAR06233
GRC
0

5770

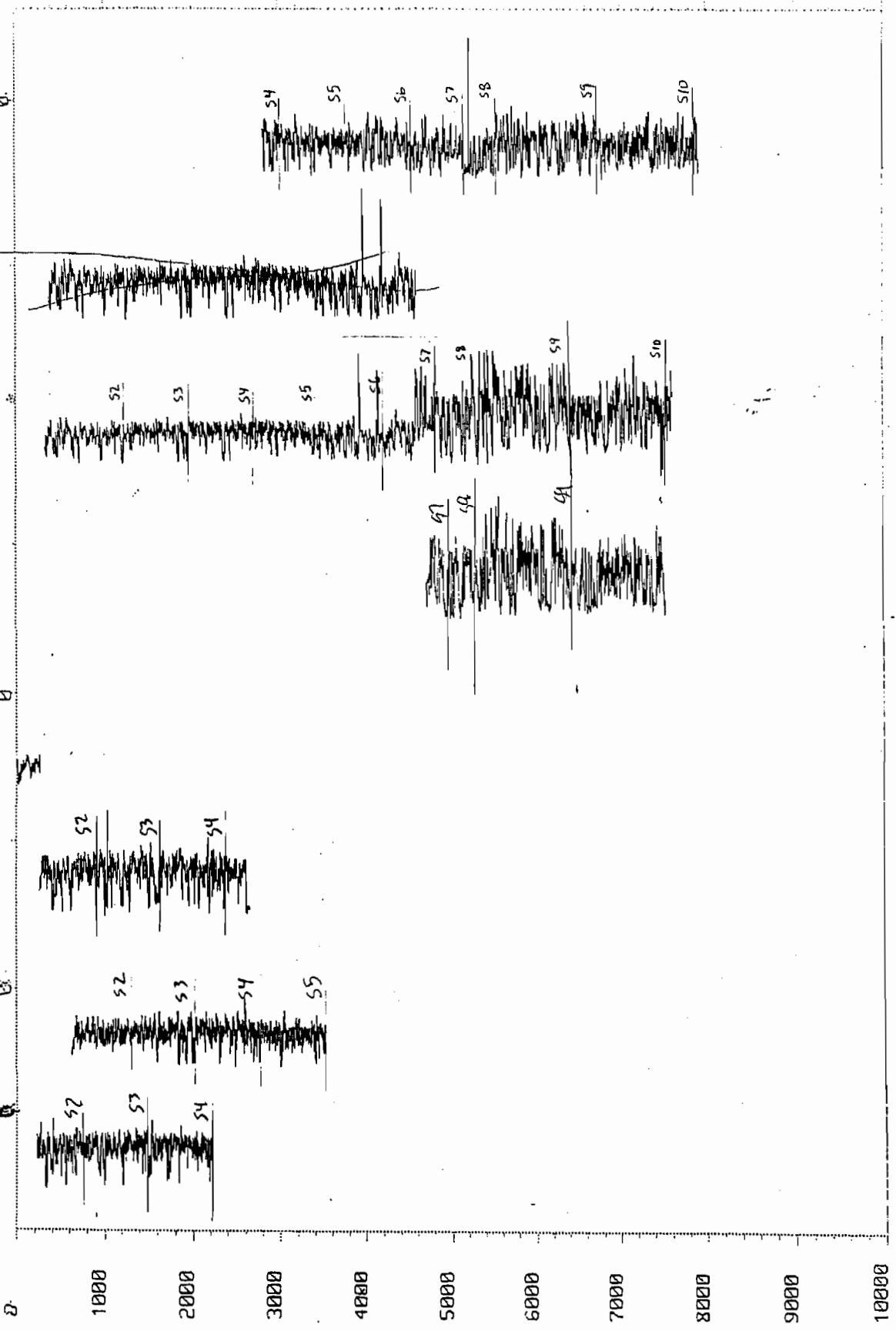
GAR06231
GR
0

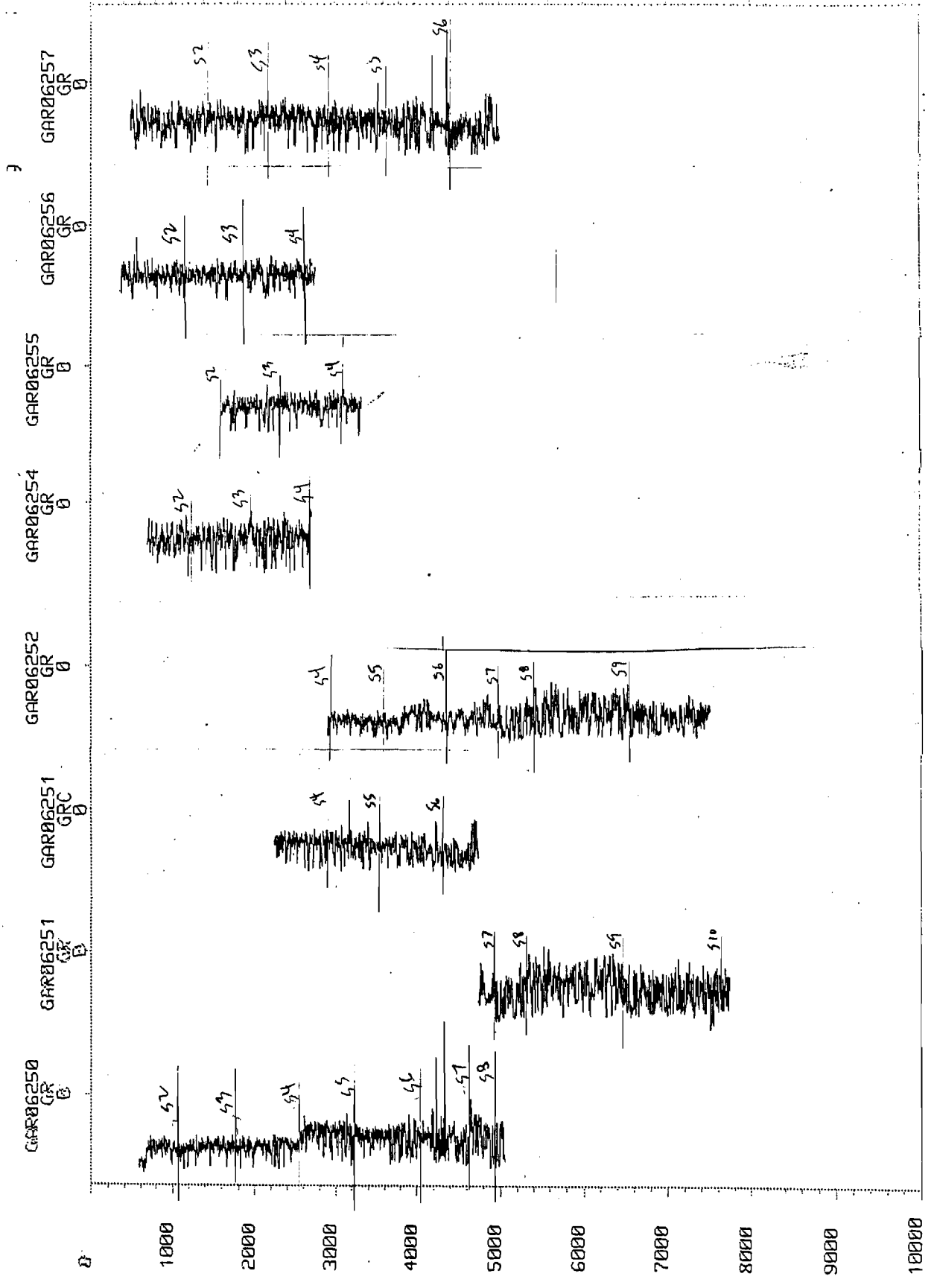
GAR06230
GRC
0

GAR06230
GR
0

GAR06229
GR
0

GAR06228
GR
0





29-JAN-87 09:34

GAR06298
GR
0

GAR06283
GR
0

GAR06277
GR
0

GAR06271
GR
0

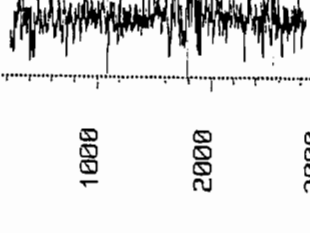
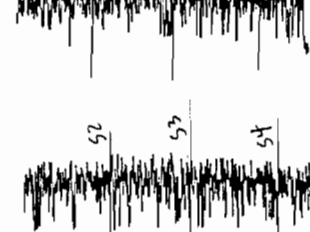
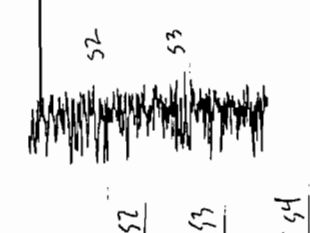
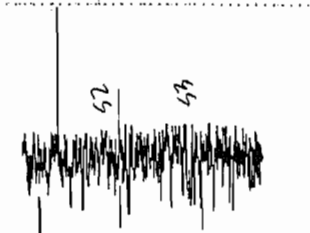
GAR06270
GR
0

GAR06268
GR
0

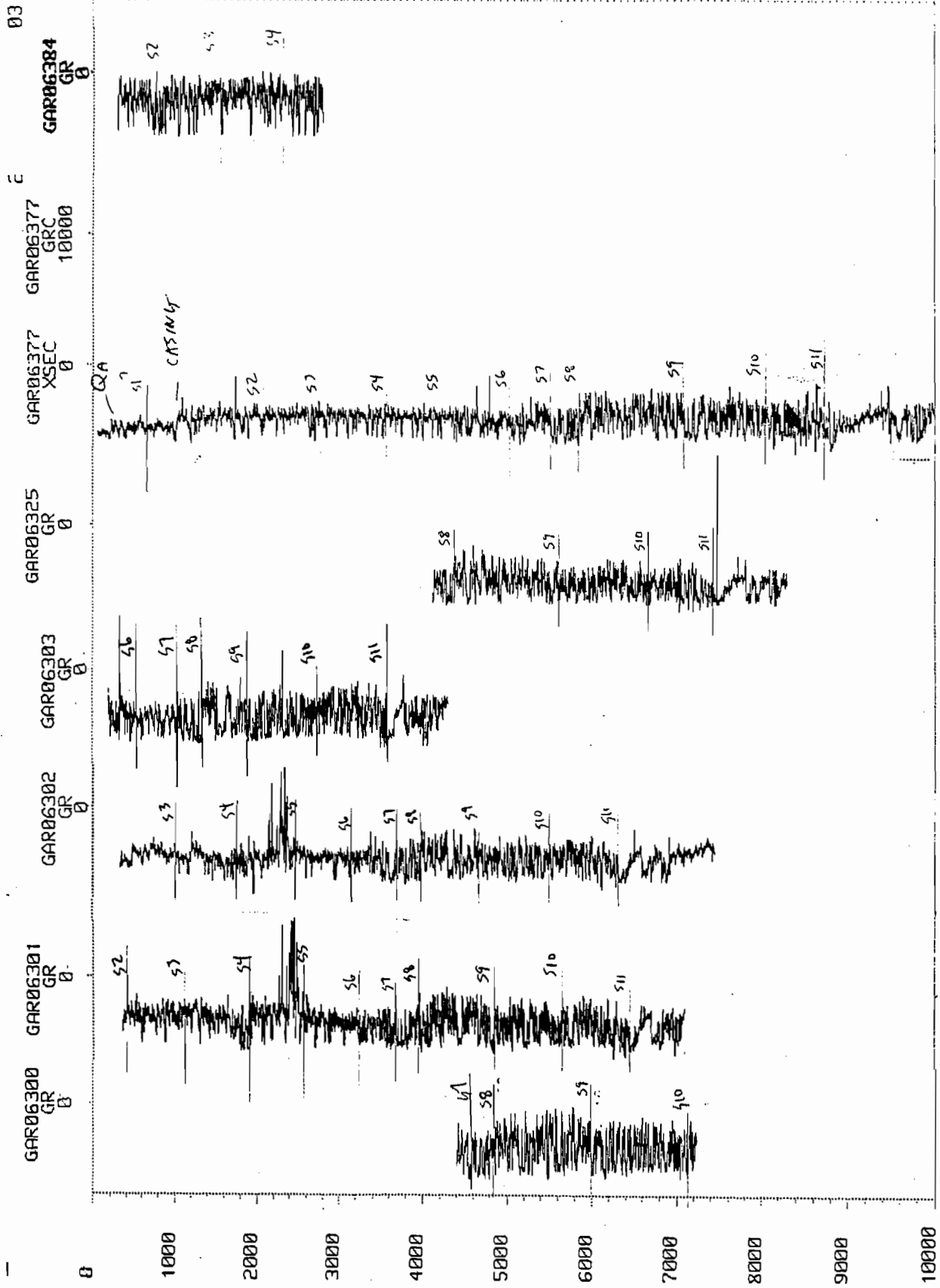
26-NOV-86 10

GAR06267
GR
0

GAR06266
GR
0



0 1000 2000 3000 4000 5000 6000 7000 8000 9000 10000



29-JAN-87 11:19

GAR06390
GR
0

GAR06390
GRC
0

GAR06393
GR
0

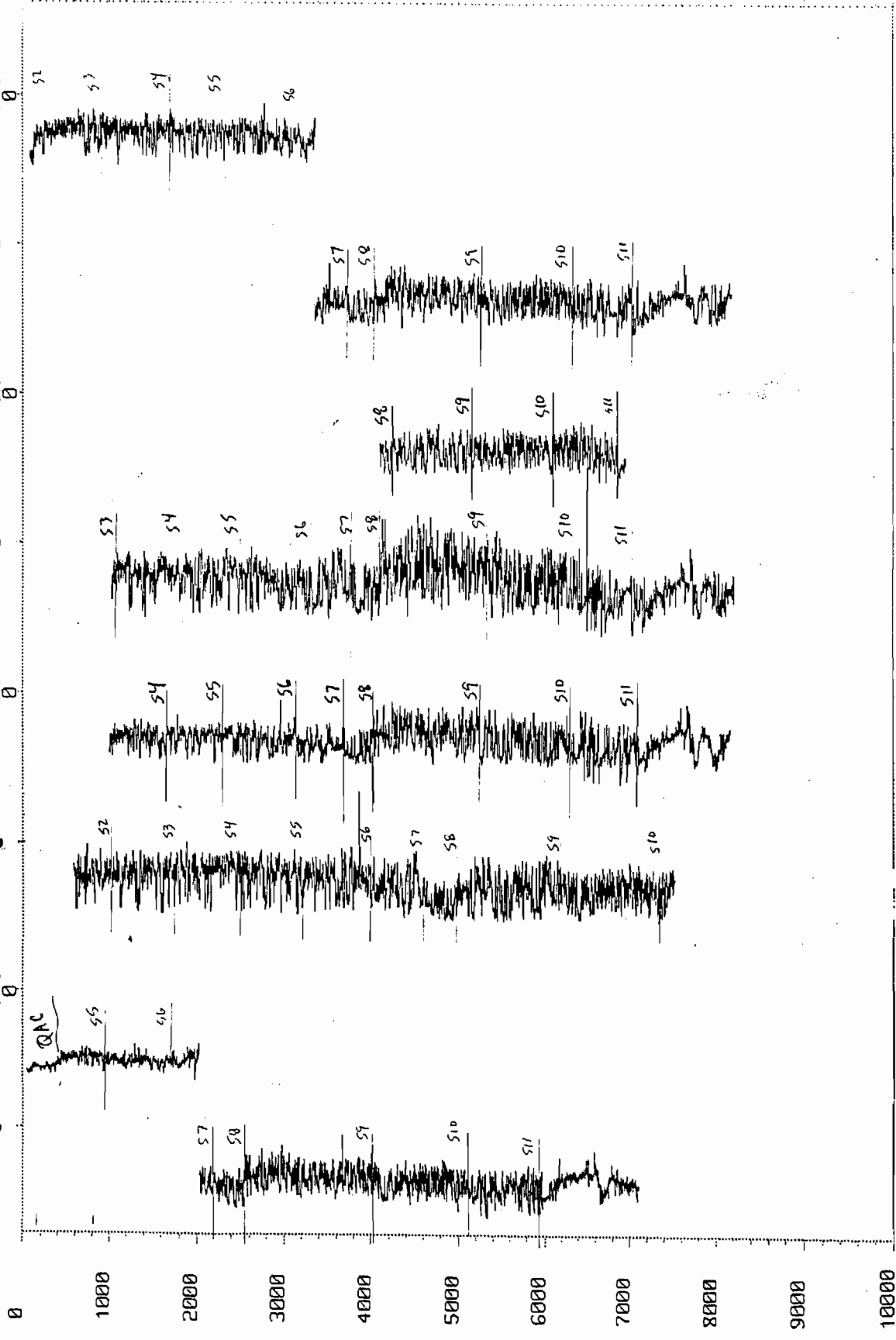
GAR06395
GR
0

GAR06410
GR
0

GAR06413
GR
0

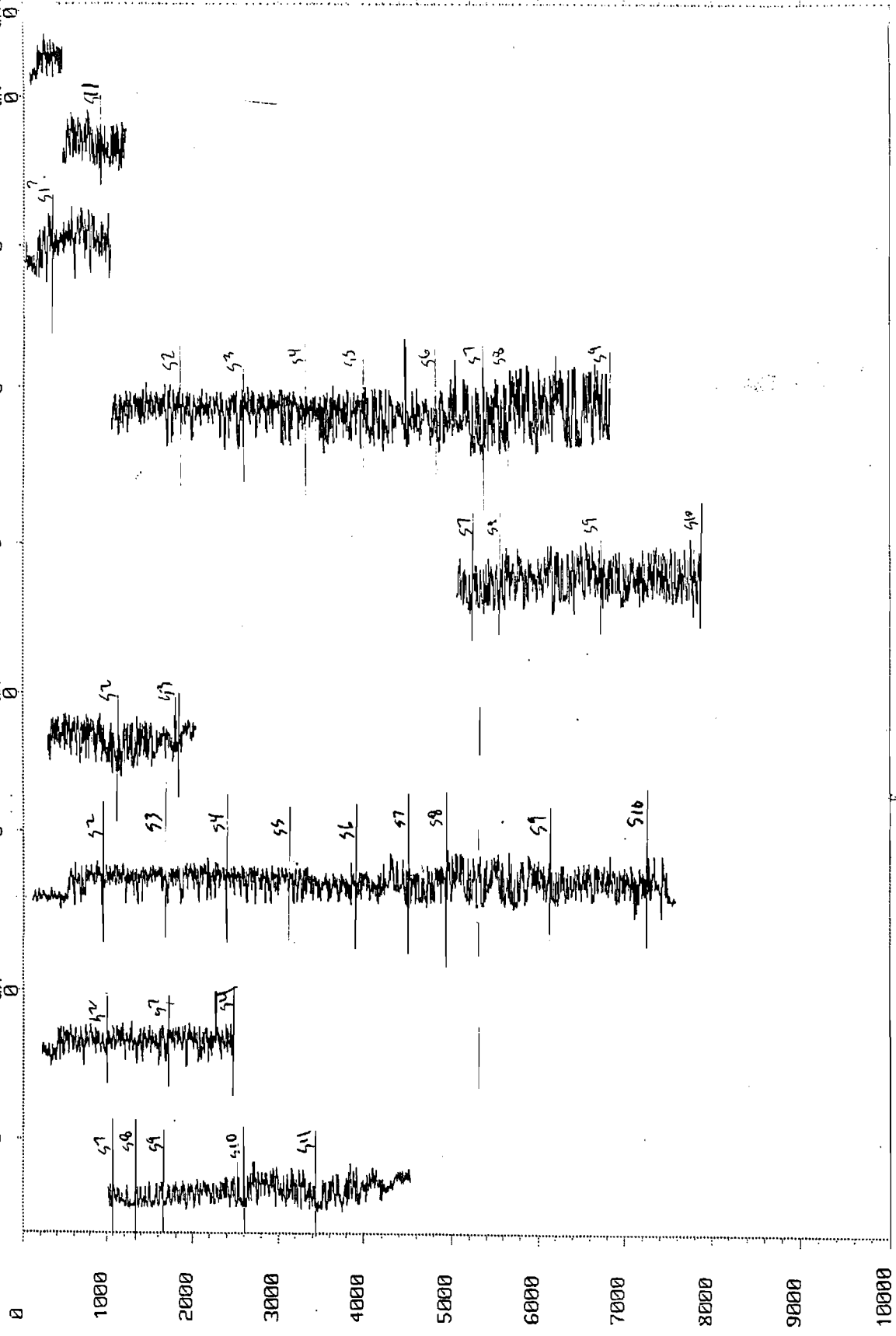
GAR06419
GR
0

GAR06419
GRC
0



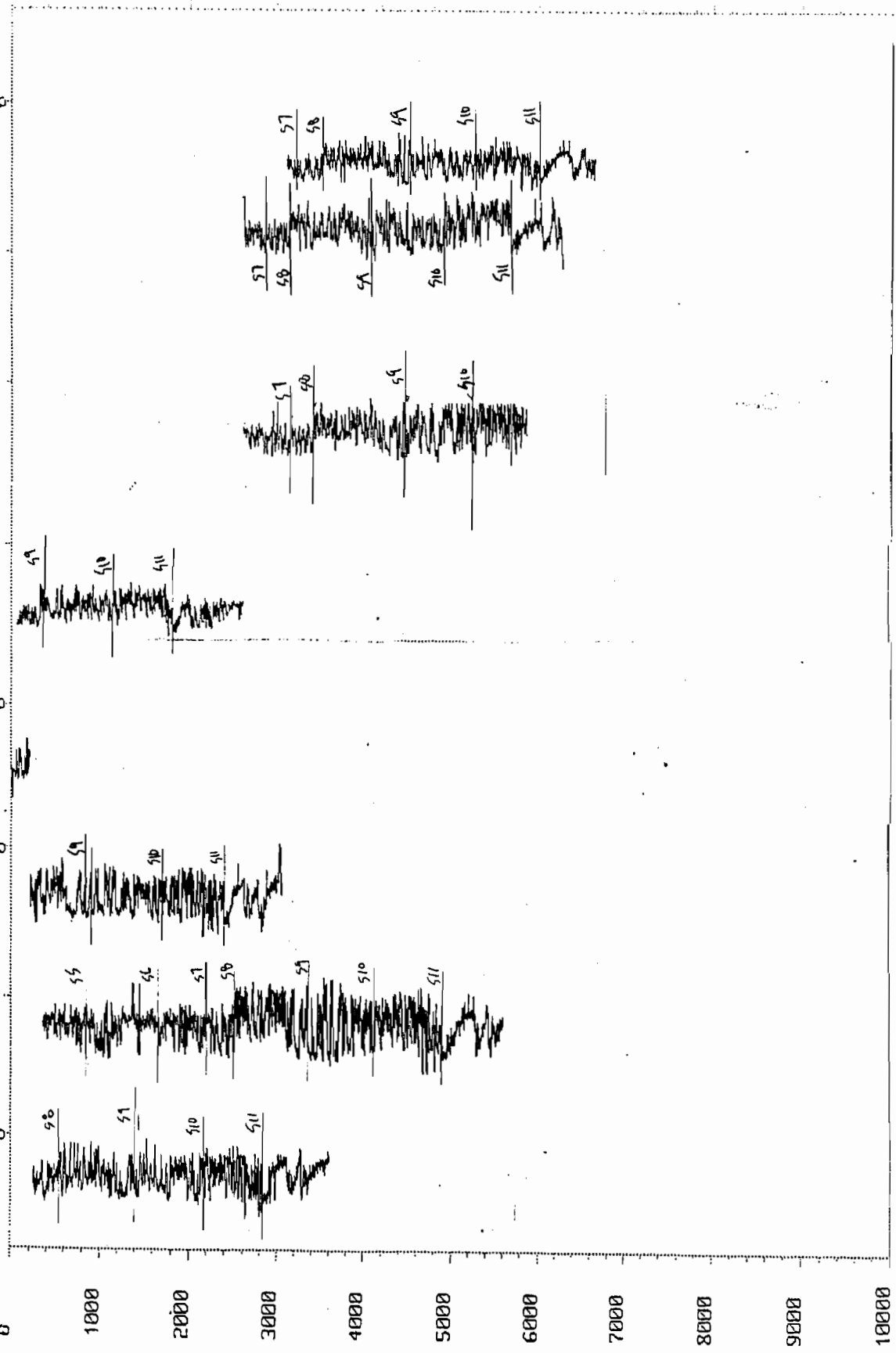
29-JAN-87 DEC-86 08.

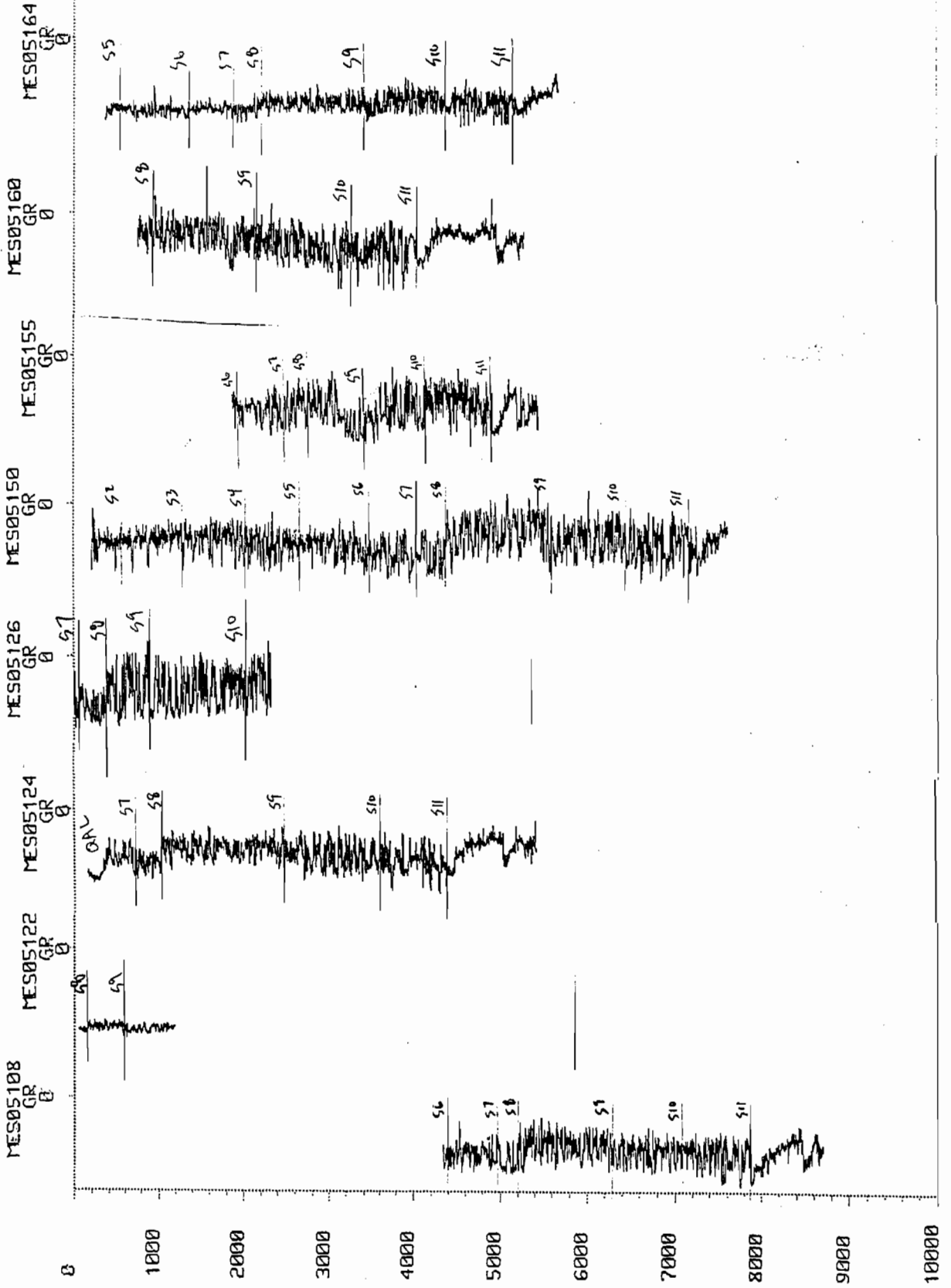
GAR06422 GR 0
GAR06440 GR 0
GAR06441 GR 0
GAR06466 GR 0
GAR09901 GR 0
GAR60005 GR 0
GAR60005 GRC 0
GAR60010 GR 0
GAR60010 GRC 0



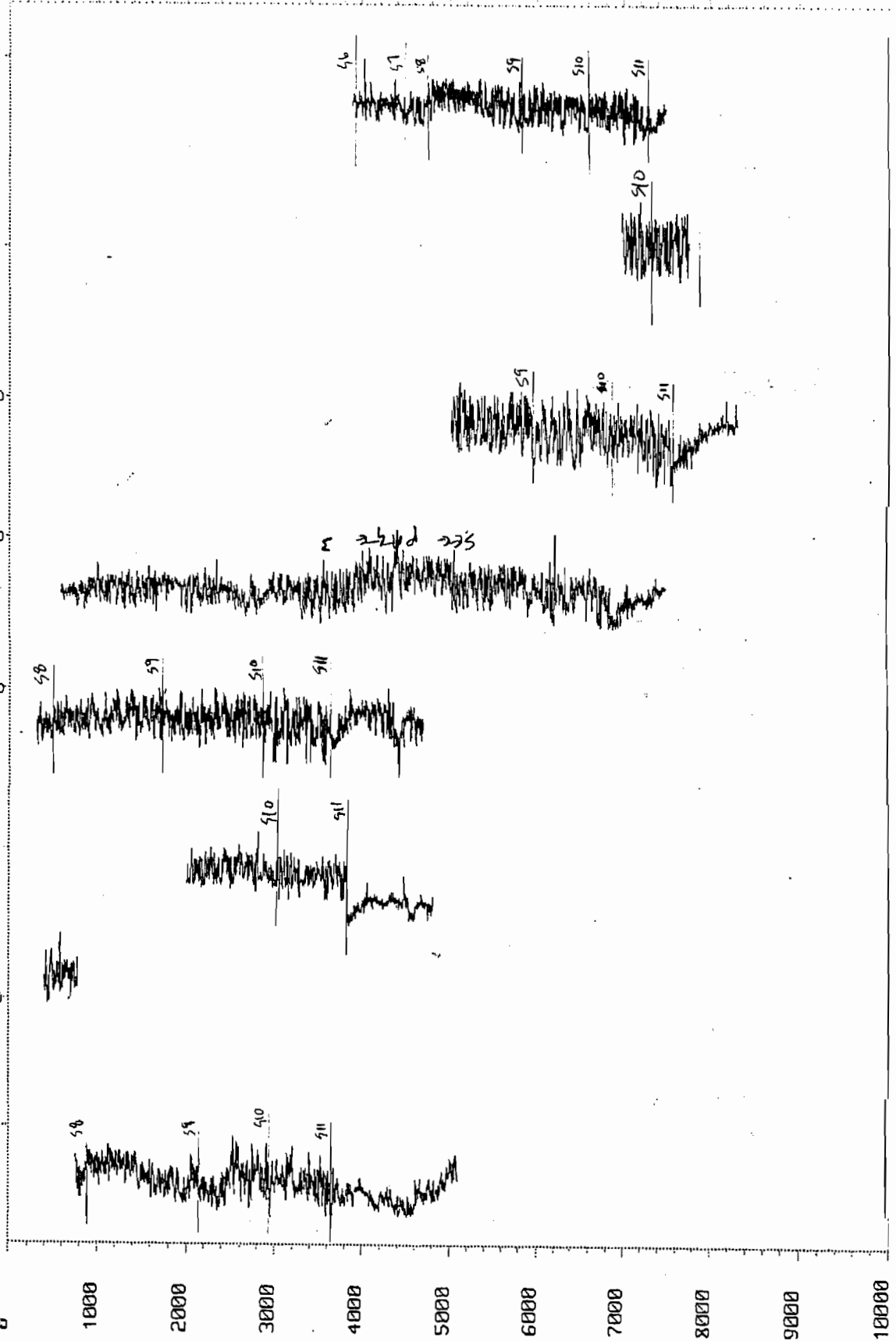
29-JAN-87 12:09

MES05025 GR 0
MES05037 GR 0
MES05044 GR 0
MES05044 GR 0
MES05045 GR 0
MES05063 GR 0
MES05080 GR 0
MES05091 GR 0





MES05167 GR 0
 MES05167 GRC 0
 MES05172 GR 0
 MES05177 GR 0
 GAR05186 GR 0
 MES07331 GR 0
 MES07353 GR 0
 29- I
 MES07360 GR 0



29-JAN-87 14:25

MES08171
GR
0

MES08150
GAM
0

MES08149
GI
0

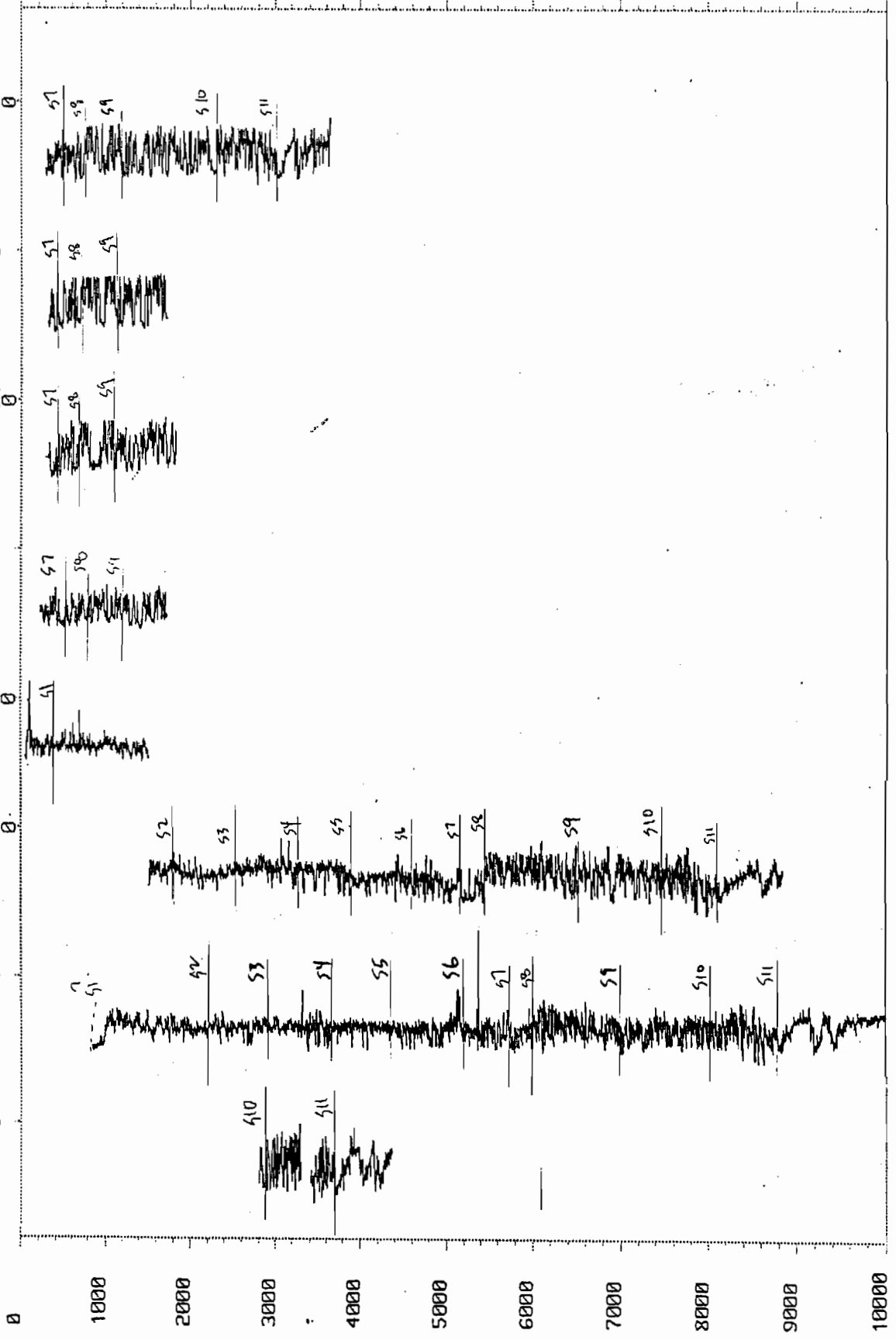
MES08148
GR
0

MES08132
GRC
0

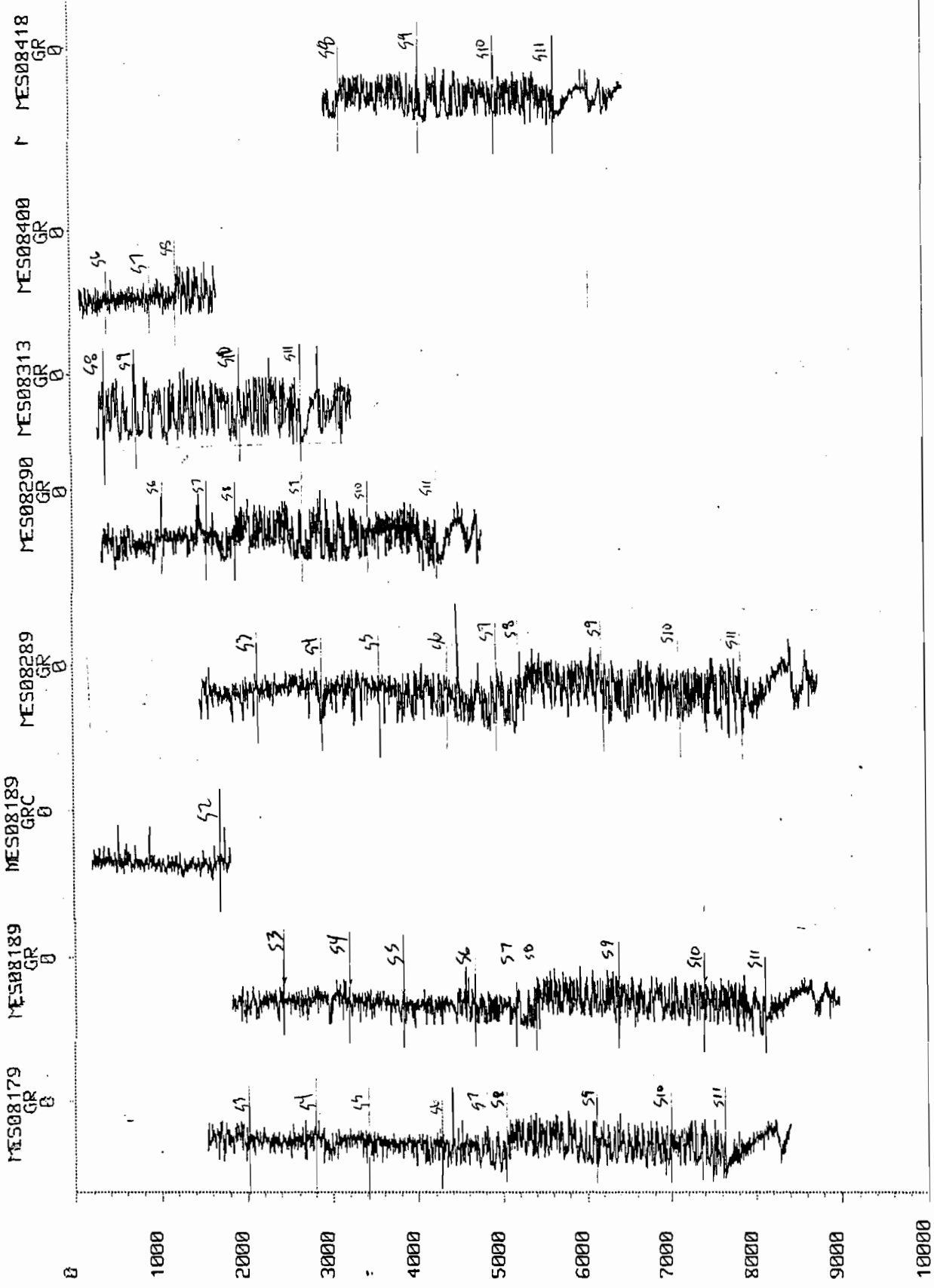
MES08132
GR
0

MES08043
GR
0

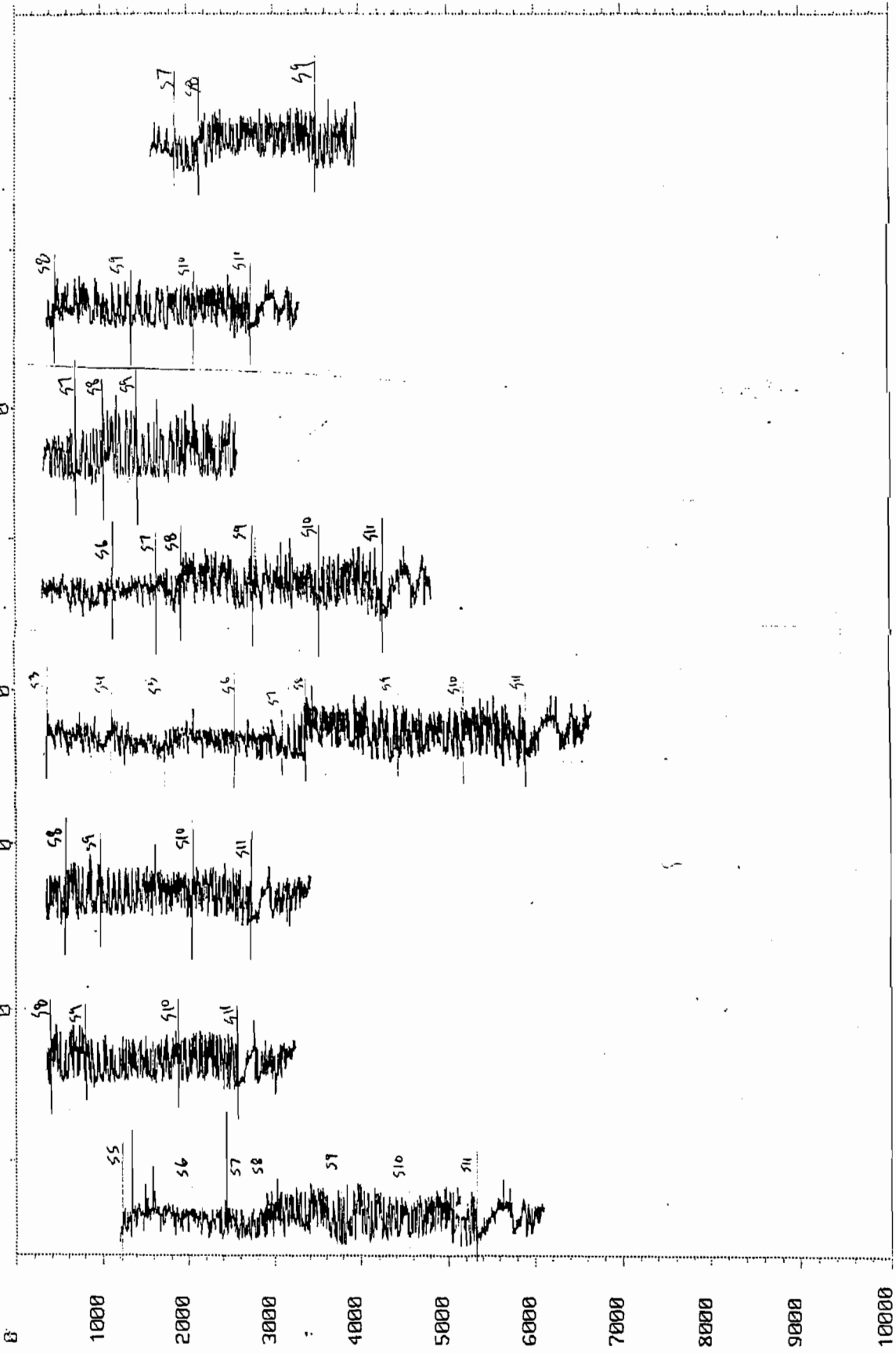
MES08004
GR
0



29-1



MES08419 GR 0
 MES08420 GR 0
 MES08432 GR 0
 MES08449 GR 0
 MES08511 GR 0
 MES08533 GR 0
 MES08542 GR 0
 MES60009 GR 0



:34

RB0503ERB05048
GR 0

RB05009
GR 0

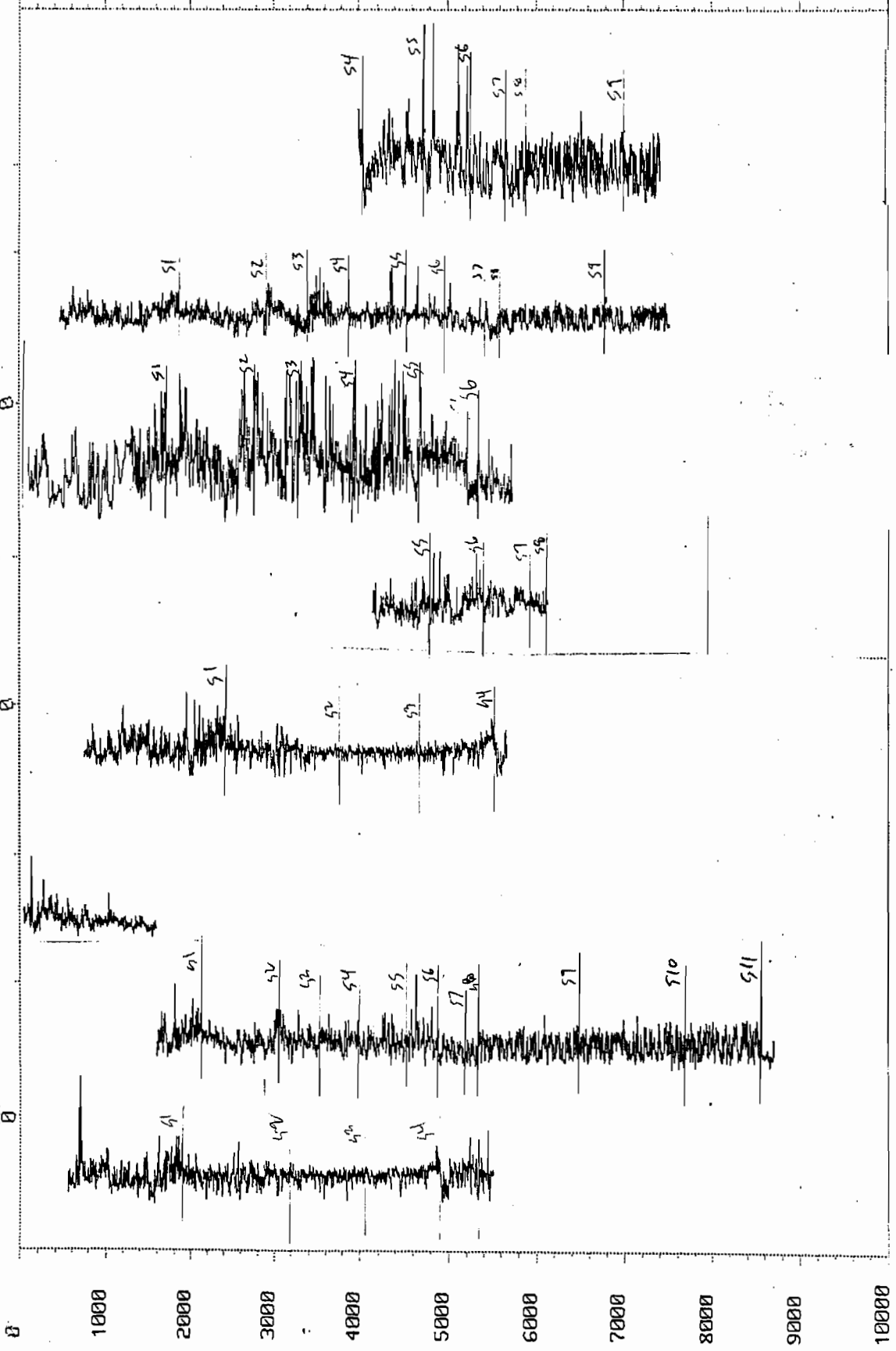
RB05006
GR 0

RB01097
GR 0

RB01095
GRC 0

RB01095
GR 0

RB01016
GR 0



30-JAN-87 07:35

RB07036
GR
0

RB05891
GR
0

RB05288
GR
0

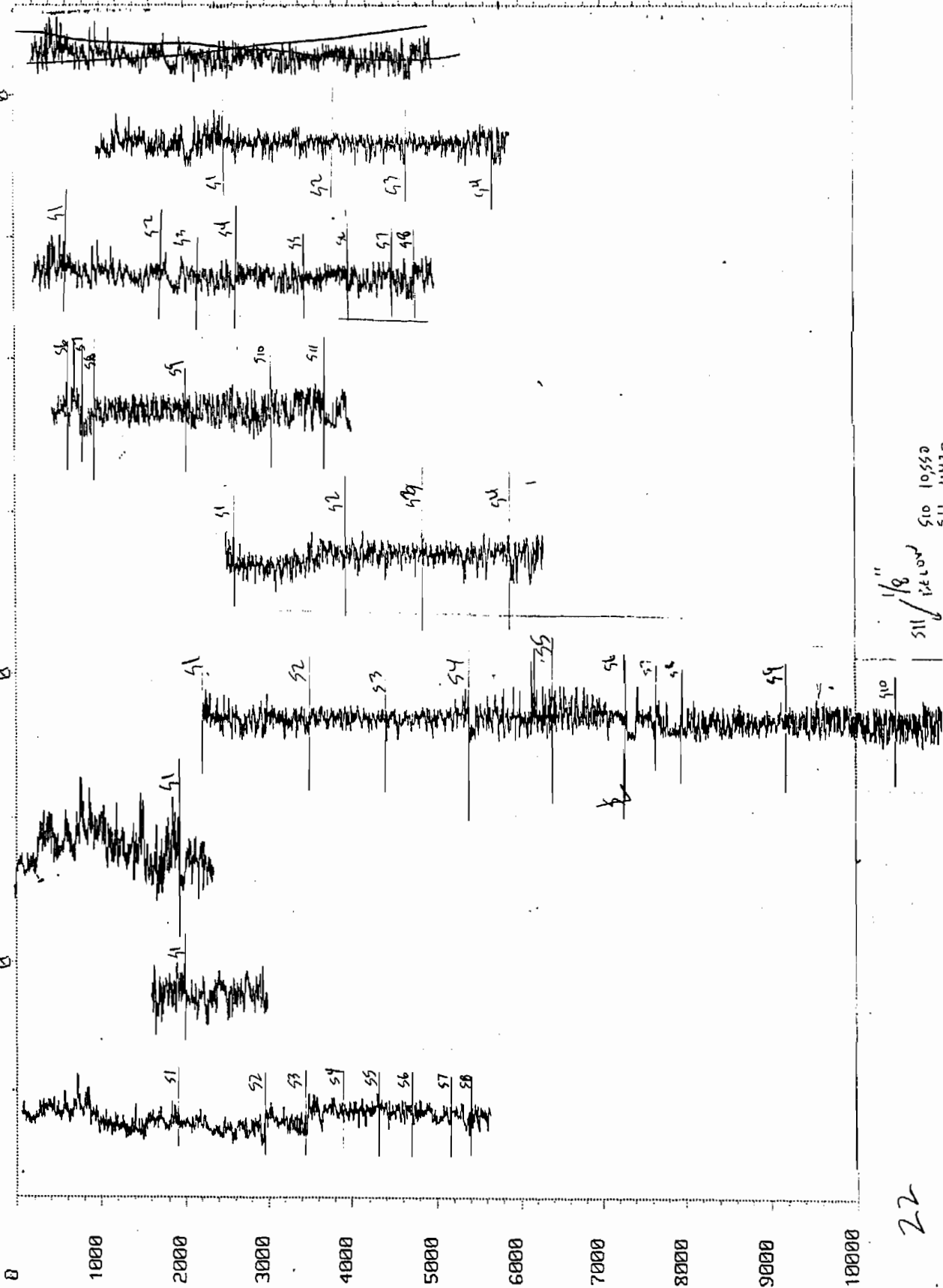
RB05173
GR
0

RB05170
GR
0

RB05151
GR
0

RB05136
GR
0

RB05072
GR
0



22

4-DEC-86 1032

RB07040
GR
0

RB07040
GRC
0

RB07048
GR
0

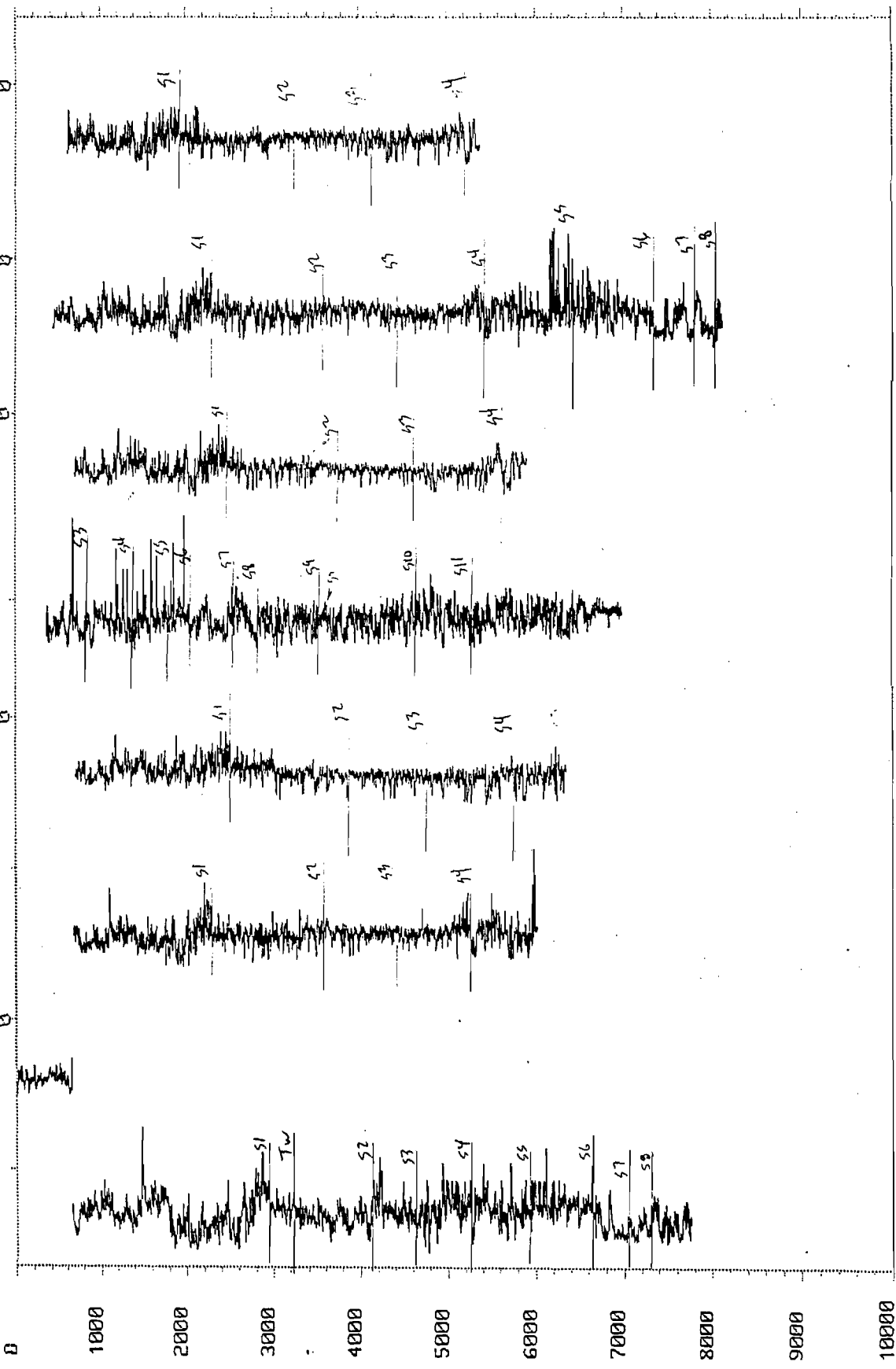
RB07052
GR
0

RB07076
GR
0

RB07091
GR
0

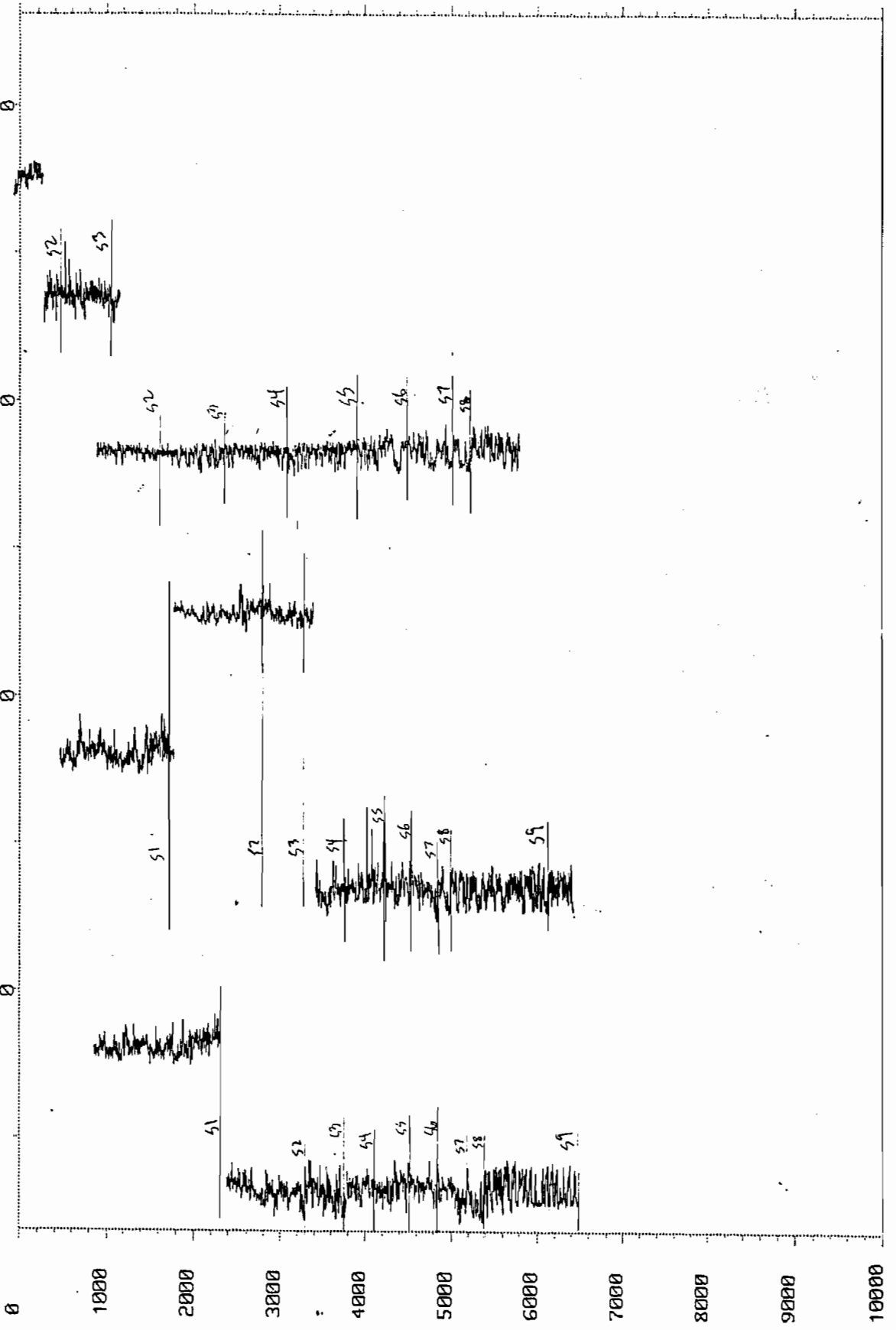
RB07096
GR
0

RB07175
GR
0



30-JAN-87 08:22

RB07234 GR 0
RB07234 GRC 0
RB07238 GR 0
RB07238 GRC 0
RB07238 GRCC 0
RB07258 GR 0
RB07302 GR 0
RB07302 GRC 0



30-JAN-87 08:45

RB07312
GR
0

RB07315
GR
0

RB07349
GR
0

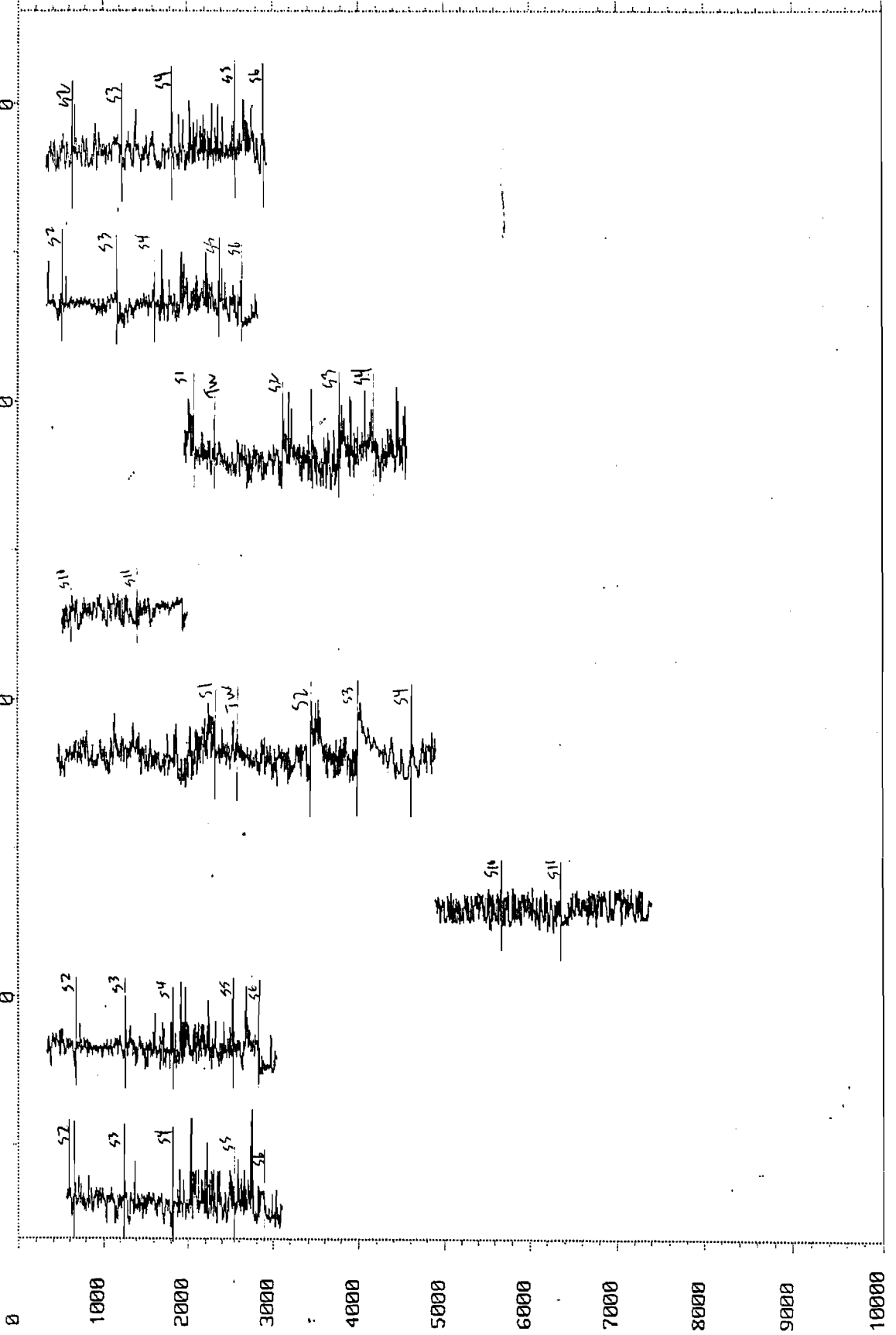
RB07355
GR
0

RB07382
GR
0

RB07399
GR
0

RB07404
GR
0

RB07411
GR
0



30-JAN-87 09:09

RB07413
GR
0

RB07418
GR
0

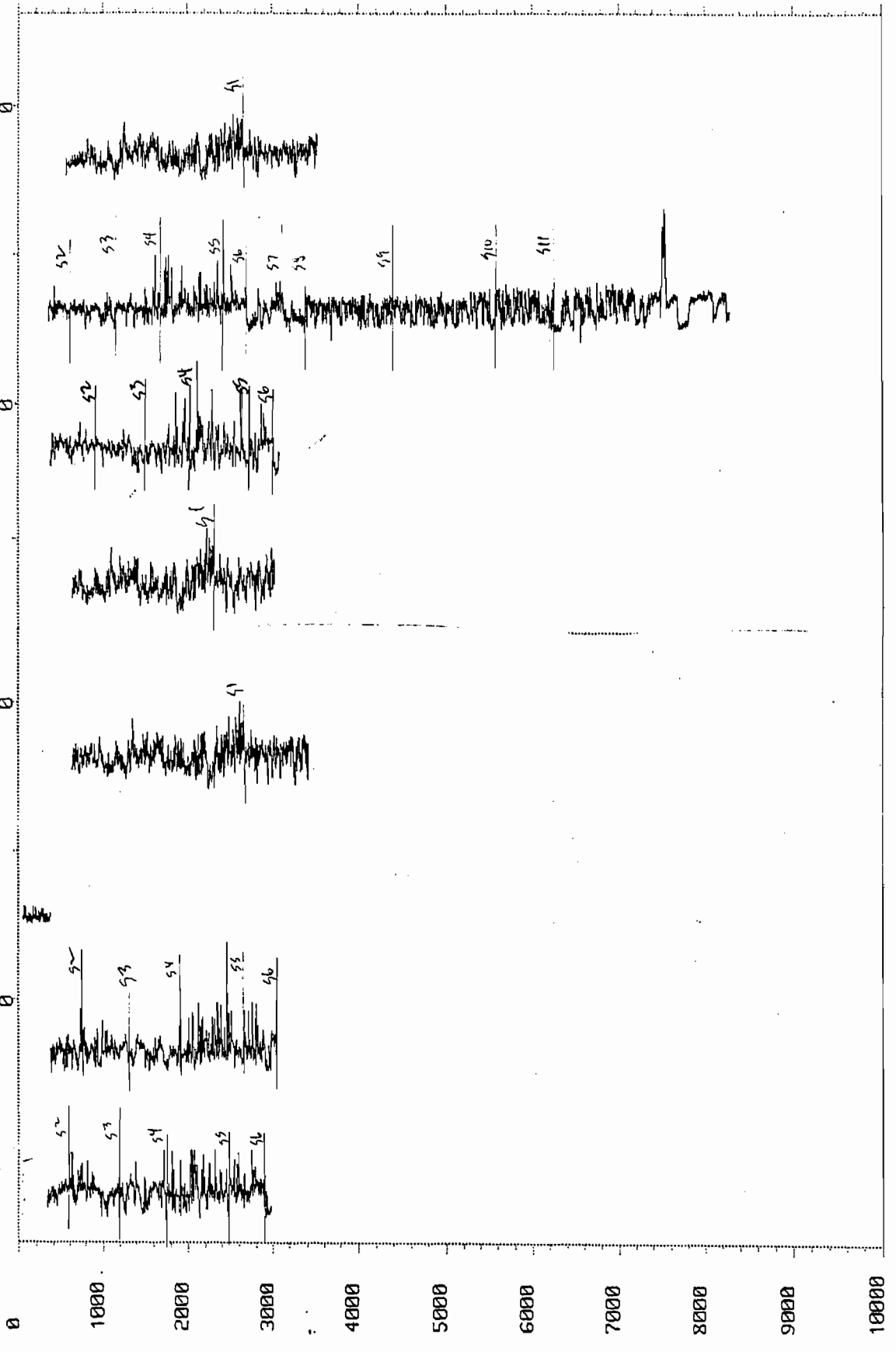
RB07435
GR
0

RB07436
GR
0

RB07467
GR
0

RB07468
GR
0

RB07476
GR
0



0-JAN-87 09:27

R807550
GR
0

R807544
GR
0

R807543
GR
0

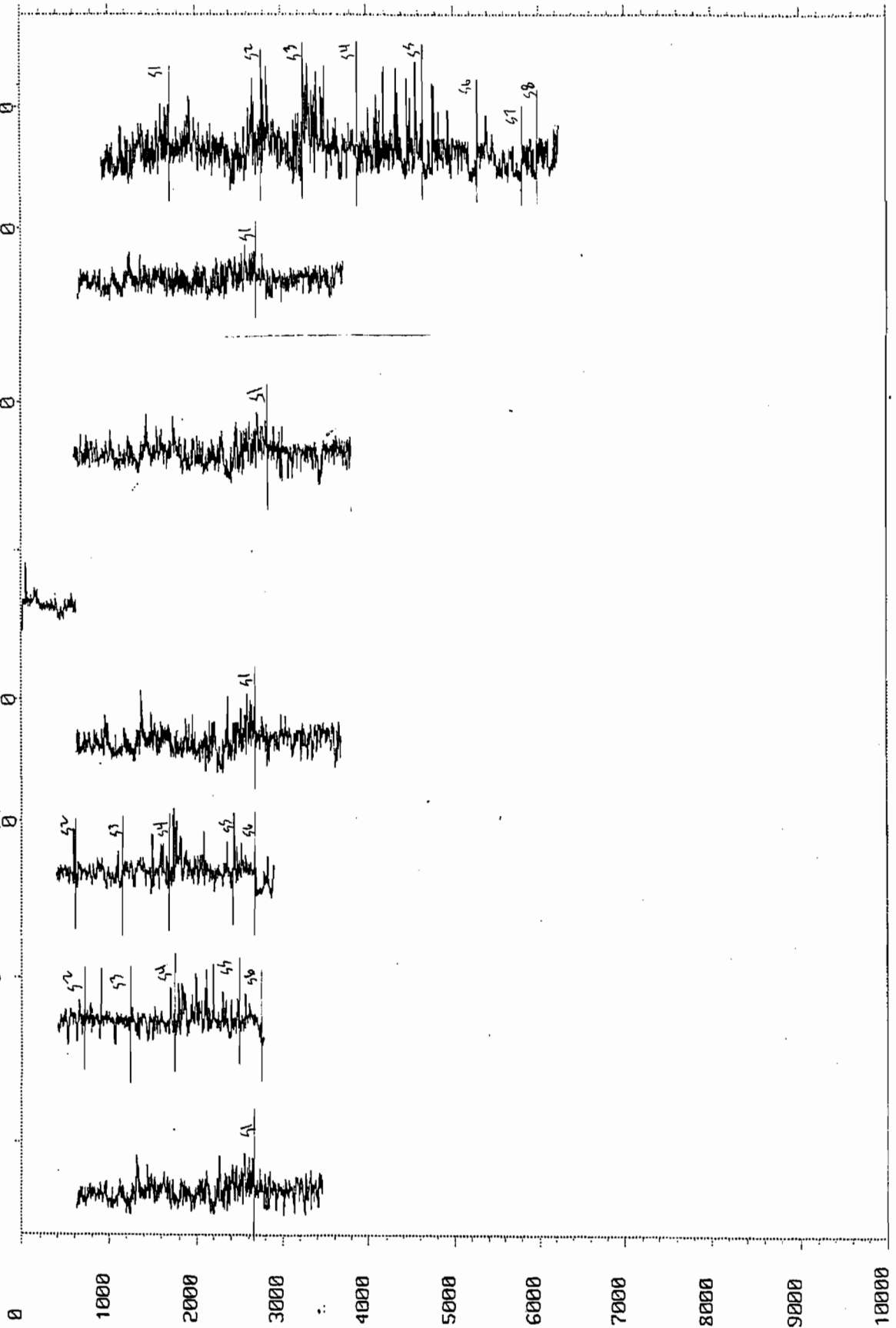
R807542
GRC
0

R807542
GR
0

R807493
GR
0

R807492
GR
0

R807477
GR
0



1-JAN-87 09:42

RB07648
GR
0

RB07617
GR
0

RB07613
GR
0

R

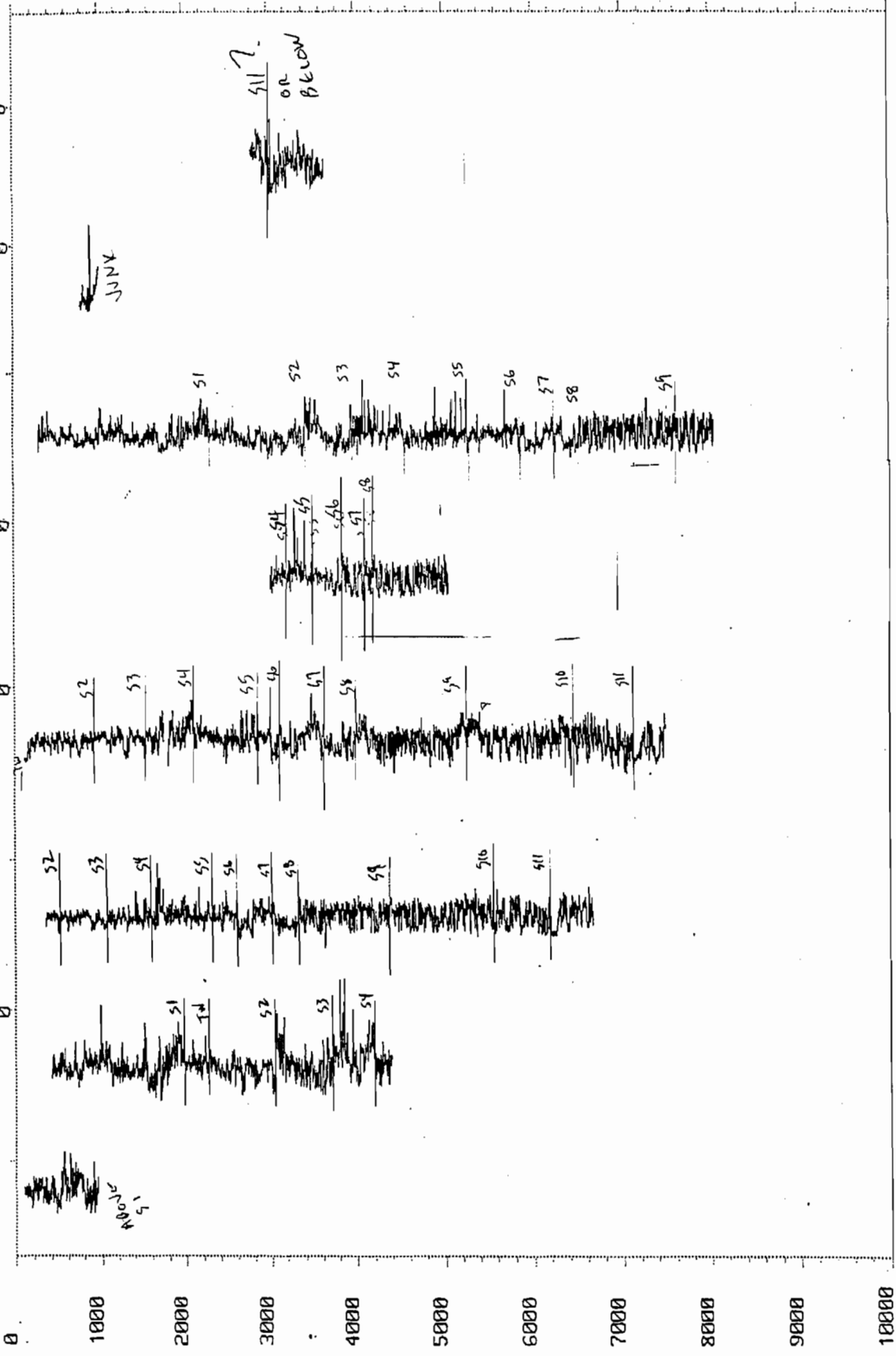
RB07611
GR
0

RB07570
GR
0

RB07564
GR
0

RB07563
GR
0

RB07550
GRC
0



55

30-

RB07693
GR
0

RB07681
GRC
0

RB07681
GR
0

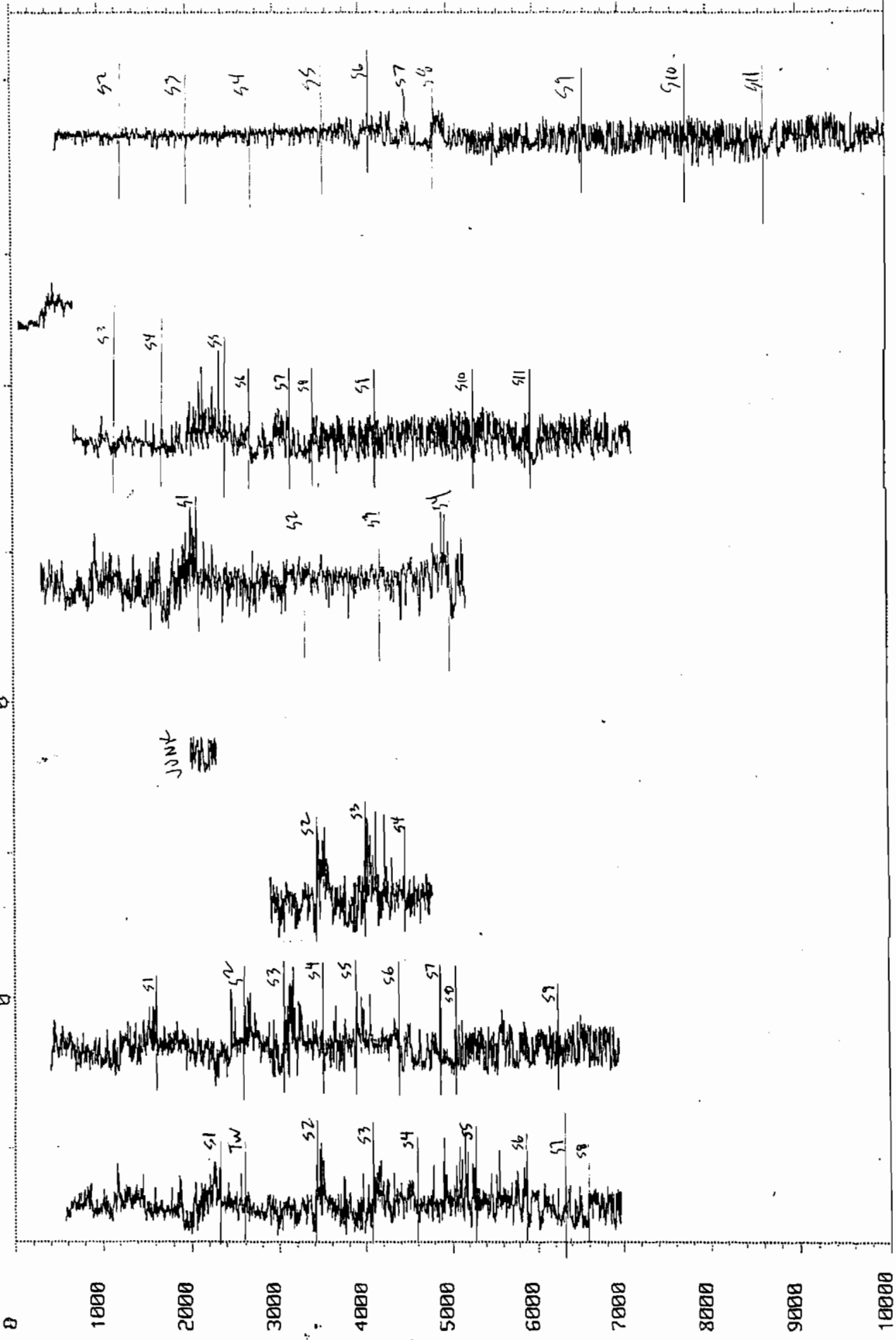
RB07678
GR
0

RB07671
GR
0

RB07662
GR
0

RB07661
GR
0

RB07659
GR
0



10-JAN-87 10:05

RB07706
GR
0

RB07707
GR
0

RB07708
GR
0

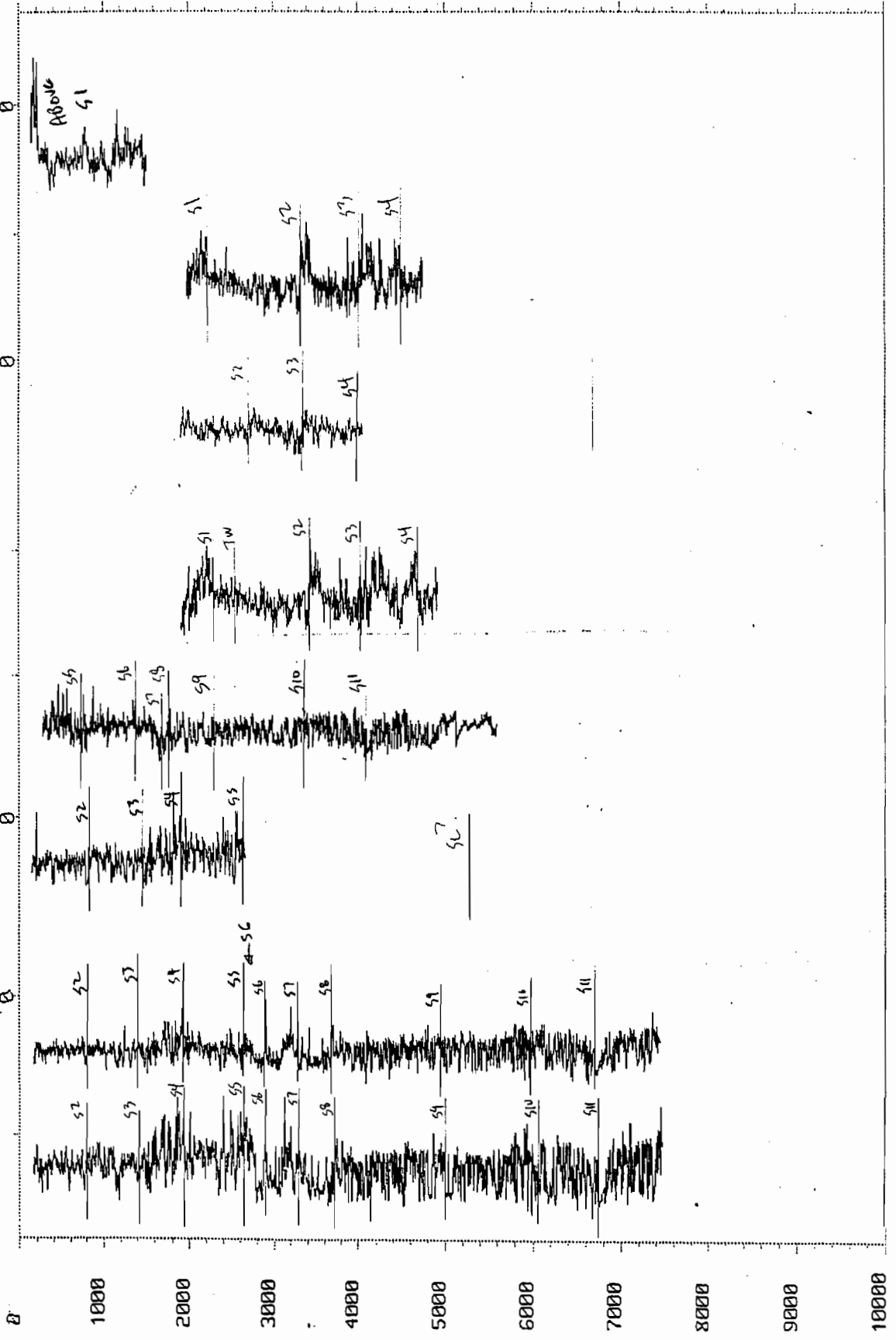
RB07747
GR
0

RB07760
GR
0

RB07761
GR
0

RB07762
GR
0

RB07890
GR
0



30-JAN-87 13:47

RB07955
GR
0

RB07959
GR
0

RB07960
GR
0

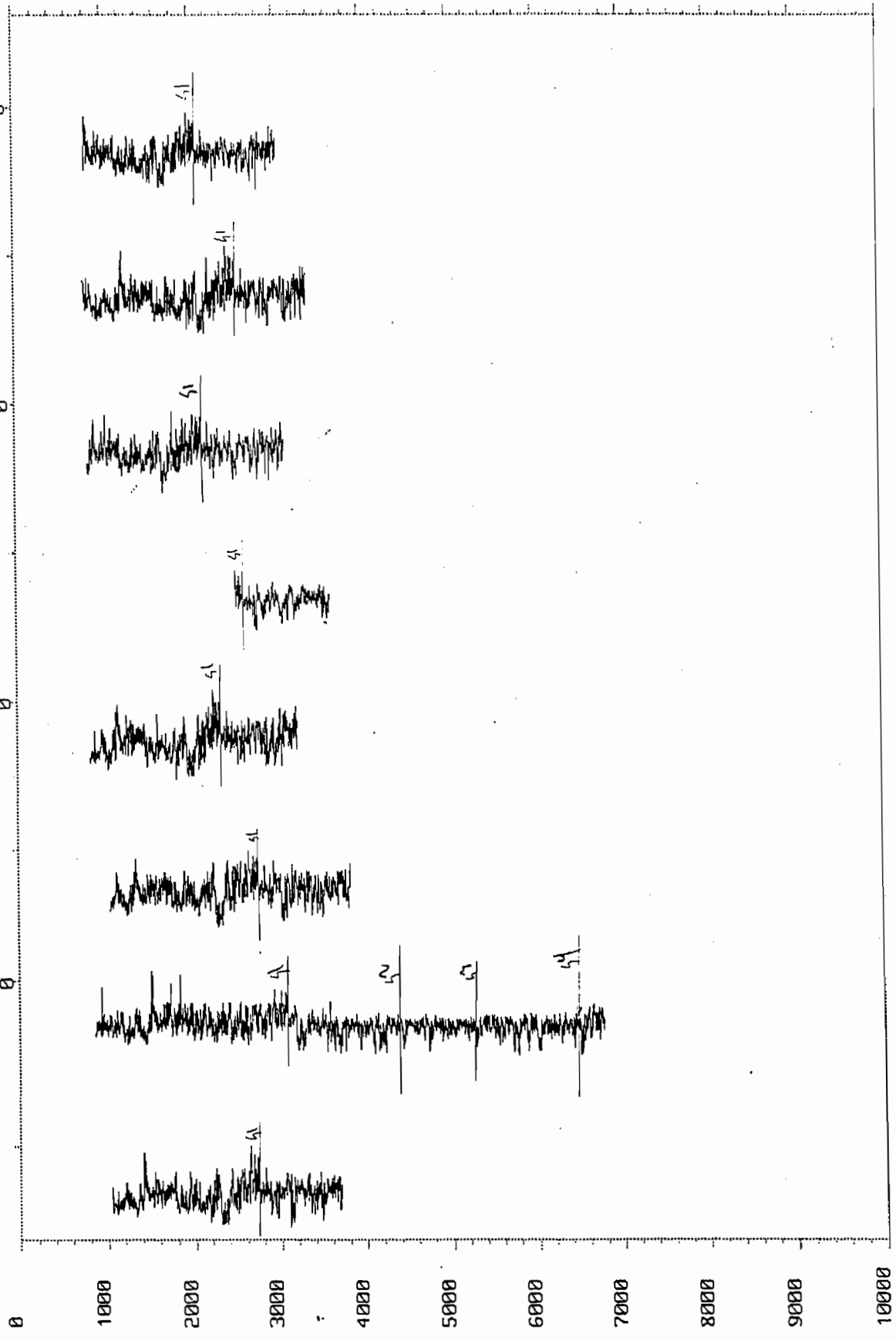
RB07961
GR
0

RB07993
GR
0

RB07994
GR
0

RB07995
GR
0

RB07996
GR
0



30-JAN-87 14:04

RB08179
GR
0

RB08178
GR
0

RB08176
GR
0

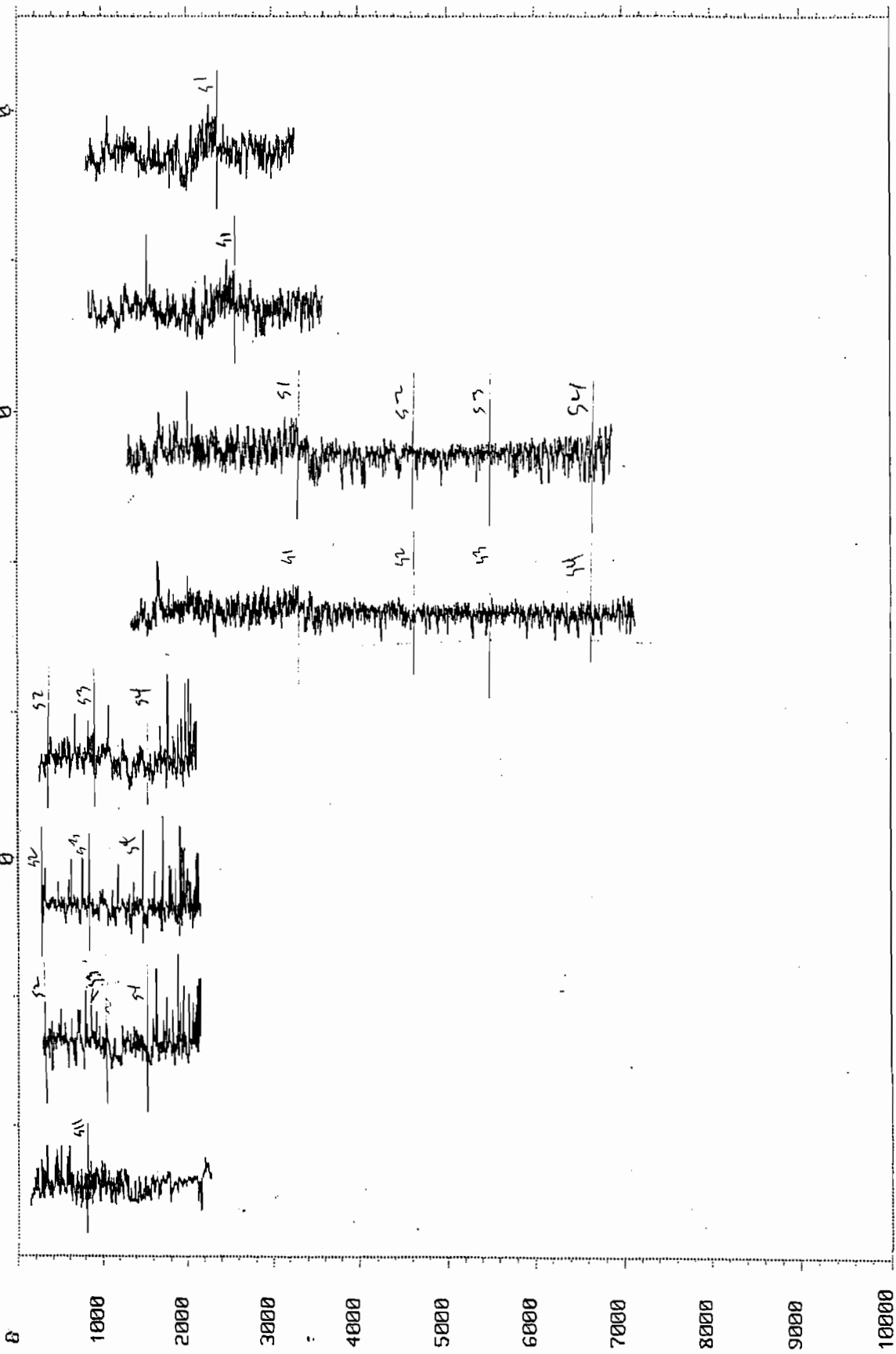
RB08175
GR
0

RB08102
GR
0

RB08101
GR
0

RB08100
GR
0

RB08002
GR
0



30-JAN-87 14:16

RB08541
GR
0

RB08316
GR
0

RB08247
GR
0

4-DEC-86 09

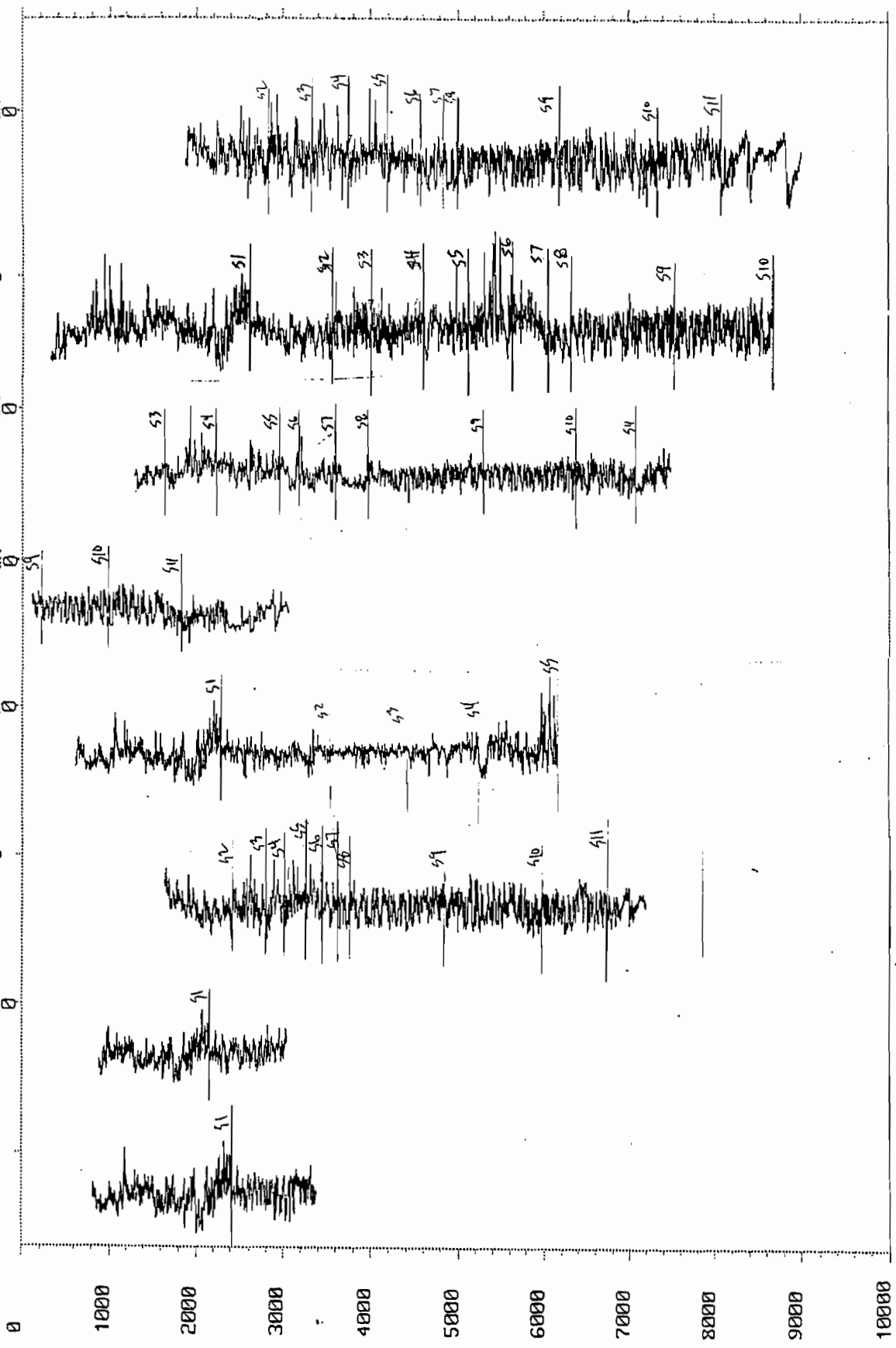
RB08233
GR
0

RB08189
GR
0

RB08183
GR
0

RB08182
GR
0

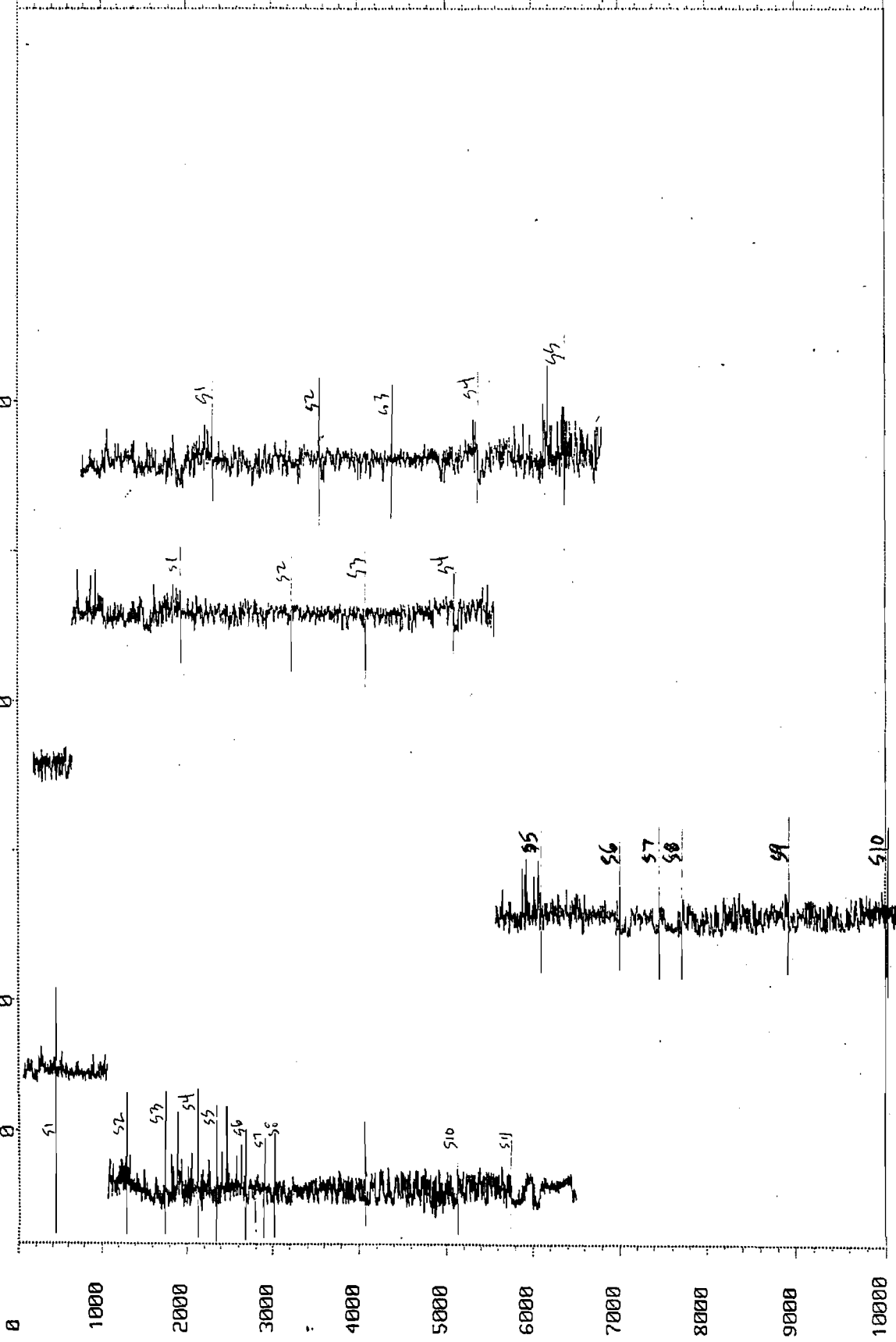
RB08181
GR
0



30-JAN-87 14:38

66V:0885

RB08711 RB08711 RB066423 RB066423 RB066423 RB066512
 GR GR GRCC GRCC GR GR GR
 0 0 0 0 0 0



XI. APPENDIX C

Portion of the Geologic Map of Colorado showing the Piceance Basin area. Note the location of the Grand Hogback monocline (L-shaped feature at center) for reference. The Grand Hogback forms the eastern most boundary of the basin.